AD-A080 969   SYSTEMS RESEARCH LABS INC DAYTON OHIO RESEARCH APPLI--ETC F/G 14/2
STUDY OF NONDESTRUCTIVE EVALUATION METHODS FOR LAYERED STRUCTUR--ETC(U)
NOV 79 N K BATRA, C M ELIAS, J S LEFFLER   F33615-77-C-5022
UNCLASSIFIED SRL-6492   AFML-TR-79-4162   NL

1 OF 2
AD-
A080969

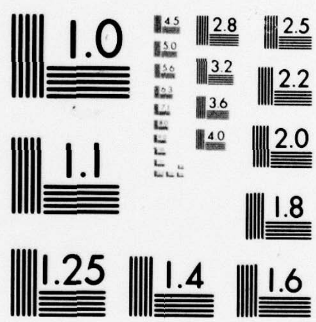

MICROCOPY RESOLUTION TEST CHART
NATIONAL BUREAU OF STANDARDS-1963-A

LEVEL II

AFML-TR-79-4162

AD A 080969

STUDY OF NONDESTRUCTIVE EVALUATION METHODS FOR LAYERED STRUCTURES

N. K. Batra
C. M. Elias
J. S. Leffler

Research Applications Division
Systems Research Laboratories, Inc.
2800 Indian Ripple Road
Dayton, Ohio 45440

November 1979

Technical Report AFML-TR-79-4162
Final Technical Report for Period 1 December 1976 - 31 July 1979

Approved for public release; distribution unlimited

AIR FORCE MATERIALS LABORATORY
AIR FORCE WRIGHT AERONAUTICAL LABORATORIES
AIR FORCE SYSTEMS COMMAND
WRIGHT-PATTERSON AIR FORCE BASE, OHIO 45433

NOTICE

When Government drawings, specifications, or other data are used for any purpose other than in connection with a definitely related Government procurement operation, the United States Government thereby incurs no responsibility nor any obligation whatsoever; and the fact that the government may have formulated, furnished, or in any way supplied the said drawings, specifications, or other data, is not to be regarded by implication or otherwise as in any manner licensing the holder or any other person or corporation, or conveying any rights or permission to manufacture, use, or sell any patented invention that may in any way be related thereto.

This report has been reviewed by the Information Office (OI) and is releasable to the National Technical Information Service (NTIS). At NTIS, it will be available to the general public, including foreign nations.

This technical report has been reviewed and is approved for publication.

R. L. Crane

R. L. CRANE
Project Engineer

FOR THE COMMANDER

D. M. FORNEY, Jr., Chief
Nondestructive Evaluation Branch
Metals and Ceramics Division

"If your address has changed, if you wish to be removed from our mailing list, or if the addressee is no longer employed by your organization please notify AFML/LLP, W-PAFB, OH 45433 to help us maintain a current mailing list".

Copies of this report should not be returned unless return is required by security considerations, contractual obligations, or notice on a specific document.

SECURITY CLASSIFICATION OF THIS PAGE (When Data Entered)

19 REPORT DOCUMENTATION PAGE

READ INSTRUCTIONS BEFORE COMPLETING FORM

18 ~~1. REPORT NUMBER~~ AFML-TR-79-4162	2. GOVT ACCESSION NO.
3. RECIPIENT'S CATALOG NUMBER	
4. TITLE (and Subtitle) 6 STUDY OF NONDESTRUCTIVE EVALUATION METHODS FOR LAYERED STRUCTURES	9 ~~5. TYPE OF REPORT & PERIOD COVERED~~ Final Technical Report, 1 Dec 76 [redacted] 31 July 79
	~~6. PERFORMING ORG. REPORT NUMBER~~ 6492 Final
7. AUTHOR(s) 10 N. K. Batra, C. M. Elias [redacted] J. S. Leffler	~~8. CONTRACT OR GRANT NUMBER(s)~~ 15 F33615-77-C-5022
9. PERFORMING ORGANIZATION NAME AND ADDRESS Systems Research Laboratories, Inc. 2800 Indian Ripple Road Dayton, Ohio 45440	10. PROGRAM ELEMENT, PROJECT, TASK AREA & WORK UNIT NUMBERS 16 ~~Project~~ 2418 Task 0507 17
11. CONTROLLING OFFICE NAME AND ADDRESS Air Force Materials Laboratory AFML/LLP Wright-Patterson Air Force Base, Ohio 45433	11 ~~12. REPORT DATE~~ Nov [redacted] 79
	~~13. NUMBER OF PAGES~~ 143
14. MONITORING AGENCY NAME & ADDRESS (if different from Controlling Office) PE 62102F 12 142	15. SECURITY CLASS. (of this report) UNCLASSIFIED
	15a. DECLASSIFICATION/DOWNGRADING SCHEDULE

16. DISTRIBUTION STATEMENT (of this Report)

Approved for public release; distribution unlimited.

409171

17. DISTRIBUTION STATEMENT (of the abstract entered in Block 20, if different from Report)

14 SRL-6492

18. SUPPLEMENTARY NOTES

19. KEY WORDS (Continue on reverse side if necessary and identify by block number)

Nondestructive evaluation, adhesively bonded layered structures, acoustic cw spectroscopy, sampled cw spectroscopy, bolt-hole cracks, ultrasonics, measurement of crack sizes, Doppler-shift studies of cracks, pseudorandom signal correlation.

20. ABSTRACT (Continue on reverse side if necessary and identify by block number)

Acoustic parameters of adhesively bonded layered structures were extracted from experimental cw spectra. Computer software was developed which yielded the best fit of the experimental spectra of such structures to theoretical spectra generated from the theoretical model of layered structures. The acoustic parameters for such a fit then corresponded to the structures under study. A sampled cw Doppler-effect technique was developed to measure radial

DD FORM 1 JAN 73 1473 EDITION OF 1 NOV 65 IS OBSOLETE

-409172 slh

SECURITY CLASSIFICATION OF THIS PAGE (When Data Entered)

bolt-hole cracks under the fasteners in single- and multi-layered adhesively bonded structures. This technique measures the size of the cracks far more accurately than any of the previously used amplitude or time delay methods. An Ultrasonic Pseudorandom-Signal-Correlation System was designed, fabricated, and experimentally characterized. This type of instrument may be useful in applications where high signal-to-noise ratios are not obtainable by conventional methods.

FOREWORD

This constitutes the final technical report on work accomplished under Contract No. F33615-77-C-5022, Project 2418, Task 0507. This program entitled, "Study of Adhesively Bonded Layered Structures using Acoustic Spectroscopy," is funded by the Air Force Materials Laboratory, Air Force Wright Aeronautical Laboratories (AFSC), and is monitored by the Air Force Materials Laboratory. Robert L. Crane, AFML/LLP, is the Air Force Materials Laboratory Program Monitor. This report covers the period 1 December 1976 through 31 July 1979.

TABLE OF CONTENTS

LIST OF ILLUSTRATIONS

SECTION I
INTRODUCTION

The objective of this research was to develop experimental techniques for the quantitative characterization of adhesively bonded multilayer structures nondestructively. These multilayered structures are very similar to the ones used in mechanically fastened aircraft wings.

Concerning the structural integrity of the wings, one is interested in characterizing the inner layer by measuring the acoustic parameters and studying these parameters as a function of aging. The acoustic reflection and transmission coefficients for a layered structure can be computed using the theoretical model of Brekhovskikh.[1] Details of this model and the computer program for calculation of reflection and transmission coefficients for layered structures developed during the initial phase of this research program were presented in an intermediate report.[2] Based upon the theoretical model, acoustic parameters such as attentuation coefficients are determined from the experimental data using a fit program which has been developed further since the intermediate report was published. The determination of these acoustic parameters using cw spectroscopy is described in Section II.

Microcracks in wing structures grow and develop because of tremendous stress which these structures experience in flight. The types of flaws most frequently produced in aircraft wing structures are radial cracks emanating at the bolt hole either at the faying surface of the first layer or at the inner layer. These cracks are caused by fatigue and develop from the surface down. Structural components can continue in service even with a crack, provided its dimensions remain below certain critical values. In view of this fact, it becomes very important to be able to measure periodically the size of these radial cracks nondestructively.

Several techniques such as amplitude, time, and spectral methods can be used to measure the radial dimensions of these cracks. Since each crack has a different reflectivity, quite inconclusive information regarding size is extracted by comparing the amplitude of the backscattered echo with the signal from a reference reflector and thus determining the equivalent dimension. The amplitude methods disregard several factors such as orientation of the crack, shape, width of the crack opening, and quality of the coupling--all of which affect measurement accuracy drastically. Timing methods measure the crack dimension from the time delay of a signal returning from a crack relative to the instant it left the transducer or some known scattering point on the sample. Although these methods yield better results with a focused beam, they are quite cumbersome since the best results are obtained only if the beam enters the specimen in the plane of the crack--which is not possible for the case of aircraft wing geometry.

Due to the particular geometry of radial bolt-hole cracks, a novel method based upon the Doppler shift was developed to measure the radial crack size. This method does not depend upon the amplitude or time delay of the reflected signal from the crack. The radial size of the crack is proportional to the maximum Doppler shift of the signal backscattered from the tip of the crack. The method is far more accurate than any previously used method and has potential for practical use in the field. Section III describes the measurement of radial cracks using the Doppler effect.

For adhesively bonded layered structures, the attenuation α is very large. Consequently, the sensitivity of the sampled cw technique is reduced drastically. The conventional pulse-echo technique cannot be used for such specimens since the received signal becomes comparable to the thermal noise of the receiver. An alternative approach to solving the above S/N problem was undertaken.

Random-signal-correlation techniques can be used in ultrasonic flaw-detection systems to overcome several disadvantages of conventional pulse-echo systems. In a conventional pulse-echo system, a high ratio

of peak-to-average transmitted power is usually required to meet the range and resolution requirements of the system. Furthermore, when strongly sound-absorbent material is present, a pulse-echo system requires large average transmitted power to maintain an acceptable S/N ratio. However, ultrasonic transducers are limited in average power-handling ability due to heating effects and are limited in peak-power input capability due to voltage-breakdown effects. An additional limitation of conventional pulse-echo systems is that they offer no improvement in the S/N ratio of the received signal.

The inherent difficulties with the conventional pulse-echo system mentioned above were very successfully overcome in a laboratory system developed by Ferguson, et al.[3] This system transmits a long burst of ultrasonic noise and performs a correlation of the received echoes with a delayed version of the transmitted burst. In this system the resolution does not depend upon the transmitted pulse width, as in conventional pulse-echo systems, but upon the bandwidth of the transmitted noise. In addition, an improved S/N ratio of the received echo can be achieved (at the expense of a longer data-acquisition time) by scanning the signal slowly.

From a practical point of view, the system just described has a serious drawback. The water delay line which was used consisted of two matched ultrasonic transducers in a water bath, and delay was varied using a micrometer drive. Even if this delay line were automated and computer controlled, it would be bulky and require two closely matched transducers. These two transducers, along with the transmitting and receiving transducers, contribute to the overall system response, making it difficult to isolate the desired response due to the flaw along.

An ultrasonic random-signal-correlation system which does not employ a delay line and which may be used with a single transducer has been designed and built. Section IV describes this Ultrasonic Pseudorandom-Signal-Correlation System.

Section V contains conclusions on the progress reported herein. Suggestions are also made for further efforts which could be initiated utilizing the results reported here.

SECTION II

CW ULTRASONIC SPECTROSCOPY

Current Air Force requirements include the ability to detect delamination and degradation of adhesive bonds or sealants in multilayered, adhesively bonded aircraft structures. For nondestructive evaluation, ultrasonic examination provides the only access to the inner layers of such sandwich-like structures. Because the ultrasonic signal will be affected by each material layer through which it travels, some means must be utilized to extract information concerning the layer of interest. Ultrasonic spectroscopy provides such a method of isolating the contribution of each material layer to the total frequency spectrum of the multilayered structure. Ultrasonic spectroscopy has been proposed as a means for determining grain-size,[4] for measuring plate thicknesses or sound velocities,[5] for detecting delaminations in bonded structures,[6] for classifying bond strength,[7] and for measuring attentuation.[8]

A method has been developed which makes use of cw ultrasonic spectroscopy in the determination of the acoustic parameters of an unknown material used singly or as the inner layer of a three-layer sandwich structure. This method utilizes a theoretical model of layered structures developed by Brekhovskikh[1-2,9-10] which incorporates a functional dependence upon the density, thickness, and longitudinal sound velocity as well as the quadratic, linear, and constant frequency-dependent attenuation coefficients for each layer of the structure. A computer fit[11] of the theoretical model of the experimental transmission-coefficient spectrum provides a resultant set of acoustic parameters which may be used to indicate material degradation such as microcrazing or to evaluate proposed models of tensile or shear-bond strength. The cw spectroscopy results are included as Appendix A in a paper entitled, "Computer Determination of Acoustic Parameters for Multilayered Structure Using cw Spectroscopy".

Table I in Appendix A gives an overall summary of the procedure used to extract the acoustic parameters and Table II shows the data flow for the computer program for the layered structures. Appendix B contains the

listing of the fit program used to extract the physical parameters of the inner layer.

SECTION III
MEASUREMENT OF CRACKS USING THE DOPPLER EFFECT

There has been considerable interest in the nondestructive detection and measurement of radial cracks under bolt holes of wing fasteners. For detection of these cracks, conventional pulse-echo ultrasonic techniques are usually employed. In general, methods for measurement of the size of cracks have depended upon echo duration from the crack or upon the attenuation of the ultrasound wave across the crack. It will be demonstrated in this section that for special geometries such as the radial cracks emanating from the bolt hole at the faying surface on the inner layer of an adhesively bonded structure, crack size can be measured using the Doppler effect. A sample having a radial crack is mounted on a rotating platform in a water bath and interrogated using a train of tone bursts from a stationary, focused transducer. The Doppler-shift spectrum of the backscattered ultrasonic beam from the rotating crack is recorded. The maximum Doppler shift is then related to the radial size of the crack. Paper describing the Doppler studies of cracks is included as Appendix C.

SECTION IV
PSEUDORANDOM-SIGNAL-CORRELATION SYSTEM

Detailed information on a pseudorandom-signal-correlation system designed and built under this program (including a logic description), on the experimental efforts with the system, and on the experimental results can be found in the papers which appear as Appendix D of this report.

This section contains a brief discussion of a cw pseudorandom-signal-correlation system for which the preliminary design is now complete. It is expected that future work on this system will give new insight into ultrasonic pseudorandom-signal correlation.

CW PSEUDORANDOM-SIGNAL-CORRELATION SYSTEM (DISCUSSION OF A PRELIMINARY DESIGN)

The pseudorandom-signal-correlation system discussed in detail in Appendix D may be characterized as a "burst-type" system. Since the bursts are subsequences of a longer sequence, they *do not have the desirable correlation properties* of a continuously transmitted complete m-sequence. Correlation of these truncated m-sequences produces range sidelobes. In the burst-type system, the magnitude of the range sidelobes is reduced by an averaging technique which consists of transmitting many bursts per correlation point. The increased signal-acquisition time inherent in this averaging technique is the price which must be paid for the advantages of a burst-type system. These advantages include the capability of using a single transducer for both transmitting and receiving and the fine control over burst length which is inherent in the burst-generation method used.

In applications where two-transducer operation is feasible, a pseudorandom-signal-correlation system which continuously transmits a complete m-sequence--a "cw" system--offers certain advantages over the burst-type system. The auto-correlation of a complete N-bit m-sequence produces a periodic waveform which consists of triangular pulses spaced N bits apart and a non-zero constant level elsewhere. For a sequence having

the binary values of +1 and -1, the pulses will be N units high and the constant level will be -1 units. (The pulse will be two bits wide at its base, regardless of sequence length.) These auto-correlation properties imply that range sidelobes are not produced in a cw system and that for any sequence length which does not produce range ambiguity, the cw system can transmit more energy to the target than the burst-type system. (Range ambiguity results when all discernible signals are not received before the m-sequence begins to repeat itself.)

The preliminary design of the cw pseudorandom-signal-correlation system was completed during this program. This system is intended for use in experimental investigations to determine how well a practical system of this type would conform to the theoretical ideal performance and how such a system could be applied to actual NDE problems.

The cw pseudorandom-signal-correlation system will be a flexible laboratory instrument incorporating the following major features:

(1) Capable of correlation and auto-correlation using N-bit m-sequences (of length $2^N - 1$, N being a positive non-zero integer) up to N = 20.

(2) Possessing two basic correlation modes:

(a) "True" continuous correlation where the correlation process continues until a halt command is given.

(b) Delayed correlation over a preset number of correlation points. In this case, transmission starts on command, but the reference sequence is gated off for a preset delay interval. At the end of this delay, both the reference and transmitter sequence generators run for a preset number of correlation points after which the entire cycle is repeated.

16

In either of the above correlation modes, a correlation point is defined as R periods of the m-sequence. R is a presettable integer and is analogous to "repetitions per correlation point" in the burst-type system. The repetitions are not used in the cw system to reduce sidelobes but to control the correlation "speed." Just as in the burst-type system, correlation speed determines the bandwidth of the correlator output.

The cw system algorithmic design is essentially complete. Since this is the crucial part of the design, any anticipated changes (except for very minor ones) in system operation should be made before proceeding. The algorithm is now being reviewed with this in mind. Future work will involve completing the review and translating the algorithmic-state machine chart into logic diagrams and then into hardware.

SECTION V
CONCLUSIONS AND FUTURE WORK

CONCLUSIONS

cw Spectroscopy

A swept-frequency, continuous-wave ultrasound technique for determining longitudinal-mode acoustic parameters in multi-layered structures has been developed. A computer program performs a nonlinear curve fit of theroretical to experimental frequency spectra. A theoretical model of layered structures derived by Brekhovskikh[1] and programmed in Fortran is used for this purpose. A computer FIT program iteratively computes the wave speed and frequency-dependent attenuation within a given layer. Although all of the <u>outer</u>-layer-parameter values must be known, characterization of the inner layer requires knowledge only of the thickness and density.

Three-layer aluminum/sealant/aluminum sandwiches, a one-layer aluminum plate, and several one-layer epoxy-resin plates have been characterized using this technique. The resultant theoretical frequency spectra nearly duplicated the experimentally determined spectra in most cases. Figures 3-5 in Appendix A (dashed curves) illustrate the FIT program output for one of the three-layer samples.

Comparison of the epoxy-resin results with independent tone-burst attenuation results suggests that the computed values for attenuation are within ± 0.5 nepers/cm of the actual values at 10 MHz (broadband 10-MHz transducers were employed). Two different thicknesses of a standard commercial sealant (RTV) used as the inner layer of three-layer aluminum plate sandwiches were evaluated. The computed values for attenuation per centimeter varied by only 0.3 nepers.

Computed wave speeds were within 3% of those measured for the epoxy-resin samples by the tone burst technique. The computed wave speeds for the sealant used were up to 9% higher than the measured values. This discrepancy is probably due to error in measuring the thickness of the inner sealant layer.

A major result of cw spectroscopy was the development of a versatile computer program for determining acoustic parameters for a variety of layered structures. This program permits the calculation of the ultrasonic attenuation of a given layer in a three-layer sandwich structure directly from the experimental frequency spectrum of that structure. It is hoped that this unique ability will aid in the detection of sealant and adhesive bond degradation in layered structures.

The following conclusions have been reached as a result of this study:

- The knowledge of either the wave speed or thickness of inner layer demands some a priori knowledge of the properties of this layer. Hence, this technique cannot be applied to an unknown sealant.

- The attenuation as determined by the above technique for the single-layer epoxy-resin samples increased with aging of the samples. This was confirmed independently by the tone-burst method. It could be inferred from this that the periodic determination of the attenuation for the inner layer of a multilayer structure may give an indication of the degradation or the mechanical integrity of the bond.

- It proved to be impractical to utilize real Air Force sealants in the present study due to their high attenuation. A commercial, silicon-based sealant (RTV) was substituted because of its ease of use and much lower

attenuation. Since the aluminum/sealant/aluminum sandwiches were immersed in a water bath, the aluminum-water impedance mismatch created another source of signal loss. The use of impedance-matching techniques--particular when real sealants are to be characterized--could prove to be necessary in overcoming this problem.

- The choice of the Simplex Method[11] to perform the nonlinear curve fit proved to be very advantageous. The method is ideally suited for the complex and (nearly) intractable Brekovskikh Model. No additional subroutines are required to invert matrices or to determine derivations. As currently implemented, the program can handle up to 100 parameters with the user having freedom to vary or fix those as desired. This flexibility was invaluable in evaluating the technique.

Measurement of Crack Size

As shown in Section III, it is indeed possible to measure the radial size of the cracks under bolt holes both in single- and multi-layer mechanically fastened aircraft wing structures. The accuracy of the present method is better than 20%. In the presence of multiple radial cracks or nonradial cracks, the method can measure only the maximum radial extent. However, this is sufficient since with knowledge of the radial extension of the crack, the bolt hole can be reamed with an over-size reamer and a crack can be repaired before it reaches a critical size.

Since the size of the radial crack is computed from the frequency shift and not from the amplitude of the backscattered ultrasound, the method is applicable for measuring radial cracks in the third layer in a multiple-layer aircraft structure. The method can be used in the field by employing a rotating transducer. The sound is coupled to the test sample through water in a boot capping the transducer. Results were similar to those obtained by rotating the disk in water.

40

Ultrasonic Pseudorandom-Signal-Correlation System

The experimental characterization of the Ultrasonic Pseudorandom-Signal-Correlation System (UPSC system) has shown that such a system can produce results comparable to those obtained with a random signal-correlation system. The UPSC system has better range resolution than a random-signal system which makes use of a narrow-band variable delay line. However, a high system clock rate is required to generate and control the wide bandwidth pseudo-noise bursts needed for good range resolution. Furthermore, the signal-to-noise ratio improvement gained with the UPSC system is obtained at the expense of long signal-acquisition times.

FUTURE WORK

Research should be initiated on the special case of a three-layer structure where two matching pieces of metal are separated by a thin liquid layer. This type of structure may improve efficiency in nondestructive inspection of cast, "near-net-shape" components such as turbine disks which contain topologically complex features which are difficult to scan in a typical water-tank inspection device. It is hoped that a matching part to the turbine disk, for instance, would limit the diffraction and focusing effects of the water-metal interface by decreasing the path length of ultrasound in water. In the final limit of an infinitesimally thin water layer, the component to be inspected should be seen only as an interior region of a larger, but topologically simpler, structure.

Initially a comparison should be made between theoretically predicted losses due to thin water interfaces at various angles and thicknesses and losses observed experimentally. Figure 1 illustrates the transmission and reflection coefficients of a 5-mil-thick aluminum/water/aluminum interface.

A proof-of-principal device to test the matching-shape hypothesis has been constructed and used with encouraging results. Figure 2 illustrates this device which consists of a cylindrical well within an aluminum cube. An

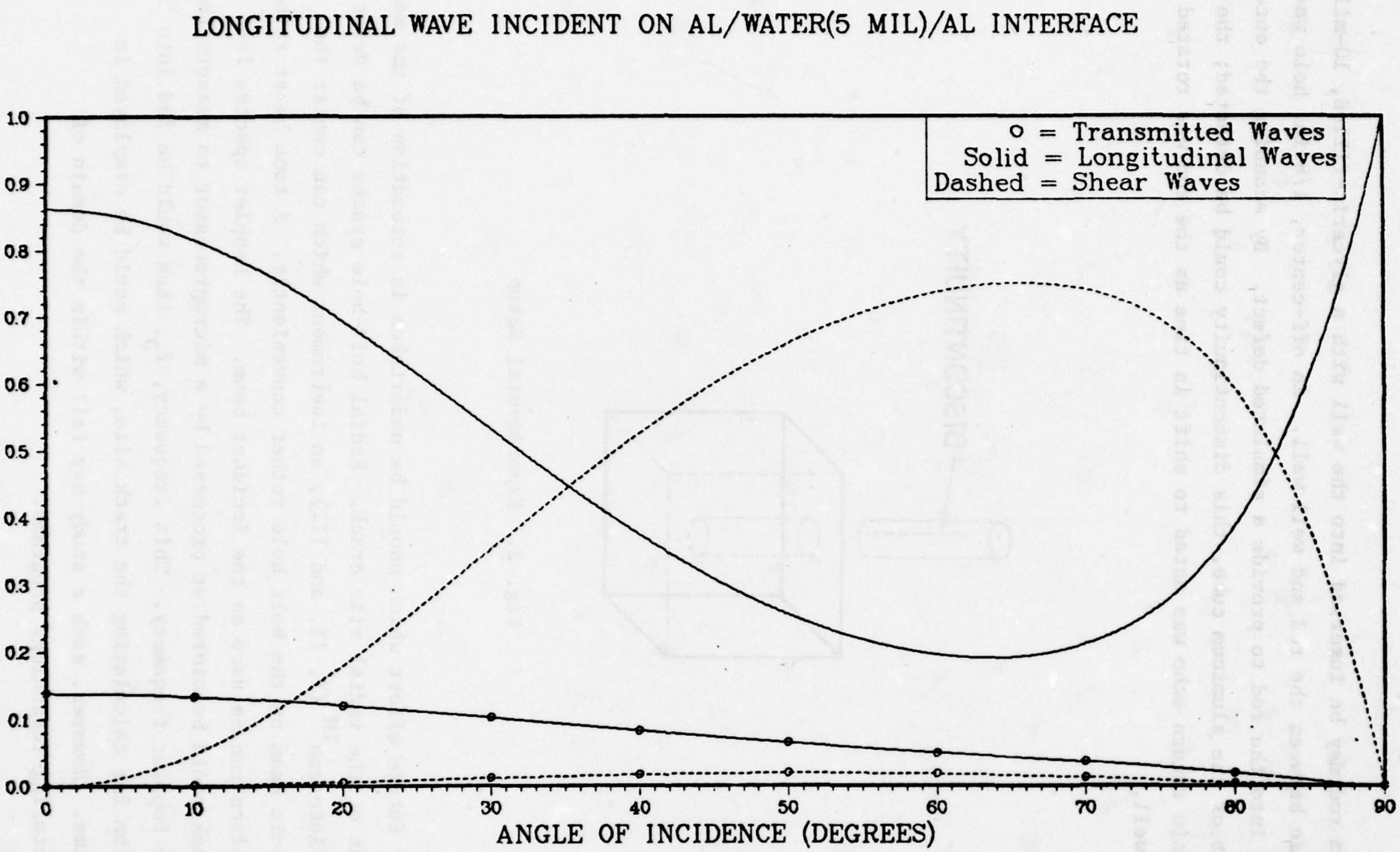

Fig. 1. **Plot of Transmission and Reflection Coefficients for Longitudinal and Shear Waves as a Function of Angle of Incidence**

aluminum rod may be inserted into the well with a glycerin-filled, 10-mil clearance between the rod and well wall. An off-center, 1/8-in. hole was drilled into the rod to provide a simulated defect. By scanning the outer surfaces of the aluminum cube, this discontinuity could be detected; the ultrasonic return echo was noted to shift in time as the rod was rotated in the well.

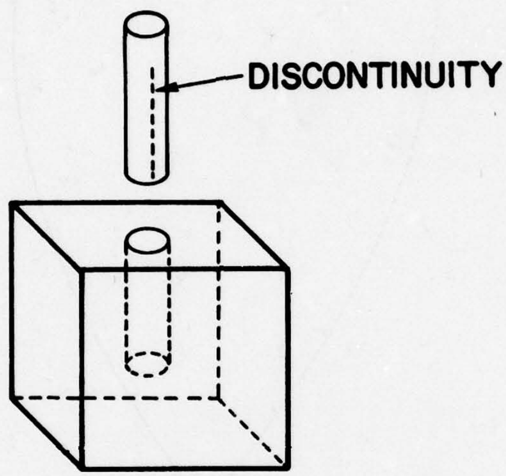

Fig. 2. Experimental Setup

Another future effort which should be undertaken is automation of the measurement of the radial size crack. Radial bolt-hole cracks can be detected by the Autoscan™ (I, II, and III), an instrument which can center the ultrasonic beam on the bolt hole rather conveniently. A tone burst rather than pulses can be used as the incident beam. The Doppler spectra from the crack could be stored or processed by a microprocessor to measure the maximum Doppler frequency. This frequency, f_D, then would be fed into the alogrithm for calculating the crack size, which could be displayed in real time. However, such a study may fall within the domain of Manufacturing-Technology programs.

A high clock rate for the UPSC system could be obtained by using emitter-coupled logic (ECL), while the signal acquisition time could be improved by using parallel processing with multiple correlators. These two system improvements might be the subject of future work on the UPSC system. Future work on pseudorandom signal-correlation systems should also include the completion of the design, fabrication, and experimental evaluation of the cw pseudorandom signal correlation system.

REFERENCES

1. L. M. Brekhovskikh, Waves in Layered Media, (New York: Academic Press, 1960).

2. J. M. Raney, C. M. Elias, and N. K. Batra, "Study of Adhesively Bonded Layered Structures using cw Acoustic Spectroscopy," Interim Technical Report under AF Contract F33615-77-C-5022 for period 1 December 1976 through 1 January 1978. (Systems Research Laboratories, Inc., Dayton, OH, 1978).

3. E. S. Ferguson, V. L. Newhouse, N. M. Bilgutay, and G. R. Cooper, "Application of Random Signal Correlation Techniques to Ultrasonic Flaw Detection," Ultrasonics 13, 11 (January 1975).

4. O. R. Gericke, Paper No. 1 in The Future of Ultrasonic Spectroscopy, (ed., P. M. Reynolds) (British Nonferrous Metals Research Association, London, 1971).

5. B. G. W. Yee, F. H. Chang, and J. C. Couchman, "Applications of Ultrasonic Inteference Spectroscopy to Materials and Flaw Characterization," Materials Evaluation 23, 193 (August 1975).

6. E. P. Papadakis, "Ultrasonic Impulse-Induced-Resonance Utilizing Damping for Adhesive Disbond Detection," Materials Evaluation 3, 37 (February 1978).

7. G. A. Alers, P. L. Flynn, and M. J. Buckley, "Ultrasonic Techniques for Measuring the Strength of Adhesive Bonds," Materials Evaluation 35, 77 (April 1977).

8. E. P. Papadakis, K. A. Fowler, and L. C. Lynnworth, "Ultrasonic Attenuation by Spectrum Analysis of Pulses in Buffer Rods," J. Acous. Soc. Am. 53, 1336 (1973).

9. D. L. Folds and L. D. Loggins, "Transmission and Reflection of Ultrasonic Waves in Layered Media," J. Acoust. Soc. Am. 62, 1102 (November 1977).

10. M. J. Buckley and J. M. Raney, "The Use of Continuous-Wave Ultrasonic Spectroscopy for Adhesive-Bond Evaluation," in Proceedings of the ARPA/AFML Review of Progress in Quantitative NDE, Technical Report AFML-TR-77-44 (Air Force Materials Laboratory, Wright-Patterson Air Force Base, OH, September 1977).

11. J. A. Nelder and R. Mead, "A Simplex Method for Function Minimization," Comp. J. 7, 308 (1965).

APPENDIX A

CW SPECTROSCOPY STUDIES

Table 1

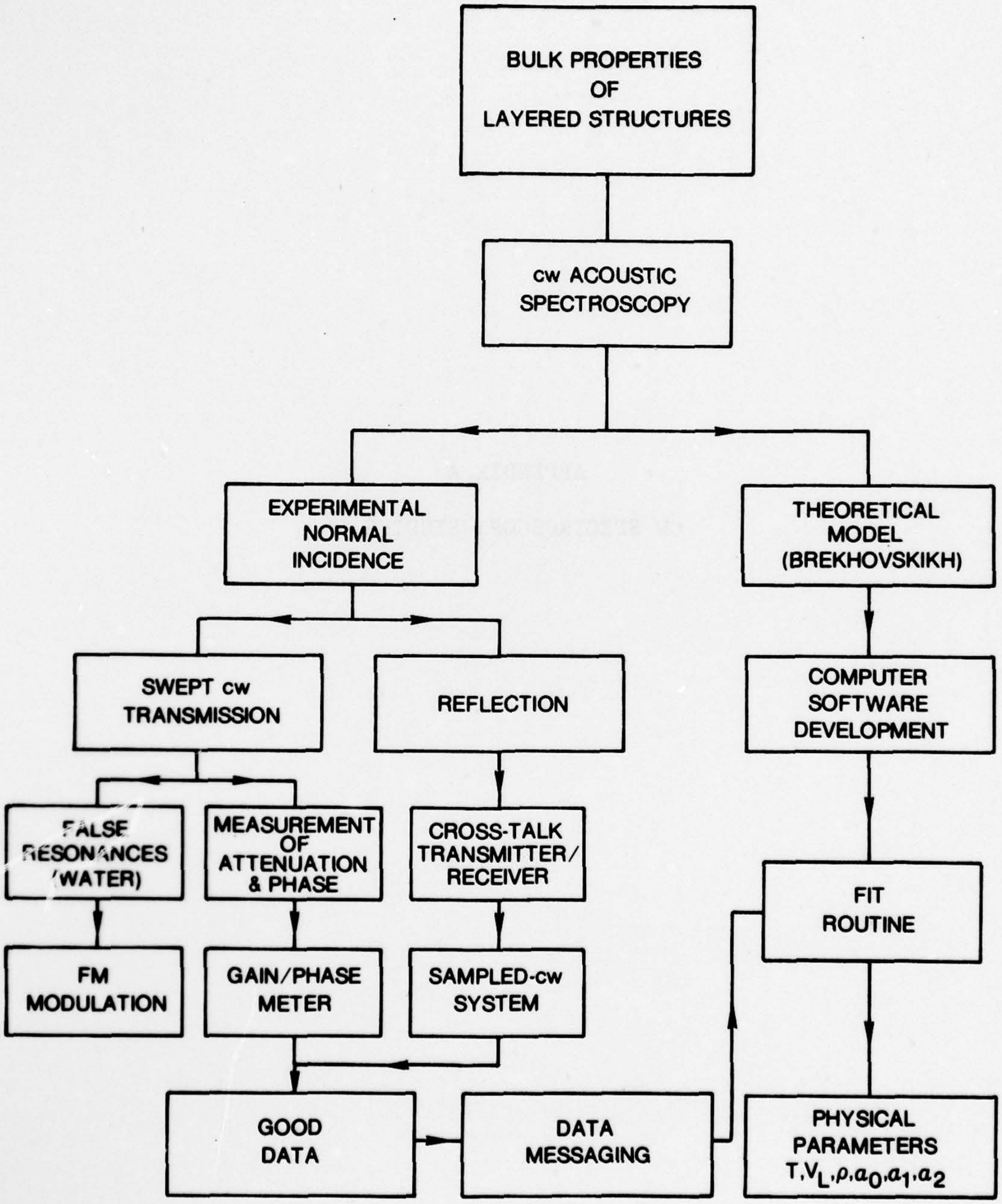
BULK PROPERTIES OF LAYERED STRUCTURES
cw ACOUSTIC SPECTROSCOPY
EXPERIMENTAL NORMAL INCIDENCE
THEORETICAL MODEL (BREKHOVSKIKH)
SWEPT cw TRANSMISSION
REFLECTION
COMPUTER SOFTWARE DEVELOPMENT
FALSE RESONANCES (WATER)
MEASUREMENT OF ATTENUATION & PHASE
CROSS-TALK TRANSMITTER/RECEIVER
FIT ROUTINE
FM MODULATION
GAIN/PHASE METER
SAMPLED-cw SYSTEM
GOOD DATA
DATA MESSAGING
PHYSICAL PARAMETERS
$T, V_L, \rho, a_0, a_1, a_2$

Table 2

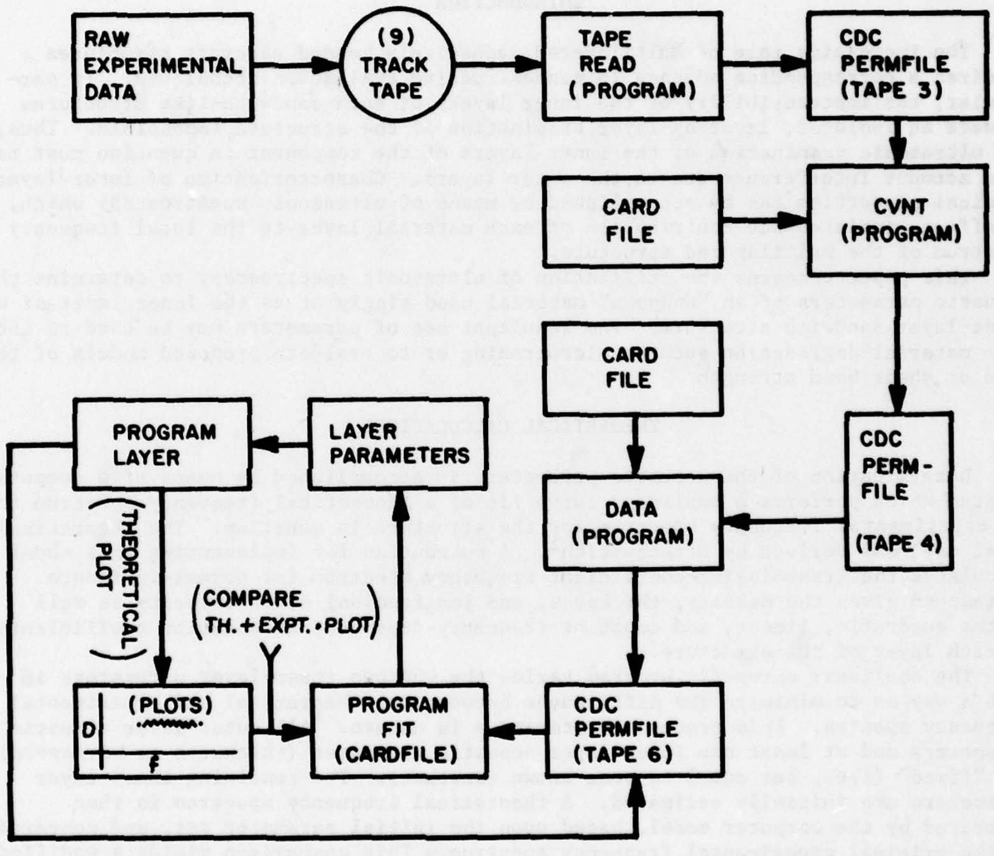
RAW EXPERIMENTAL DATA
(9) TRACK TAPE
TAPE READ (PROGRAM)
CDC PERMFILE (TAPE 3)
CARD FILE
CVNT (PROGRAM)
CARD FILE
CDC PERM-FILE (TAPE 4)
DATA (PROGRAM)
PROGRAM LAYER
LAYER PARAMETERS
(THEORETICAL PLOT)
(COMPARE TH. + EXPT. PLOT)
(PLOTS)
D
f
PROGRAM FIT (CARDFILE)
CDC PERMFILE (TAPE 6)

Published in Paper Summaries, National Fall Conference, American Society for Nondestructive Testing, Oct. 15 - 18, 1979, St. Louis (American Society for Nondestructive Testing, Columbus, OH, 1979), pp. 268-274.

COMPUTER DETERMINATION OF ACOUSTIC PARAMETERS FOR MULTILAYERED STRUCTURES USING CW ULTRASONIC SPECTROSCOPY*

J. S. Leffler and N. K. Batra
Systems Research Laboratories, Inc.
Dayton, OH

INTRODUCTION

The increasing role of multilayered, adhesively bonded aircraft structures requires a corresponding advance in nondestructive evaluation techniques. In particular, the inaccessibility of the inner layers of such sandwich-like structures renders an isolated, layer-by-layer examination of the structure impossible. Thus, any ultrasonic examination of the inner layers of the component in question must take into account interference due to the outer layers. Characterization of inner-layer physical properties can be accomplished by means of ultrasonic spectroscopy which, in effect, isolates the contribution of each material layer to the total frequency spectrum of the multilayered structure.

This paper concerns the utilization of ultrasonic spectroscopy to determine the acoustic parameters of an "unknown" material used singly or as the inner layer of a three-layer sandwich structure. The resultant set of parameters may be used to indicate material degradation such as microcrazing or to evaluate proposed models of tensile or shear bond strength.

THEORETICAL CALCULATIONS

Determination of the acoustic parameters is accomplished by means of a computer program which performs a nonlinear curve fit of a theoretical frequency spectrum to the experimental frequency spectrum for the structure in question. The theoretical model used was derived by Brekhovskikh[1]. A subroutine for implementing this model calculates the transmission-coefficient frequency spectrum for normal-incidence ultrasound given the density, thickness, and longitudinal sound velocity as well as the quadratic, linear, and constant frequency-dependent attenuation coefficients of each layer of the structure.

The nonlinear curve-fit program varies the unknown inner-layer parameters in such a way as to minimize the differences between the theoretical and experimental frequency spectra. This process is iterative in nature. All outer-layer acoustic parameters and at least one inner-layer acoustic parameter (thickness or wavespeed) are "fixed" (i.e., set equal to some known constant). The remaining inner-layer parameters are initially estimated. A theoretical frequency spectrum is then generated by the computer model, based upon the initial parameter set, and compared to the original experimental frequency spectrum. This comparison yields a modified chi-squared value which is related to the "closeness-of-fit" of the two spectra. The nonlinear fit program makes use of this chi-squared value as a guide in generating a new parameter set which will better fit the experimental results. The computer model utilizes the new parameter set in calculating another theoretical frequency spectrum, and the iteration continues until the best chi-squared fit is achieved. The acoustic parameters for the inner layer of the structure are then given by the last iterated parameter set.

*Work supported under U.S. Air Force Contract No. F33615-77-C-5022.

EXPERIMENTAL PROCEDURE

The experimental set-up is illustrated in Figure 1. A digital synthesizer is swept in frequency (0-20 MHz) by a 1024-channel signal averager. The output sine wave is fed to an immersion transducer and to the reference input of a gain/phase meter. The incident ultrasound is coupled through water to the sample at normal incidence setting up standing-wave resonances at certain frequencies. The ultrasound transmitted through the sample is received by a second transducer and compared to the reference signal by the gain/phase meter. An analog output which can selectively represent either the relative attenuation (in dB) or the phase change (in degrees) of the transmitted versus the incident signal is digitized by the signal averager and stored on magnetic tape.

Figure 2 shows a three-layer sample spectra which has been deconvolved to eliminate the effects of the particular transducers or equipment used. The peaks correspond to standing-wave resonances induced in the three material layers.

RESULTS

Three-layer structures (aluminum/sealant/aluminum) (see Figures 3-5) and several one-layer epoxy-resin plates (Figures 6-7) have been characterized using the computer program. Each figure contains a table giving the complete acoustic parameter set for that sample. T, ρ, and C represent thickness (cm), density (gm/cc), and longitudinal wave velocity, respectively. The total frequency-dependent longitudinal attentuation is given by

$$\alpha(\omega) = C2 \cdot \omega^2 + C1 \cdot \omega + C\emptyset ,$$

where C2, C1, and CØ are the quadratic, linear, and constant attenuation coefficients, respectively. (The shear-mode parameters, B, B2, B1, and BØ in the figures were not used in this longitudinal wave study and were set equal to zero.) Since the first- and third-layer aluminum plates were identical, parameters are specified for the first layer only. In the lower section of each figure, FMIN and FMAX denote the frequency range of interest and WN(2) is a scale factor normally set equal to one. Theoretical and experimental spectra are signified by dashed and solid lines, respectively.

Three-Layer Structures

Figure 3 shows the theoretical frequency spectrum derived from the initial parameter estimation for a particular three-layer structure. The theoretical spectrum based upon computer-derived acoustic parameters for that same structure is shown in Figure 4. The value of chi-squared goes from 16.1 in Figure 3 to 2.21 in Figure 4, which reflects a much better agreement between the theoretical and experimental spectra in the latter plot. Figure 5 shows computer-determined acoustic parameters for a similar sandwich structure but one having a "double-thick" inner layer (sealant). The constant attenuation coefficient, CØ, computed for the sealant (same type in both samples) was 2.03 nepers/cm in Figure 5 and 1.89 nepers/cm in Figure 4. This close agreement tends to validate the procedure for determining inner-layer parameters.

Single-Layer Structures

Single-layer epoxy-resin samples which had been hydrothermally spiked to create scattering centers were studied to determine the effect of sample degradation upon the attenuation of ultrasound. Figures 6 and 7 show the computer-determined

30

attenuation parameters (C2, C1, and CØ) for both unaged and aged (hydrothermally, 318 days) cases. Notice the quadratic frequency dependence of the attenuation in both cases. A comparison of typical nonlinear-fit-program results with those from an independent analysis using a tone-burst method is shown in Table 1. It should be pointed out that the attenuation increases with aging.

SUMMARY

Continuous-wave ultrasonic spectroscopy indeed provides a tool for the characterization of the inner layer of multilayered structures. Through the use of a computer curve-fit technique and a suitable theoretical model, acoustic parameters can be determined from analysis of experimental frequency spectra. The determined parameters can be used to characterize the layered structure.

TABLE 1

ATTENUATION RESULTS FOR EPOXY-RESIN SAMPLES

$$\alpha = C2\cdot\omega^2 + C1\cdot\omega + C\emptyset \text{ (nepers/cm)}$$

	C2	C1	CØ	α (10 MHz)
Unaged				
Tone Burst	-0.127×10^{-15}	0.517×10^{-7}	0.043	3.00
Fit Program	-0.066×10^{-15}	0.464×10^{-7}	0.056	2.71
Partially Aged*				
Tone Burst	-0.134×10^{-15}	0.606×10^{-7}	0.258	3.45
Fit Program	-0.051×10^{-15}	0.570×10^{-7}	0.045	3.42
Fully Aged**				
Tone Burst	-0.216×10^{-15}	0.928×10^{-7}	0.488	5.18
Fit Program	-0.202×10^{-15}	0.866×10^{-7}	0.037	4.68

*Hydrothermally spiked for 37 days.

**Hydrothermally spiked for 463 days.

REFERENCES

1. Brekhovskikh, L.M., Waves in Layered Media, New York: Academic Press, 1960.

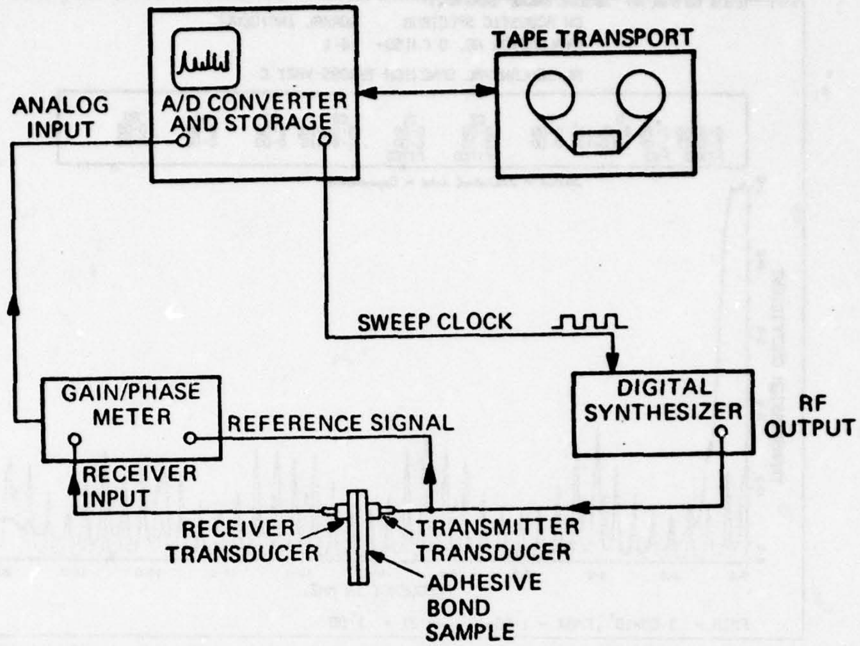

FIGURE 1--CW ultrasonic spectroscopy experimental arrangement.

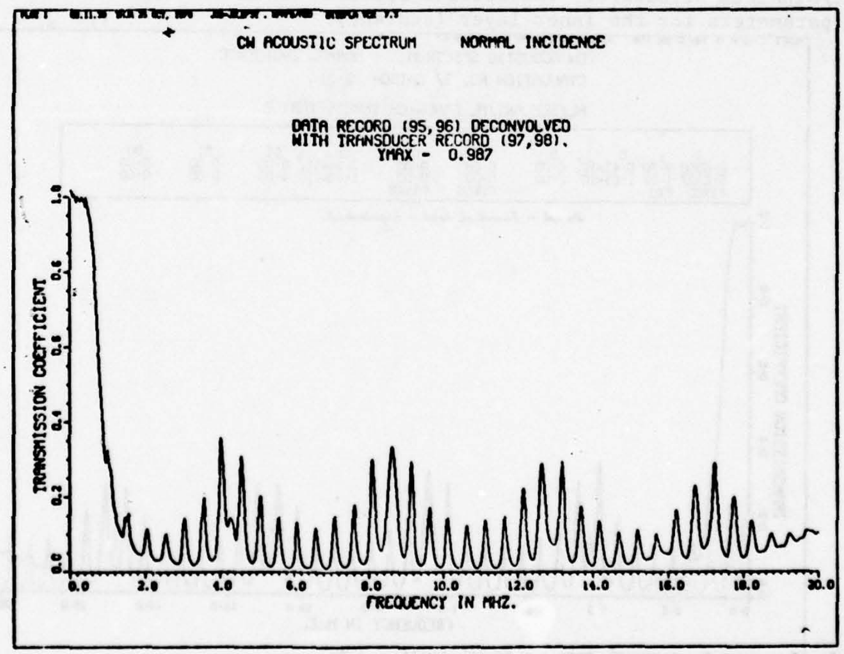

FIGURE 2--Deconvolved experimental frequency spectrum for three-layer aluminum/ sealant/aluminum structure.

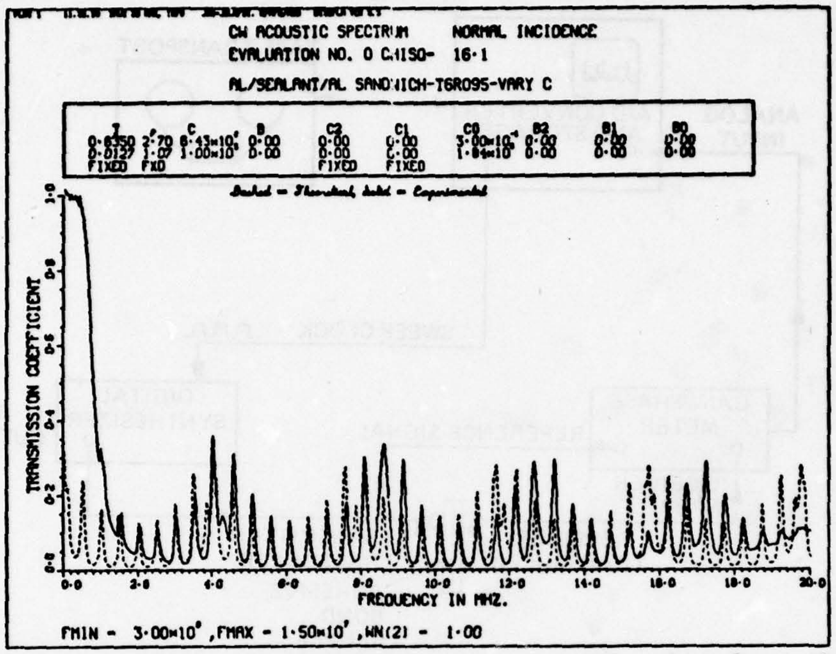

FIGURE 3--Theoretical and experimental frequency spectra for three-layer aluminum/sealant/aluminum structure. Theoretical spectrum is based upon initial estimates of the parameters for the inner layer (sealant).

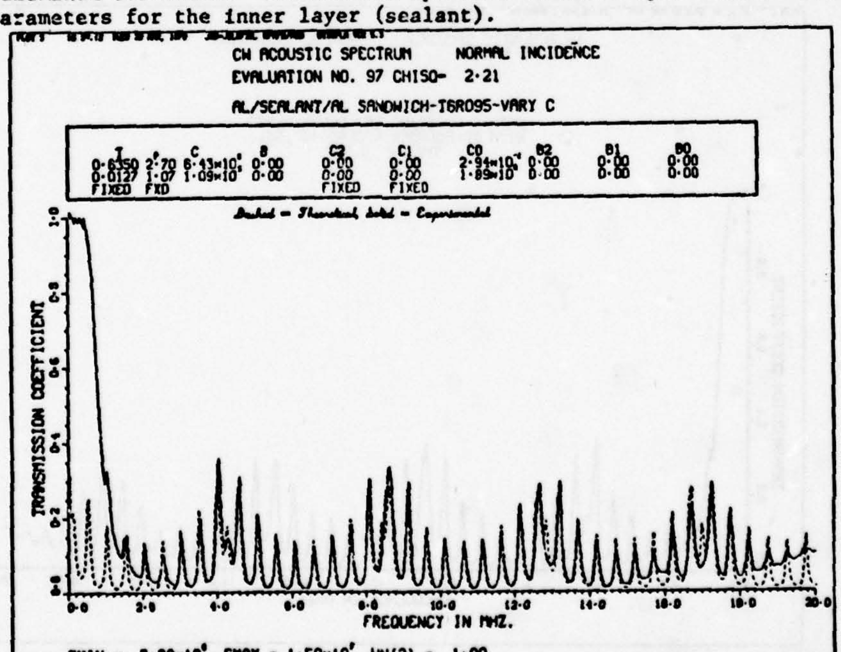

FIGURE 4--Comparison of theoretical spectrum (based upon computer-determined acoustic parameters for sealant) and experimental data of Figure 2.

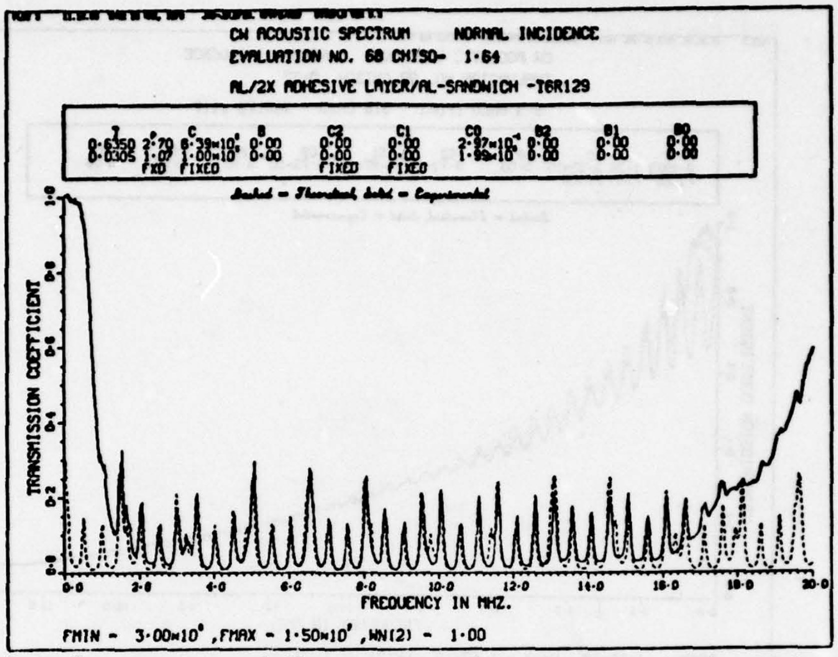

FIGURE 5--Data for structure similar to Figure 4 but having a double thickness of sealant.

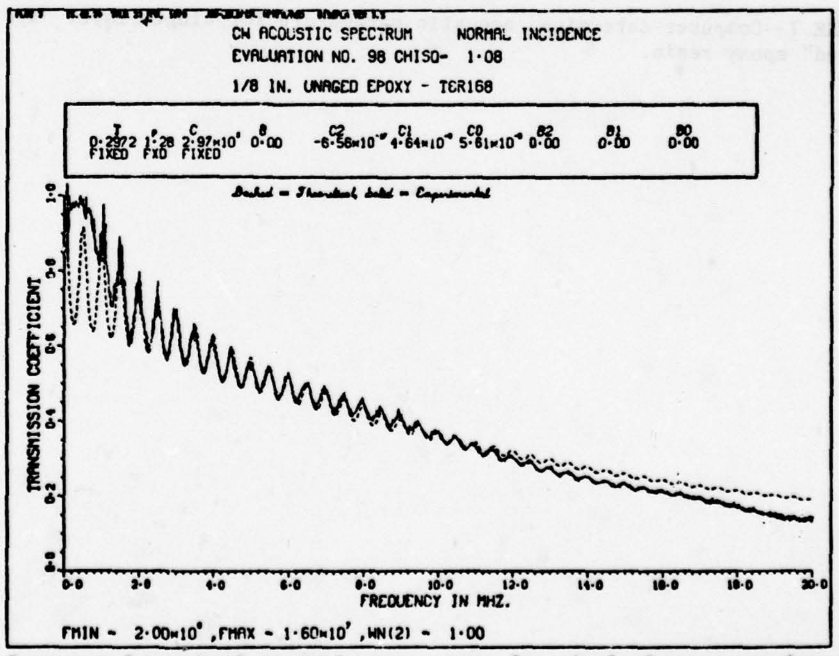

FIGURE 6--Computer-determined acoustic parameters for single-layer unaged epoxy resin.

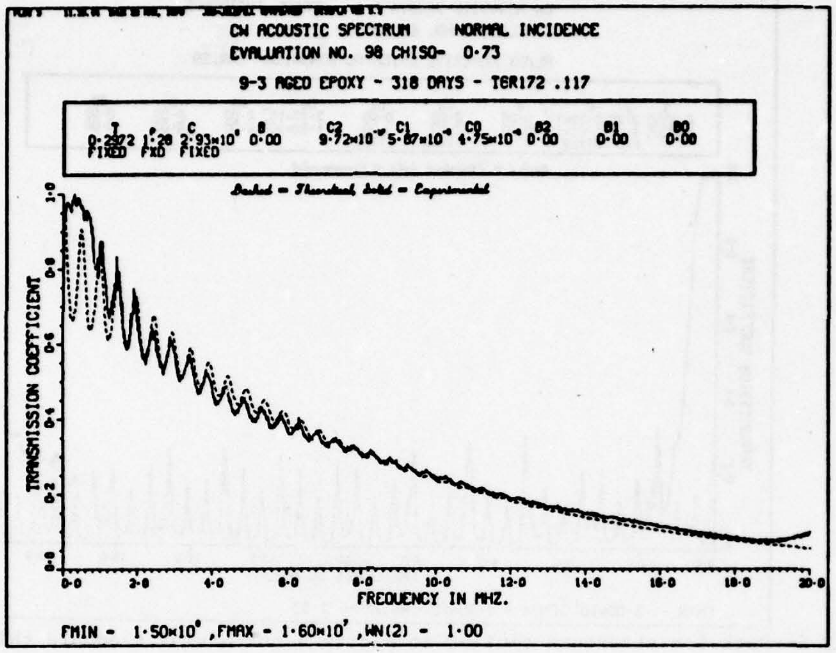

FIGURE 7--Computer-determined acoustic parameters for single-layer "hydrothermally spiked" epoxy resin.

APPENDIX B

COMPUTER PROGRAMS

```
      PROGRAM FIT(INPUT,OUTPUT,TAPE6,DEBUG=OUTPUT,PLFILE=0)
      COMMON/FIT1/NPTS,NPAR,YD(1050),WD(1050),PZ(100),TD(1050)
      COMMON /FITB/ FMIN,FMAX,ITITLE(5)
      COMMON /FITC/ IPD(100),IPSWCH
      COMMON /FITD/ B(2),B2(2),B1(2),B0(2)
      COMMON/STEPIT/NV,NTRACE,CHISQ,MASK(100),
     1               X(100),DELTAX(100),DELMIN(100),NF
      COMMON /BEST/ BX(100),NFBEST,NRPBST,BCHISQ
      COMMON /CONSTS/ NPLN,NPLSW,NPINT,NEVAL
      EXTERNAL FCN
      IPSWCH = 1
C     PLOT EXPERIMENTAL CURVE?
C     NPLWS = 0 ; PLOT THEORETICAL & EXPERIMENTAL
C     NPLSW = 2 ; PLOT ONLY THEORETICAL
      NPLSW = 0
C     LIMIT # OF EVALUATIONS
      NEVAL=99
C     PLOT EVERY 50 EVALUATIONS
      NPINT = 50
C
C     SET UP FOR BEST FIT
      BCHISQ = 1.0E20
      NF = 0
C     NORMAL INCIDENCE ONLY
      DO 7 I = 1,2
      B(I) = 0.0
      B2(I) = 0.0
      B1(I) = 0.0
      B0(I) = 0.0
    7 CONTINUE
C
C     ******************************************************************
C     *                                                                *
C     *          FFFF  IIII  TTTT                                      *
C     *          F      II    TT                                       *
C     *          FFFF   II    TT                                       *
C     *          F     IIII   TT                                       *
C     *                                                                *
C     ******************************************************************
C     *                                                                *
C     *   THIS PROGRAM WILL ACCEPT EXPERIMENTAL OR THEORETICAL DATA IN *
C     * FILE TAPE6 ALONG WITH KNOWN AND "GUESSTIMATED" PARAMETERS FOR  *
C     * A THREE LAYER METAL-BOND-METAL SYSTEM AND ATTEMPT TO FIT THE   *
C     * UNKNOWN PARAMETERS TO THE DATA.                                *
C     *                                                                *
C     *----------------------------------------------------------------*
C     *                                                                *
C     *   FOR THE THREE LAYER SYSTEM, 12 PARAMETERS ARE INPUTTED AND   *
C     * STORED IN THE PZ ARRAY BY THE INDATA SUBROUTINE AS FOLLOWS:    *
C     *                                                                *
C     *   PZ( 1) = T(1) - THICKNESS OF FIRST LAYER (CM).               *
C     *   PZ( 2) = T(2) - THICKNESS OF SECOND (MIDDLE) LAYER (CM).     *
C     *   PZ( 3) = C(1) - VELOCITY OF SOUND IN FIRST LAYER (CM/SEC).   *
C     *   PZ( 4) = C(2) - VELOCITY OF SOUND IN SECOND LAYER (CM/SEC).  *
C     *   PZ( 5) = R(1) - RELATIVE DENSITY OF FIRST LAYER.             *
C     *   PZ( 6) = R(2) - RELATIVE DENSITY OF SECOND LAYER.            *
C     *   PZ( 7) =A2(1) - OMEGA SQUARED LONGITUDINAL ATTENUATION       *
```

```
C        *                   COEFFICIENT FOR FIRST LAYER.                  *
C        *  PZ( 8) =A2(2) -  OMEGA SQUARED LONGITUDINAL ATTENUATION         *
C        *                   COEFFICIENT FOR SECOND LAYER.                 *
C        *  PZ( 9) =A1(1) -  OMEGA LONGITUDINAL ATTENUATION COEFFICIENT    *
C        *                   FOR FIRST LAYER.                              *
C        *  PZ(10) =A1(2) -  OMEGA LONGITUDINAL ATTENUATION COEFFICIENT    *
C        *                   FOR SECOND LAYER.                             *
C        *  PZ(11) =A0(1) -  CONSTANT LONGITUDINAL ATTENUATION TERM FOR    *
C        *                   FIRST LAYER.                                  *
C        *  PZ(12) =A0(1) -  CONSTANT LONGITUDINAL ATTENUATION TERM FOR    *
C        *                   SECOND LAYER.                                 *
C        *                                                                 *
C        *  THE THIRD LAYER IS ASSUMED TO BE IDENTICAL TO THE FIRST.       *
C        *                                                                 *
C        *-----------------------------------------------------------------*
C        *                                                                 *
C        *  MASK(I) INDICATES WHETHER OR NOT THE I'TH PARAMETER IS KNOWN.  *
C        *  IF MASK(I)=1, THE I'TH PARAMETER IS DETERMINED AND MAY NOT BE  *
C        *  VARIED IN ORDER TO OBTAIN A FIT. IF MASK(I)=0, THE I'TH        *
C        *  PARAMETER IS UNKNOWN AND REPRESENTS A "GUESSTIMATE" WHICH MAY  *
C        *  BE VARIED WHILE OBTAINING A FIT TO THE DATA.                   *
C        *                                                                 *
C        *-----------------------------------------------------------------*
C
C        *-----------------------------------------------------------------*
C        *                                                                 *
C        *     THE YD ARRAY CONTAINS THE REAL PART OF THE COMPLEX          *
C        *  TRANSMISSION FUNCTION ARRAY READ IN FROM FILE TAPE6 IN         *
C        *  SUBROUTINE INDATA. THIS FILE IS PRODUCED FROM EXPERIMENTAL DATA*
C        *  BY THE DATA PROGRAM OR FROM A THEORETICAL MODEL BY THE LAYER   *
C        *  PROGRAM.  EACH CHOICE OF PARAMETERS LEADS TO A THEORETICAL     *
C        *  COMPLEX TRANSMISSION FUNCTION WHICH IS COMPARED TO YD IN ORDER *
C        *  TO SURMISE THE CLOSENESS OF THE FIT. THIS IS DONE BY THE       *
C        *  FCN SUBROUTINE.                                                *
C        *-----------------------------------------------------------------*
C        *                                                                 *
C        *     THE WD ARRAY IS USED AS A WEIGHTING FUNCTION TO FIT THE DATA *
C        *  WITH REGARD TO THE TRANSDUCER RESPONSE. MORE IMPORTANCE IS     *
C        *  GIVEN TO MATCHING THE THEORETICALLY GENERATED TRANSMISSION     *
C        *  FUNCTION WITH THE EXPERIMENTAL TRANSMISSION FUNCTION AT THE    *
C        *  FREQUENCIES WHERE THE TRANSDUCER RESPONSE IS THE GREATEST.     *
C        *                                                                 *
C        *-----------------------------------------------------------------*
C        *                                                                 *
C        *  THE SEARCH SUBROUTINE PERFORMS A NON-LINEAR FUNCTION           *
C        *  MINIMIZATION BY THE USE OF A SIMPLEX METHOD. IT VARIES THE     *
C        *  UNKNOWN PARAMETERS AND CALLS SUBROUTINE FCN TO DETERMINE       *
C        *  THE SUCCESS OF THE LATEST ITERATION BY USE OF A CHI-SQUARED    *
C        *  TEST.                                                          *
C        *******************************************************************
C
C        *******************************************************************
C        *                                                                 *
C        *  VARIABLES                                                      *
C        *******************************************************************
C        *                                                                 *
C        *  NAME   TYPE           FORMAT  DEFINITION.                      *
C        *------  -------------  ------  ---------------------------------*
```

```
C      *                                                                     *
C      *     A0  REAL ARRAY       E10.2 - CONSTANT ATT. TERM IN LAYER         *
C      *     A1  REAL ARRAY       E10.2 - W ATT. COEFFICIENT IN LAYER         *
C      *     A2  REAL ARRAY       E10.2 - W**2 ATT. COEFFICIENT IN LAYER      *
C      *BCHISQ   REAL                   - BEST FIT CHI-SQUARED VALUE          *
C      *     BX  REAL ARRAY       (100) - BEST FIT PARAMETER VALUES           *
C      *      C  REAL ARRAY       E10.2 - VELOCITY OF SOUND IN LAYER (CM/S)*
C      * CHISQ   REAL                   - CHI-SQUARED                         *
C      *      D  COMPLEX ARRAY    E15.5 - TEMPORARY STORAGE,TRANS. FUNCTION*
C      *DELMIN   REAL ARRAY       (100) - SMALLEST STEP SIZE FOR X(I)         *
C      *DELTAF   REAL              FREE - FREQUENCY INCREMENT FOR DATA SET *
C      *DELTAX   REAL ARRAY       (100) - INITIAL STEP SIZE FOR X(I)          *
C      *    DUM  REAL ARRAY             - DUMMY FILLER FOR COMMON STATEMENT*
C      *DUM1-8   REAL ARAAYS            - DUMMY FILLER FOR COMMON STATEMENT*
C      *    EYE  COMPLEX CONST.         - =SQRT(-1)                           *
C      *   FMAX  REAL             E10.2 - MAXIMUM FREQUENCY FOR VALID FIT *
C      *   FMIN  REAL             E10.2 - MINIMUM FREQUENCY FOR VALID FIT *
C      *  FZERO  REAL              FREE - STARTING FREQUENCY FOR DATA SET *
C      *      I  INTEGER                - DO LOOP PARAMETER                   *
C      *    IPD  INTEGER ARRAY    (100) - PEAK (S.W. RESONANCE)  INDICES      *
C      *IPSWCH   INTEGER                - IF =1,UTILIZES DATA PEAKS IN FIT *
C      *ITITLE   INTEGER ARRAY     4A10 - CONTAINS PLOT TITLE                 *
C      *   MASK  INTEGER ARRAY    (100) - FIXED VARIABLE MASK                 *
C      *  NEVAL  INTEGER                - MAX # OF EVALUATIONS                *
C      *     NF  INTEGER                - CURRENT NUMBER OF EVALUATIONS       *
C      * NFBEST   NTEGER                - BEST FIT # OF ITERATIONS            *
C      *   NPAR  INTEGER                - # OF PARAMETERS                     *
C      *  NPAR1  INTEGER                - =NPAR-1, DUMMY VARIABLE             *
C      *  NPINT  INTEGER                - PLOT INTERVAL (#EVAL'S/PLOT)        *
C      *   NPLN  INTEGER                - PLOT NUMBER                         *
C      *  NPLSW  INTEGER                - =2,PLOT ONLY THEORETICAL,0=BOTH *
C      *   NPTS  INTEGER           FREE - NUMBER OF POINTS IN DATA SET        *
C      *NRPBST   INTEGER                - # REJECT PEAKS(FCN)(NOT YET IMPL.*
C      *NTRACE   INTEGER                - =0,NO TRACE; =1,TRACE SEARCH        *
C      *     NV  INTEGER                - # OF PARAMETERS TO BE VARIED        *
C      *                                                                     *
C      ***********************************************************************
C      *---------------------------------------------------------------------*
C
C      *---------------------------------------------------------------------*
C      *  NAME   TYPE            FORMAT  DEFINITION                          *
C      *------   ------------    ------  ------------------------------------*
C      *                                                                     *
C      *     PI  REAL CONSTANT          - =3.14159                            *
C      *     PZ  REAL ARRAY       (100) - CONTAINS INITIAL PARAMETERS         *
C      *      R  REAL ARRAY       E10.2 - RELATIVE DENSITY(RHO) OF LAYER      *
C      *      T  REAL ARRAY       E10.2 - THICKNESS OF LAYER (CM)             *
C      *     TD  REAL ARRAY      (1050) - THEOR. DATA POINTS AT EACH FREQ.    *
C      *     TI  REAL              FREE - ANGLE OF INCIDENCE (DEG.)           *
C      *     WD  REAL ARRAY       (100) - WEIGHTING FUNCTION - T. RESPONSE *
C      *      X  REAL ARRAY       (100) - CONTAINS BEST-FIT COMPUTED PARAMS*
C      * XJUMP   REAL                   - DUMMY VARIABLE = 10%                *
C      *     YD  REAL ARRAY       (100) - REAL (D)-REAL PART OF TRANS. FNC.   *
C      *     Z1  REAL CONSTANT          - IMPEDANCE OF FIRST LIQUID MEDIA *
C      *    ZN1  REAL CONSTANT          - IMPEDANCE OF LAST  LIQUID MEDIA *
C      *                                                                     *
C      ***********************************************************************
C
```



```
C      ***************************************************************************
C      *                                                                         *
C      *                                                                         *
C      *   INPUT DATA CARDS                                                      *
C      *                                                                         *
C      *-------------------------------------------------------------------------*
C      *                                                                         *
C      * CARD #1                                                                 *
C      *   - FIRST LAYER  (6E10.2)                                               *
C      *                                                                         *
C      * CC  1-10 -  R : RELATIVE DENSITY                                        *
C      * CC 11-20 -  T : THICKNESS (CM)                                          *
C      * CC 21-30 -  C : VELOCITY OF SOUND (CM/SEC)                              *
C      * CC 31-40 - A2 : OMEGA-SQUARED LONGITUDINAL ATTEN. COEFFICIENT           *
C      * CC 41-50 - A1 : OMEGA LONGITUDINAL ATTENUATION COEFFICIENT              *
C      * CC 51-60 - A0 : CONSTANT ATTENUATION COEFFICIENT                        *
C      *                                                                         *
C      * CARD #2                                                                 *
C      *   - SECOND (MIDDLE) LAYER                                               *
C      * SAME FORMAT AS FIRST LAYER PARAMETERS                                   *
C      *                                                                         *
C      * CARD #3                                                                 *
C      *   - SECOND LAYER MASK (80I1)                                            *
C      * CC 1 : =1 IF T FIXED,0 (OR BLANK) IF NOT FIXED.                         *
C      * CC 2 : =1 IF C FIXED,0 (OR BLANK) IF NOT FIXED.                         *
C      * CC 3 : =1 IF R FIXED,0 (OR BLANK) IF NOT FIXED.                         *
C      * CC 4 : =1 IF A2 FIXED,0 (OR BLANK) IF NOT FIXED.                        *
C      * CC 5 : =1 IF A1 FIXED,0 (OR BLANK) IF NOT FIXED.                        *
C      * CC 6 : =1 IF A0 FIXED,0 (OR BLANK) IF NOT FIXED.                        *
C      * CC 11-20 -   FMIN   : MINIMUM FREQUENCY FOR FIT,DEFAULT=0.0             *
C      * CC 21-30 -   FMAX   : MAXIMUM FREQUENCY FOR FIT,DEFAULT=20.0E06         *
C      * CC 31-70 -   ITITLE: PLOT TITLE, 40 CHARACTERS                          *
C      * CC80 : =1 IF WEIGHTING FUNCTION NOT NECESSARY                           *
C      *                                                                         *
C      ***************************************************************************
C
C
C
C
C
C
C
C
C
C
C
C
C      ***************************************************************************
C      *                                                                         *
C      *   INPUT FILE  TAPE6   ( FROM DATA OR LAYER PROGRAM)                     *
C      *                                                                         *
C      *-------------------------------------------------------------------------*
C      *                                                                         *
C      *     4I10 - (TRN(I),I=1,4); EXPERIMENTAL DATA TAPE RECORD NUMBERS        *
C      *     FREE - NPTS  ; NUMBER OF DATA POINTS IN DATA SET                    *
C      *     FREE - FZERO ; START FREQUENCY (HZ)                                 *
C      *     FREE - DELTAF; FREQUENCY INCREMENT (HZ)                             *
C      *     FREE - TI    ; ANGLE OF INCIDENCE (DEG.)                            *
C      *  2E15.5 - (D(I),I=1,NPTS); COMPLEX TRANSMISSION FUNCTION                *
C      *                                                                         *
```


40

```
C     **************************************************************
C
C
C
C     MAIN PROGRAM-------------------------------------------------*
C
C     CALL PLOTTER INITIALIZATION ROUTINE
      CALL COMPRS
      NPLN = 0
      PRINT 4
      PRINT 6
C     GET DATA
      CALL INDATA
C
C     SET UP FOR DO LOOPS
      NPAR1 = NPAR - 1
C
C     LOCATE DATA PEAKS
      CALL PEAK(YD,NPTS,IPD,1)
C     TOP OF FORM
      PRINT 4
      PRINT 5
C     PRINT OUT INITIAL PARAMETERS
      PRINT 11
      PRINT 13,(ITITLE(I), I=1,4)
      PRINT 10, ( 1,PZ(I), I=1,NPAR1,2),(2,PZ(I),I=2,NPAR,2)
      IF ( MASK(2) .EQ. 1 ) PRINT 22
      IF ( MASK(4) .EQ. 1 ) PRINT 24
      IF ( MASK(6) .EQ. 1 ) PRINT 26
      IF ( MASK(8) .EQ. 1 ) PRINT 28
      IF (MASK(10) .EQ. 1) PRINT 30
      IF (MASK(12) .EQ. 1) PRINT 32
C     --------------------------------------------------------------
C     COMPUTE STEP SIZE
      DO 1 I=1,NPAR
      XJUMP=0.1
      DELTAX(I)=XJUMP*PZ(I)
      IF(DELTAX(I) .EQ. 0.0) DELTAX(I)=0.01
C     WATCH OUT FOR A2(2)
      IF ( I .EQ. 8 ) DELTAX(I)=1.0E-14
      DELMIN(I)=XJUMP*XJUMP*DELTAX(I)
    1 CONTINUE
C
C     TOP OF FORM
      PRINT 4
C
C     COMPUTE CORRECT PARAMETERS
C     PLOT FIRST GUESS
      CALL FCN ------------------------------------------------------
      CALL PICTR(1)
      CALL SMPLEX(FCN)
C     PLOT COMPUTED FIT
      CALL FCN
      CALL PICTR(1)
C
C     TOP OF FORM
      PRINT 4
      PRINT 5
```

```
C
C      PRINT OUT INITIAL PARAMETERS
       PRINT 11
       PRINT 13,(ITITLE(I), I=1,4)
       PRINT 10, ( 1,PZ(I), I=1,NPAR1,2),(2,PZ(I),I=2,NPAR,2)
       PRINT 5
C
C      PRINT OUT BEST COMPUTED PARAMETERS
       PRINT 12
       PRINT 14, BCHISQ, NFBEST
       PRINT 10, (1,BX(I), I=1,NPAR1,2),(2,BX(I),I=2,NPAR,2)
       IF ( MASK(2) .EQ. 1 ) PRINT 22
       IF ( MASK(4) .EQ. 1 ) PRINT 24
       IF ( MASK(6) .EQ. 1 ) PRINT 26
       IF ( MASK(8) .EQ. 1 ) PRINT 28
       IF (MASK(10) .EQ. 1) PRINT 30
       IF (MASK(12) .EQ. 1) PRINT 32
       PRINT 5
       PRINT 3,NF
       CALL DONEPL
C
C      FORMAT STATEMENTS
C
     2 FORMAT(10X,6E15.5)
     3 FORMAT(10X,*NUMBER OF FUNCTIONAL EVALUATIONS = *,I5)
     4 FORMAT(1H1)
     5 FORMAT(/////)
     6 FORMAT(*-*,10X, *FIT PROGRAM EXECUTION*)
    10 FORMAT (*0*,10X, *T(*,I1,*) = *,E15.5,5X,*C(*,I1,*) = *,E15.5,5X,
     1         *RHO(*,I1,*) = *,E15.5,/* *,10X,*A2(*,I1,*) = *,E15.5,5X,
     2         *A1(*,I1,*) = *,E15.5,5X,*A0(*,I1,*) = *,E15.5,5X,
     3         *WN(*,I1,*) = *,F5.2)
    11 FORMAT (*-        INITIAL PARAMETERS *)
    12 FORMAT (*-        COMPUTED PARAMETERS*)
    13 FORMAT(*0*,10X,4A10,//)
    14 FORMAT (*0*,5X,*CHISQ = *,F12.3,*, EVALUATION NUMBER = *,I5,//)
    22 FORMAT (*0*,10X, *FIX THICKNESS*)
    24 FORMAT (*0*,10X, *FIX VELOCITY*)
    26 FORMAT (*0*,10X,*FIX DENSITY*)
    28 FORMAT (*0*,10X,*FIX A2*)
    30 FORMAT (*0*,10X,*FIX A1*)
    32 FORMAT (*0*,10X,*FIX A0*)
       STOP
       END
       SUBROUTINE SMPLEX(FUNK)
C
C  *  *  *  *  *  *  *  *  *  *  *  *  *  *  *  *  *  *
C
C      FUNCTION MINIMIZATION BY THE SIMPLEX METHOD                  SMPLX
C   (NELDER AND MEAD, THE COMPUTER JOURNAL, JANUARY 1965)           SMPLX   4
C
C   COMMANDMENT 1 ....  THOU SHALT NOT OMIT THINE "EXTERNAL" CARD.  SMPLX   8
C
C  *  *  *  *  *  *  *  *  *  *  *  *  *  *  *  *  *  *
C
C                    ***** SEARCH COMMON ******
C
       COMMON/STEPIT/NV,NTRACE,CHISQ,MASK(100),
```

```
     1               X(100),DELTAX(100),DELMIN(100),NF
      COMMON /CONST6/ NPLN,NPLSW,NPINT,LIM
C
C                    ***** INTERNAL DIMENSIONS *****
C
      DIMENSION CHI(21),Z(21,20),ZBAR(20),ZSTAR(20)                     SMPLX 12
C
C *  *  *  *  *  *  *  *  *  *  *  *  *  *  *  *  *  *  *
C
C     THE SEARCH PARAMETERS ARE DEFINED AS FOLLOWS
C
C     NV              THE NUMBER OF PARAMETERS TO BE VARIED
C     NTRACE          = 1  PRINT OUT MAP OF SEARCH SEQUENCE
C                     = 0  NO MAP
C     X               PARAMETER ARRAY
C     MASK            =0   SEARCH ON PARAMETER I
C                     =1   HOLD PARAMETER I FIXED
C     DELTAX          INITIAL STEP SIZE FOR VARIABLE X(I)
C     DELMIN          SMALLEST STEP SIZE ALLOWED FOR VARIABLE X(I)
C
C
C     CHISQ           RETURNED FUNCTION VALUE
C
C *  *  *  *  *  *  *  *  *  *  *  *  *  *  *  *  *  *  *
C
      ALPHA=1.0                                                         SMPLX 14
      BETA=0.5                                                          SMPLX 15
      GAMMA=2.0                                                         SMPLX 16
      HUGE=1.0E37
      SIGNIF=1.E5
      NVP=NV+1                                                          SMPLX 20
C     LIM IS # OF EVALUATIONS PERMITTED BEFORE TERMINATION.
      DO 10 J=1,NV                                                      SMPLX 21
   10 Z(NV+1,J)=X(J)                                                    SMPLX 22
      CALL FUNK                                                         SMPLX 23
      NF=1                                                              SMPLX 24
      CHI(NV+1)=CHISQ                                                   SMPLX 25
C
C *  *  *  *  *  *  *  *  *  *  *  *  *  *  *  *  *  *  *
C
C  CALCULATE INITIAL P(I) AND Y(I).                                     SMPLX 29
C
C *  *  *  *  *  *  *  *  *  *  *  *  *  *  *  *  *  *  *
C
      DO 30 J=1,NV                                                      SMPLX 31
      DO 20 K=1,NV                                                      SMPLX 32
   20 Z(J,K)=X(K)                                                       SMPLX 33
       SIGN = 1.0
   23  IF(MASK(J) .EQ. 1) GO TO 21
      Z(J,J) = Z(J,J)+SIGN*DELTAX(J)
   21 XS=X(J)
      X(J)=Z(J,J)                                                       SMPLX 36
      CALL FUNK                                                         SMPLX 37
      NF=NF+1                                                           SMPLX 38
      IF ( NF .GE. LIM) GO TO 500
      X(J)=XS                                                           SMPLX 39
      IF(CHI(NV+1)-CHISQ) 22,30,30
   22  IF(SIGN .EQ. -2.0) GO TO 30
```

```
      SIGN = -2.0
      GO TO 23
   30 CHI(J)=CHISQ                                                      SMPLX 40
C
C  *  *  *  *  *  *  *  *  *  *  *  *  *  *  *  *  *  *  *  *
C
C  DETERMINE H AND L.                                                   SMPLX 42
C
C  *  *  *  *  *  *  *  *  *  *  *  *  *  *  *  *  *  *  *  *
C
   40 JH=1                                                              SMPLX 44
      JL=1                                                              SMPLX 45
      DO 80 J=2,NVP                                                     SMPLX 46
      IF(CHI(J)-CHI(JH))60,60,50                                        SMPLX 47
   50 JH=J                                                              SMPLX 46
   60 IF(CHI(J)-CHI(JL))70,80,80                                        SMPLX 49
   70 JL=J                                                              SMPLX 50
   80 CONTINUE                                                          SMPLX 51
C
C  *  *  *  *  *  *  *  *  *  *  *  *  *  *  *  *  *  *  *  *
C
C  CALCULATE PBAR.                                                      SMPLX 54
C
C  *  *  *  *  *  *  *  *  *  *  *  *  *  *  *  *  *  *  *  *
C
   90 DO 120 J=1,NV                                                     SMPLX 56
      ZBAR(J)=0.0                                                       SMPLX 57
      DO 110 K=1,NVP                                                    SMPLX 58
      IF(K-JH)100,110,100                                               SMPLX 59
  100 ZBAR(J)=ZBAR(J)+Z(K,J)                                            SMPLX 60
  110 CONTINUE                                                          SMPLX 61
  120 ZBAR(J)=ZBAR(J)/FLOAT(NV)                                         SMPLX
C
C  *  *  *  *  *  *  *  *  *  *  *  *  *  *  *  *  *  *  *  *
C
C  ATTEMPT A REFLECTION.                                                SMPLX 64
C  FORM P* .                                                            SMPLX 65
C
C  *  *  *  *  *  *  *  *  *  *  *  *  *  *  *  *  *  *  *  *
C
      DO 130 J=1,NV                                                     SMPLX 67
       IF(MASK(J) .EQ. 1) GO TO 130
      X(J)=(1.0+ALPHA)*ZBAR(J)-ALPHA*Z(JH,J)                            SMPLX 68
  130 ZSTAR(J)=X(J)                                                     SMPLX 69
      CALL FUNK                                                         SMPLX 70
      NF=NF+1                                                           SMPLX 71
      IF ( NF .GE. LIM) GO TO 600
      CHISTA =CHISQ                                                     SMPLX 72
      IF(CHISQ-CHI(JL))140,180,180                                      SMPLX 73
C
C  *  *  *  *  *  *  *  *  *  *  *  *  *  *  *  *  *  *  *  *
C
C  THE REFLECTION SUCCEEDED.  ATTEMPT AN EXPANSION.                     SMPLX 75
C  FORM P** .                                                           SMPLX 76
C
C  *  *  *  *  *  *  *  *  *  *  *  *  *  *  *  *  *  *  *  *
C
  140 IF(NTRACE)150,160,150                                             SMPLX 78
```

```
150 PRINT 43, CHISQ
 43 FORMAT(1JX8HCHISQ = E15.8,10X20HREFLECTION SUCCEEDED  )      SMPLX 80
    PRINT 44, (X(J),J=1,NV)
 44 FORMAT(5X8HX(I)..../(10(1XE12.5)))                           SMPLX 82
    PRINT 155
155 FORMAT(1H )                                                  SMPLX 84
160 DO 170 J=1,NV                                                SMPLX 85
     IF(MASK(J) .EQ. 1) GO TO 170
    X(J)=GAMMA*X(J)+(1.0-GAMMA)*ZBAR(J)
170 CONTINUE
    CALL FUNK                                                    SMPLX 87
    NF=NF+1                                                      SMPLX 88
    IF ( NF .GE. LIM) GO TO 600
    IF(CHISQ-CHI(JL)) 175,210,210
175 IF(CHISQ-CHISTA) 400,210,210
C
C * * * * * * * * * * * * * * * * * * *
C
C THE REFLECTION FAILED.                                         SMPLX 91
C
C * * * * * * * * * * * * * * * * * * *
C
180 DO 200 J=1,NVP                                               SMPLX 93
    IF(J-JH)190,200,190                                          SMPLX 94
190 IF(CHISQ-CHI(J))230,200,200                                  SMPLX 95
200 CONTINUE                                                     SMPLX 96
    IF(CHISQ-CHI(JH))250,270,270                                 SMPLX 97
C
210 IF(NTRACE)220,230,220                                        SMPLX 99
220 PRINT 46
 46 FORMAT(43X16HEXPANSION FAILED  )                             SMPLX101
C
C * * * * * * * * * * * * * * * * * * *
C
C REPLACE P(JH) BY P* .                                          SMPLX103
C
C * * * * * * * * * * * * * * * * * * *
C
230 DO 240 J=1,NV                                                SMPLX105
240 Z(JH,J)=ZSTAR(J)                                             SMPLX106
    CHI(JH)=CHISTA
    GO TO 440                                                    SMPLX108
C
250 DO 260 J=1,NV                                                SMPLX110
260 Z(JH,J)=X(J)                                                 SMPLX111
    CHI(JH)=CHISQ                                                SMPLX112
C
C * * * * * * * * * * * * * * * * * * *
C
C ATTEMPT A CONTRACTION.                                         SMPLX114
C FORM P** .                                                     SMPLX115
C
C * * * * * * * * * * * * * * * * * * *
C
270 DO 280 J=1,NV                                                SMPLX117
     IF(MASK(J) .EQ. 1) GO TO 280
    X(J)=BETA*Z(JH,J)+(1.0-BETA)*ZBAR(J)
280 CONTINUE
```

```
      CALL FUNK                                                         SMPLX119
      NF=NF+1                                                           SMPLX120
      IF ( NF .GE. LIM) GO TO 600
      IF(CHISQ-CHI(JH))290,330,330                                      SMPLX121
  290 IF(NTRACE)300,420,300                                             SMPLX122
  300 IF(CHISQ-CHI(JL))310,320,320                                      SMPLX123
  310 PRINT 303, CHISQ
  303 FORMAT(10X8HCHISQ = E15.8,10X21HCONTRACTION SUCCEEDED  )          SMPLX125
      PRINT 44,  (X(J),J=1,NV)
      PRINT 155
      GO TO 420                                                         SMPLX128
  320 PRINT 49
   49 FORMAT(43X21HCONTRACTION SUCCEEDED  )                             SMPLX130
      GO TO 420                                                         SMPLX131
C
C     *  *  *  *  *  *  *  *  *  *  *  *  *  *  *  *  *  *
C
C     THE CONTRACTION FAILED.                                           SMPLX133
C     REPLACE ALL P(I) BY (P(I)+P(JL))/2.0                              SMPLX134
C
C     *  *  *  *  *  *  *  *  *  *  *  *  *  *  *  *  *  *
C
  330 IF(NTRACE)340,350,340                                             SMPLX136
  340 PRINT 56
   56 FORMAT(43X18HCONTRACTION FAILED  )                                SMPLX138
  350 JS=JL                                                             SMPLX139
      DO 390 J=1,NVP                                                    SMPLX140
      IF(J-JL)360,390,360                                               SMPLX141
  360 DO 370 K=1,NV                                                     SMPLX142
      Z(J,K)=0.5*(Z(J,K)+Z(JL,K))                                       SMPLX143
  370 X(K)=Z(J,K)                                                       SMPLX144
      CALL FUNK                                                         SMPLX145
      NF=NF+1                                                           SMPLX146
      IF ( NF .GE. LIM) GO TO 600
      IF(CHISQ-CHI(JL))380,390,390                                      SMPLX147
  380 JS=J                                                              SMPLX148
  390 CHI(J)=CHISQ                                                      SMPLX149
      JL=JS                                                             SMPLX150
      GO TO 440                                                         SMPLX151
C
  400 IF(NTRACE)410,420,410                                             SMPLX153
  410 PRINT 52, CHISQ
   52 FORMAT(10X8HCHISQ = E15.8,10X19HEXPANSION SUCCEEDED  )            SMPLX155
      PRINT 44,  (X(J),J=1,NV)
      PRINT 155
C
C     *  *  *  *  *  *  *  *  *  *  *  *  *  *  *  *  *  *
C
C     REPLACE P(JH) BY P* OR P**  .                                     SMPLX160
C
C     *  *  *  *  *  *  *  *  *  *  *  *  *  *  *  *  *  *
C
  420 DO 430 J=1,NV                                                     SMPLX161
  430 Z(JH,J)=X(J)                                                      SMPLX162
      CHI(JH)=CHISQ                                                     SMPLX163
C
C     *  *  *  *  *  *  *  *  *  *  *  *  *  *  *  *  *  *
```

```
C
C  TEST FOR CONVERGENCE.                                              SMPLX165
C
C  *  *  *  *  *  *  *  *  *  *  *  *  *  *  *  *  *  *  *
C
  440 DO 470 J=1,NV                                                   SMPLX167
       IF(MASK(J) .EQ. 1) GO TO 470
      ZMAX=-HUGE                                                      SMPLX168
      ZMIN=HUGE                                                       SMPLX169
      DO 450 K=1,NVP                                                  SMPLX170
      ZMAX=AMAX1(ZMAX,Z(K,J))                                         SMPLX
  450 ZMIN=AMIN1(ZMIN,Z(K,J))                                         SMPLX
      IF(SIGNIF*(ZMAX-ZMIN)-AMIN1(ABS(ZMAX),ABS(ZMIN)))470,470,460    SMPLX
  460 IF(ZMAX-ZMIN-ABS(DELMIN(J)))470,470,475
  470 CONTINUE                                                        SMPLX175
      GO TO 480
  475 JH=1
      JL=1
      DO 479 J=2,NVP
      IF(CHI(J)-CHI(JH)) 477,477,476
  476 JH=J
  477 IF(CHI(J)-CHI(JL)) 478,479,479
  478 JL=J
  479 CONTINUE
      IF(SIGNIF*(CHI(JH)-CHI(JL))-CHI(JL)) 480,480,90
C
  480 IF(CHI(JH)-CHI(JL))490,500,500                                  SMPLX177
  490 JL=JH                                                           SMPLX178
  500 CHISQ=CHI(JL)                                                   SMPLX179
      DO 510 J=1,NV                                                   SMPLX184
  510 X(J)=Z(JL,J)                                                    SMPLX185
      RETURN                                                          SMPLX188
C     OUT OF TIME
  600 CONTINUE
      PRINT 610, NF, LIM
  610 FORMAT(*0FUNCTIONAL ITERATION LIMIT REACHED, NF =*,I5)
      RETURN
      END                                                             SMPLX
      SUBROUTINE FCN
      COMMON/FIT1/NPTS,NPAR,YD(1050),WD(1050),PZ(100),TD(1050)
      COMMON /FITB/ FMIN,FMAX,ITITLE(5)
      COMMON /FITC/ IPD(100),IPSWCH
      COMMON/STEPIT/NV,NTRACE,CHISQ,MASK(100),T(2),C(2),R(2),
     1         A2(2),A1(2),A0(2),WN(2),DUM(86),DELTAX(100),DELMIN(100),NF
      COMMON /BEST/ BX(100),NFBEST,NRPBST,BCHISQ
      COMMON/CONST1/Z1,ZN1,PI,EYE
      COMMON/CONST4/DELTAF,FZERO
      COMMON /CONST6/ NPLN,NPLSW,NPINT,NEVAL
      COMMON /DISP/ DSP(2,3)
      COMPLEX K(2),CC(2),SINP(2),COSP(2),EYE
      COMPLEX Q231,Q232,Q23,Q321,Q322,Q32,Q221,Q222,Q22,Q331,Q332,Q33
      DIMENSION ITD(100)
      COMPLEX VB1,VB2,VB
      COMPLEX K1
      REAL K2
C     NPINT IS HOW OFTEN TO PLOT. I.E., EVERY 50 EVALUATIONS, ETC..
C
C     THIS SUBROUTINE IS USED TO DETERMINE THE ADEQUACY OF THE FIT
```

```
C     ACHIEVED BY THE CURRENT PARAMETER VALUES.  IT PRODUCES A
C     CHI-SQUARED ESTIMATE OF THE DIFFERENCE BETWEEN A THEORETICAL
C     MODEL UTILIZING THE CURRENT PARAMETERS AND THE EXPERIMENTAL DATA
C     VALUES. IT IS A MODIFIED "XLAYER" SUBROUTINE WHERE THE THIRD
C     LAYER IS ASSUMED TO BE IDENTICAL TO THE FIRST.
C
      CHISQ=0.0
C     INIT PEAK DETECTION
      N = 1
C     DON'T PRINT PEAK MATCHES
      MPSWCH = 0
C     NEGATIVE PARAMETERS UNPHYSICAL
      IF ( T(2) .LT. 0) GO TO 4
      IF ( C(2) .LT. 0) GO TO 4
      IF ( R(2) .LT. 0) GO TO 4
      IF ( A0(2) .LT. 0) GO TO 4
      DO 1 I=1,NPTS
      F=(FLOAT(I)*DELTAF+FZERO)
      OMEGA=2.0*PI*F
      DO 6 J=1,2
      ATT=A2(J)*OMEGA*OMEGA+A1(J)*OMEGA+A0(J)
      K(J)=CMPLX(OMEGA/C(J),-ATT)
C     KEEP SQUARE-ROOT ARG. FROM BLOWING UP
      IF ( CABS( K(J) ) .LT. 1.0E-99 ) PRINT 11,F,J
   11 FORMAT (* K(J) TOO SMALL, FREQ = *,E15.5, *,J= *,I2)
      CC(J)=CSQRT((OMEGA*OMEGA)/(K(J)*K(J)))
      K1 = K(J)*T(J)
C     KEEP FUNCTION FROM BLOWING UP - IMAGINARY PART MAG. >300.
      IF (ABS(AIMAG(K1)) .GT. 300.0) PRINT 10,F,J
   10 FORMAT (* K1 BLOW UP, FREQ = *,E15.5,*, J= *,I2)
      IF (ABS(AIMAG(K1) ) .GT. 300.0 ) GO TO 4
      SINP(J) = CSIN(K1)
      COSP(J) = CCOS(K1)
    6 CONTINUE
      Q231=(1.0/(R(2)*CC(2)))*SINP(2)*COSP(1)
      Q232=(1.0/(R(1)*CC(1)))*SINP(1)*COSP(2)
      Q23=-EYE*(Q231+Q232)
      Q321=R(2)*CC(2)*SINP(2)*COSP(1)
      Q322=R(1)*CC(1)*SINP(1)*COSP(2)
      Q32=-EYE*(Q321+Q322)
      Q221=Q331=COSP(2)*COSP(1)
      Q222=((R(1)*CC(1))/(R(2)*CC(2)))*SINP(2)*SINP(1)
      Q332=((R(2)*CC(2))/(R(1)*CC(1)))*SINP(2)*SINP(1)
      Q22=Q221-Q222
      Q33=Q331-Q332
      VB1=COSP(1)+((EYE*ZN1)/(R(1)*CC(1)))*SINP(1)
      VB2=ZN1*COSP(1)+EYE*R(1)*CC(1)*SINP(1)
      VB=VB1*(Q32-Z1*Q33)-VB2*(Q22-Z1*Q23)
      Y = CABS((-2.0*Z1)/VB)
C     STORE THEORETICAL RESULTS
C     NORMALIZE THEORETICAL
      Y = WN(2)*Y
      TD(I) = Y
C     FMIN IS MINIMUM FIT FREQUENCY
C     FMAX IS MAXIMUM FIT FREQUENCY
      IF (F .LT. FMIN) GO TO 1
      IF (F .GT. FMAX) GO TO 1
      RES=YD(I)-Y
```

```
      CHISQ=CHISQ+(RES*RES*WD(I))
    1 CONTINUE
      GO TO 5
C     UNPHYSICAL PARAMETER
    4 CHISQ = 1E10
    5 CONTINUE
C     COMPARE PEAKS?
      CNFACT = CHISQ
      PWEIGH = 0.0
      MATCH = 0
      IF (IPSWCH .NE. 1) GO TO 29
C     GET THEORETICAL PEAKS
      CALL PEAK(TD,NPTS,ITD,0)
      N=1
      M = 1
C     SEE IF PEAKS MATCH
      DO 21 M = 1,100
      IF (IABS (IPD(N)-ITD(M)) .LT. 10) MATCH=1
      IF (MATCH .EQ. 1) PRINT 31
      IF ( MATCH .EQ. 1) GO TO 22
   31 FORMAT (* THEORETICAL & EXPERIMENTAL PEAKS MATCH*)
   21 CONTINUE
C     NO MATCH
      GO TO 29
C     MATCH - COMPUTE PEAK AMPLITUDE DIFF
   22 DO 24 I = N,100
C     END LOOP IF OUT OF PEAKS
      IF ( IPD(I) .GE. NPTS) GO TO 29
      F = FLOAT(IPD(I))*DELTAF + FZERO
C     DON'T COMPARE IF OUT OF RANGE
      IF ( F .LT. FMIN) GO TO 24
      IF ( F .GT. FMAX) GO TO 24
C     SEE IF EXTRA PEAK
   26 CONTINUE
      IF (M+1 .GT. 100) GO TO 23
      I1 = IABS (IPD(I)-ITD(M+1))
      I2 = IABS (IPD(I)-ITD(M))
      IF ( I1 .LT. I2) M = M+1
      IF ( I1 .LT. I2) GO TO 26
      IF ( I2 .GT. 10) PRINT 34, IPD(I)
   34 FORMAT (* REJECT DATA PEAK INDEX:*,I4)
      IF ( I2 .GT. 10) GO TO 24
   23 CONTINUE
C     PRINT PEAK MATCH-UPS IF MPSWCH = 1
      IF (MPSWCH .EQ. 0) GO TO 27
      PRINT 33, IPD(I), ITD(M)
   33 FORMAT(* MATCH DATA PEAK INDEX:*,I4,* WITH THEORETICAL:*,I4)
   27 CONTINUE
      PRES = YD(IPD(I))-TD(ITD(M))
      PWEIGH = PWEIGH +(PRES*PRES)
      M = M+1
      IF ( M .GT. 100) GO TO 25
   24 CONTINUE
   29 CONTINUE
      PWEIGH = PWEIGH*100.0
   25 CHISQ = CHISQ + PWEIGH
      PRINT 32, PWEIGH
   32 FORMAT(* PWEIGHT = *, E15.5)
```

```
      PRINT 2, NF, CHISQ
    2 FORMAT(20X,*EVALUATION NUMBER *,I5,*      CHI SQUARED = *,E13.5)
      PRINT 3,(T(I),C(I),R(I),A2(I),A1(I),A0(I),WN(I),I=1,2)
    3 FORMAT(10X,7E15.5)
C     PLOT EVERY NPINT EVALUATIONS.
C     NEW BESTFIT?
      IF (CHISQ .LT. BCHISQ) CALL BFIT
      IF ( NF .EQ. 0) GO TO 15
      X = FLOAT(NF)/NPINT
      IF ( X-(NF/NPINT) .EQ. 0.0) CALL PICTR(1)
   15 RETURN
      END
      SUBROUTINE INDATA
      INTEGER TRN(4)
      COMPLEX EYE,D(1050)
      COMMON/FIT1/NPTS,NPAR,YD(1050),WD(1050),PZ(100),TD(1050)
      COMMON /FITB/ FMIN,FMAX,ITITLE(5)
      COMMON/STEPIT/NV,NTRACE,CHISQ,MASK(100),T(2),C(2),R(2),
     1              A2(2),A1(2),A0(2),  WN(3),DUM2(3),DUM3(3),DUM4(3),
     2              DUM5(3),DUM6(3),DUM7(3),DUM8(67),DELTAX(100),
     3              DELMIN(100),NF
      COMMON/CONST1/Z1,ZN1,PI,EYE
      COMMON/CONST4/DELTAF,FZERO
C
C     THIS SUBROUTINE INPUTS THE EXPERIMENTAL DATA AND TRANSDUCER
C     RESPONSE FROM FILE TAPE6, AND ALSO INPUTS INITIAL LAYER PARAMETERS
C     FROM DATA CARDS.
C
C
C     INITIALIZE NUMBER OF PARAMETERS
      NPAR = 14
C     INITIALIZE NUMBER OF PARAMETERS NOT VARIED
      NV=NPAR
C
C
C     TURN OFF TRACE OF SEARCH PROCEDURE
      NTRACE=0
C
C     INITIALIZE CONSTANTS
      EYE=CMPLX(0.0,1.0)
      PI=3.141592654
C     IMPEDANCE AT NORMAL INCIDENCE - FIRST MEDIUM
      Z1=1.48E05
C     IMPEDANCE AT NORMAL INCIDENCE - LAST MEDIUM
      ZN1=1.48E05
C
C     READ DATA SET.
      READ(6,1)(TRN(I),I=1,4)
    1 FORMAT(4I10)
C
      PRINT 10
   10 FORMAT (*-*,10X,*DATA SET*)
      PRINT 11, TRN(1),TRN(3)
   11 FORMAT (*0*,10X,*DATA RECORD (*,I3,*,* ,I3,*)* )
      PRINT 12, TRN(2), TRN(4)
   12 FORMAT (*0*,10X, *TRANSDUCER RECORD (*,I3,*,*, I3,*)* )
C
      READ(6,*)NPTS,FZERO,DELTAF,TI
```

```
C
C     READ COMPLEX TRANSMISSION FUNCTION
      READ(6,5)(D(I),I=1,NPTS)
    5 FORMAT(2E15.5)
C
C     READ PARAMETERS
      READ 2, (T(I),C(I),R(I),A2(I),A1(I),A0(I), WN(I),I=1,2)
    2 FORMAT(7E10.2)
C
C     STORE PARAMETERS IN PZ ARRAY
C
      PZ(1)=T(1)
      PZ(2)=T(2)
      PZ(3)=C(1)
      PZ(4)=C(2)
      PZ(5)=R(1)
      PZ(6)=R(2)
      PZ(7)=A2(1)
      PZ(8)=A2(2)
      PZ(9)=A1(1)
      PZ(10)=A1(2)
      PZ(11)=A0(1)
      PZ(12)=A0(2)
C     SET UP NORMALIZING PARAMETER
      PZ(13) = WN(1) = 0.0
C     DEFAULT VALUE OF WN(2) = 1
      IF (WN(2) .EQ. 0.0) WN(2) = 1.0
      PZ(14) = WN(2)
C
C     USE ONLY REAL PART OF COMPLEX TRANSMISSION FUNCTION
      DO 7 I=1,NPTS
      YD(I)= CABS(D(I))
    7 CONTINUE
C
C     INITIALIZE WEIGHTING FUNCTION
      DO 4 I =1,NPTS
      WD(I) =1
    4 CONTINUE
C
C     FIX FIRST LAYER PARAMETERS
      MASK(1)=MASK(3)=MASK(5)=MASK(7)=MASK(9)=MASK(11)=MASK(13)=1
C
C     READ SECOND LAYER MASK,FMIN,FMAX,ITITLE & WEIGHTING FLAG
      READ 6,(MASK(I),I=2,NPAR,2),FMIN,FMAX,(ITITLE(I),I=1,4),IWFLAG
    6 FORMAT (7I1,3X,2E10.2,4A10,9X,I1)
C     SET UP DEFAULT VALUE FOR FMAX
      IF (FMAX .LE. 0.0) FMAX=20.0E06
C     END TITLE
      ITITLE(5)=10H$
      PRINT 17, FMIN, FMAX
   17 FORMAT(* *,10X,*FMIN = *,E15.5,* FMAX = *,E15.5)
C
C     SEE IF TRANSDUCER RESPONSE CURVE TO BE USED AS WEIGHTING FUNCTION.
      IF (IWFLAG .EQ. 1) PRINT 15
   15 FORMAT (*-*,10X,*WEIGHTING FUNCTION = 1*)
      IF ( IWFLAG .EQ. 1) GO TO 8
C
C
```

```
C       READ TRANSDUCER RESPONSE CURVE
        READ(6,1)(TRN(I),I=1,4)
        READ(6,*)NPTS,FZERO,DELTAF,TI
        READ(6,5)(D(I),I=1,NPTS)
C
C
        PRINT 16, TRN(1),TRN(3)
   16   FORMAT(*-*,10X,*WEIGHTING FUNCTION RECORD (*,I3,*,*,I3,*)* )
C       USE ABSOLUTE MAGNITUDE FOR WEIGHTING FUNCTION
        DO 3 I=1,NPTS
        WD(I)=CABS(D(I))
    3   CONTINUE
C
    8   RETURN
        END
        SUBROUTINE PICTR(LOOP)
        COMMON /CONST4/ DELTAF,FZERO
        COMMON/FIT1/NPTS,NPAR,YD(1050),WD(1050),PZ(100),TD(1050)
        COMMON /FITB/ FLO,FHI,ITITLE(5)
        DIMENSION X(1050), Y(1050), Y2(1050)
        COMMON /FITD/ B(2),B2(2),B1(2),B0(2)
C       BEST FIT PARAMETERS
        COMMON /STEPIT/ NV,NTRACE,SCHISQ,MASK(100),
     1             XX(100),DELTAX(100),DELMIN(100),SNF
        COMMON /BEST/ THICK(2),C(2),ROW(2),C2(2),C1(2),C0(2),WN(2),
     1              DUM(66),NF,NRPBST,CHISQ
        DIMENSION LBLX(10),LBLY(10),LBLH(10),LSTRG(10),LPAK(150)
        COMPLEX VSV,DSD
        COMPLEX D(1024),V(1024)
        COMMON /CONST5/ NPLN,NPLSW,NPINT,NEVAL
        NLAYER=2
        TI = 0.0
        RTD=57.29577951
        LBLX(1)=10HFREQUENCY
        LBLX(2)=10HIN MHZ.$
        LBLH(1)=10H    T    (
        LBLH(2)=10HR)     C
        LBLH(3)=10H     B
        LBLH(4)=10H    C2
        LBLH(5)=10H   C1
        LBLH(6)=10H  C0
        LBLH(7)=10H B2
        LBLH(8)=10HB1        B
        LBLH(9)=10H0$
        XL=10.0
        YL=5.0
        XSF=XL/10.0
        YSF=YL/5.0
        HITE=0.12*YSF
        WIDTH=HITE*6.0/7.0
        XLEFT=0.25*XSF
        YBTM=YL+0.50*YSF
        XLC=0.0
        XRC=85.0*WIDTH+2.0*XLEFT
        YBC=YBTM-0.25*YSF
        YTC=YBC+0.50*YSF+1.35*HITE*(FLOAT(NLAYER)+1.0)
C       SET UP HORIZONTAL SPACING FOR PARAMETERS IN BOX.
        XJUMP=9.0*WIDTH
```

```
      XJ0=XLEFT
      XJ1=XJ0+7.0*WIDTH.
      XJ2=XJ1+5.0*WIDTH
      XJ3=XJ2+XJUMP
      XJ4=XJ3+XJUMP
      XJ5=XJ4+XJUMP
      XJ6=XJ5+XJUMP
      XJ7=XJ5+XJUMP
      XJ8=XJ7+XJUMP
      XJ9=XJ8+XJUMP
      PRINT 1, LOOP
    1 FORMAT (*0LOOP = *, I5)
      GO TO(6,7,8,9,10,11,12,13,21)LOOP
    6 CONTINUE
      DO 5 I=1,NPTS
      X(I)=(FLOAT(I)*DELTAF+FZERO)/1.0E06
C     THEORETICAL DATA
      Y(I) = TD(I)
C     EXPERIMENTAL
      Y2(I) = YD(I)
    5 CONTINUE
      LBLY(1)=10HTRANSMISSI
      LBLY(2)=10HON COEFFIC
      LBLY(3)=10HIENT$
      GO TO 100
    7 CONTINUE
      DO 14 I=1,NPTS
      X(I)=(FLOAT(I)*DELTAF+FZERO)/1.0E06
      Y(I)=CABS(V(I))
   14 CONTINUE
      LBLY(1)=10HREFLECTION
      LBLY(2)=10H COEFFICIE
      LBLY(3)=10HIENT$
      GO TO 100
    8 CONTINUE
      DO 15 I=1,NPTS
      X(I)=(FLOAT(I)*DELTAF+FZERO)/1.0E06
      Y(I)=RTD*ATAN(AIMAG(D(I))/REAL(D(I)))
      IF(REAL(D(I)).LT.0.0.AND.AIMAG(D(I)).GT.0.0)Y(I)=Y(I)+180.0
      IF(REAL(D(I)).LT.0.0.AND.AIMAG(D(I)).LT.0.0)Y(I)=Y(I)-180.0
   15 CONTINUE
      LBLY(1)=10HPHASE OF D
      LBLY(2)=10H IN DEG.$
      GO TO 100
    9 CONTINUE
      DO 16 I=1,NPTS
      X(I)=(FLOAT(I)*DELTAF+FZERO)/1.0E06
      Y(I)=RTD*ATAN(AIMAG(V(I))/REAL(V(I)))
      IF(REAL(V(I)).LT.0.0.AND.AIMAG(V(I)).GT.0.0)Y(I)=Y(I)+180.0
      IF(REAL(V(I)).LT.0.0.AND.AIMAG(V(I)).LT.0.0)Y(I)=Y(I)-180.0
   16 CONTINUE
      LBLY(1)=10HPHASE OF V
      LBLY(2)=10H IN DEG.$
      GO TO 100
   10 CONTINUE
      DO 17 I=1,NPTS
      X(I)=(FLOAT(I)*DELTAF+FZERO)/1.0E06
      Y(I)=REAL(D(I))
```

```
 17 CONTINUE
    LBLY(1)=10HREAL COMPO
    LBLY(2)=10HNENT OF D$
    GO TO 100
 11 CONTINUE
    DO 18 I=1,NPTS
    X(I)=(FLOAT(I)*DELTAF+FZERO)/1.0E06
    Y(I)=AIMAG(D(I))
 18 CONTINUE
    LBLY(1)=10HIMAGINARY
    LBLY(2)=10HCOMPONENT
    LBLY(3)=10HOF D$
    GO TO 100
 12 CONTINUE
    DO 19 I=1,NPTS
    X(I)=(FLOAT(I)*DELTAF+FZERO)/1.0E06
    Y(I)=REAL(V(I))
 19 CONTINUE
    LBLY(1)=10HREAL COMPO
    LBLY(2)=10HNENT OF V$
    GO TO 100
 13 CONTINUE
    DO 20 I=1,NPTS
    X(I)=(FLOAT(I)*DELTAF+FZERO)/1.0E06
    Y(I)=AIMAG(V(I))
 20 CONTINUE
    LBLY(1)=10HIMAGINARY
    LBLY(2)=10HCOMPONENT
    LBLY(3)=10HOF V$
    GO TO 100
 21 CONTINUE
    DO 22 I=1,NPTS
    X(I)=(FLOAT(I)*DELTAF+FZERO)/1.0E06
    VSV=V(I)*CONJG(V(I))
    DSD=D(I)*CONJG(D(I))
    Y(I)=REAL(VSV+DSD)
 22 CONTINUE
    LBLY(1)=10HENERGY CON
    LBLY(2)=10HSERVATION
    LBLY(3)=10H(VSV+DSD)$
100 CONTINUE
    FMIN=FZERO/1.0E06
    FMAX=(FLOAT(NPTS)*DELTAF+FZERO)/1.0E06
    FSTEP=(FMAX-FMIN)/10.0
    NPLN=NPLN+1
    PRINT 2, NPLN
  2 FORMAT (*0 CALL BGNPL, NPLN = *,I5)
    CALL BGNPL(NPLN)
    XFO=(11.0-XL)*0.75
    YFO=(8.50-YL)*0.29
    CALL PHYSOR(XFO,YFO)
    CALL XTICKS(10)
    CALL YTICKS(4)
    CALL TITLE(1H ,-1,LBLX,100,LBLY,100,XL,YL)
    IF(TI.GT.0.0)CALL MESSAG("CW ACOUSTIC SPECTRUM      THETA = $",100,
   12.25*XSF,7.1*YSF)
    IF (TI.GT.0.0)CALL REALNO (TI,1,"ABUT","ABUT")
    IF(TI.GT.0.0)CALL MESSAG(" DEG.$",100,"ABUT","ABUT")
```

```
      IF(TI.EQ.0.0)CALL MESSAG("CW ACOUSTIC SPECTRUM      NORMAL INCIDENC
     1E$",100,2.25*XSF,7.1*YSF)
C     PRINT: EVALUATION #, CHISQ
      CALL MESSAG ("EVALUATION NO. $",100,2.25*XSF,6.8*YSF)
      CALL INTNO(NF,"ABUT","ABUT")
      CALL MESSAG(" CHISQ= $",100,"ABUT","ABUT")
      CALL REALNO(CHISQ,103,"ABUT","ABUT")
      CALL MESSAG(ITITLE,100,2.25*XSF,6.4*YSF)
      CALL  MESSAG("FMIN = $",100,0.0,-.9*YSF)
      CALL REALNO (FLO, 103,"ABUT","ABUT")
      CALL  MESSAG(" ,FMAX =$",100,"ABUT","ABUT")
      CALL  REALNO (FHI,103,"ABUT","ABUT")
      CALL MESSAG (" ,WN(2) = $",100,"ABUT","ABUT")
      CALL REALNO (WN(2),103,"ABUT","ABUT")
      CALL BLNK1(XLC,XRC,YBC,YTC,2)
      IF(LOOP.EQ.3.OR.LOOP.EQ.4)CALL GRAF(FMIN,FSTEP,FMAX,-180.0,60.0,18
     10.0)
      IF(LOOP.GT.4.AND.LOOP.LT.9)CALL GRAF(FMIN,FSTEP,FMAX,-1.0,0.2,1.0)
      IF (LOOP .EQ. 1 .OR. LOOP .EQ. 2 .OR. LOOP .EQ. 9)
     1    CALL GRAF (FMIN,FSTEP,FMAX,0.0,"SCALE",1.0)
      IF(LOOP.GT.2.AND.LOOP.LT.9)CALL XSTAXS(FMIN,FSTEP,XL,1H ,1,0.0,YL/
     12.0)
      CALL MIXALF("L/CGREEK")
      CALL HEIGHT(HITE)
      DYM=1.35*HITE
      YML=YBTM+FLOAT(NLAYER)*DYM
      CALL RESET("BLNK1")
      CALL MESSAG(LBLH,100,XLEFT,YML)
      DO 3 I=1,NLAYER
C     SKIP INITIAL LAYER IF ZERO THICKNESS
      IF ( THICK(I) .EQ. 0.0) GO TO 3
      YML=YML-DYM
      CALL REALNO(THICK(I),105,XJ0,YML)
      CALL REALNO(ROW(I),103,XJ1,"ABUT")
      CALL REALNO(C(I),103,XJ2,"ABUT")
      CALL REALNO(B(I),103,XJ3,"ABUT")
      CALL REALNO(C2(I), -2,XJ4,"ABUT")
      CALL REALNO(C1(I), -2,XJ5,"ABUT")
      CALL REALNO(C0(I), -2,XJ6,"ABUT")
      CALL REALNO(B2(I), -2,XJ7,"ABUT")
      CALL REALNO(B1(I), -2,XJ8,"ABUT")
      CALL REALNO(B0(I), -2,XJ9,"ABUT")
    3 CONTINUE
C     INDICATE "FIXED" PARAMETERS IN BOX
      YML = YML-DYM
      W=WIDTH
      IF(MASK(2).EQ.1) CALL MESSAG("FIXED$",100,XJ0+W,YML)
      IF(MASK(3).EQ.1) CALL MESSAG("FXD$"  ,100,XJ1+W,YML)
      IF(MASK(4).EQ.1) CALL MESSAG("FIXED$",100,XJ2+W,YML)
      IF(MASK(8).EQ.1) CALL MESSAG("FIXED$",100,XJ4+W,YML)
      IF(MASK(10).EQ.1)CALL MESSAG("FIXED$",100,XJ5+W,YML)
      IF(MASK(12).EQ.1)CALL MESSAG("FIXED$",100,XJ6+W,YML)
      CALL SIMPLX
      CALL BASALF ("L/CSCRIPT")
      CALL MIXALF ("SCRIPT")
      CALL MESSAG ("(D)ASHED = (T)HEORETICAL, (S)OLID = (E)XPERIMENTAL$"
     1            ,100,2.25*XSF,5.00*YSF)
      CALL CARTOG
```

```
      CALL RESET ("BASALF")
      IF (NPLSH .GT. 1) GO TO 4
C     PLOT ACTUAL DATA - SOLID LINE
      CALL CURVE(X,Y2,NPTS,0)
    4 CONTINUE
C     PLOT THEORETICAL CURVE - SOLID LINE
      CALL DASH
      CALL CURVE(X,Y,NPTS,0)
      CALL RESET("DASH")
      CALL ENDPL(NPLN)
      RETURN
      END
      SUBROUTINE PEAK(Y,NPTS,IPD,NPRINT)
C
C         THIS SUBROUTINE DETERMINES THE LOCATION OF DATA PEAKS
C         IT STORES THE PEAK INDICES IN IPD UP TO 100 PEAKS.
C     IF NPRINT = 1, PEAK INFORMATION IS PRINTED
C
      DIMENSION  Y(NPTS), IPD(100)
      COMMON /CONST4/ DELTAF,FZERO
C     INITIALIZE
C     NFLAG INDICATES POSITIVE SLOPE IF = 1
      YMAX = 0.0
      YMIN= 1.0
      NFLAG = 0
      J = 1
      IPD(1) = NPTS+1
      DO 11 I = 1,NPTS
C     REJECT INITIAL GARBAGE
      IF ( Y(I) .GT. 0.95) GO TO 10
      IF  (Y(I) .GT. YMAX .AND. NFLAG .EQ. 1) YMAX = Y(I)
C     FOUND PEAK
      IF  ( Y(I) .LT. YMAX .AND. NFLAG .EQ. 1) GO TO 5
      IF  (Y(I) .LT. YMIN .AND. NFLAG .EQ. 0) YMIN = Y(I)
C     POSITIVE SLOPE?
      IF ( Y(I) .EQ. YMIN) GO TO 10
C     SEE IF STILL ON DOWNTREND
      K1 = I+1
      K2 = I+5
      IF (K2 .GT. NPTS) GO TO 10
C     SCAN NEXT 10 POINTS
      DO 3 K = K1,K2
      IF ( YMIN .GT. Y(K)) GO TO 10
    3 CONTINUE
      NFLAG=1
      GO TO 10
C     FOUND PEAK - STORE INDEX
    5 CONTINUE
C     LOOK-AHEAD, MAKE SURE YMAX = PEAK
      K1 = I
      K2 = I+20
      IF (K2 .GT. NPTS) K2 = NPTS
C     SCAN NEXT 20 POINTS
      DO 7 K = K1,K2
C     YMAX REALLY PEAK OR GLITCH?
      IF ( YMAX .LT. Y(K) ) GO TO 10
    7 CONTINUE
C     YMAX REALLY PEAK
```

```
C
      IF (J .LE. 100) IPD(J)= I-1
      J = J+1
      IF(J .LE. 100) IPD(J) = NPTS+1
      IF (NPRINT .LT. 1) GO TO 25
      F = (FLOAT(I-1)*DELTAF + FZERO)/1.0E06
      PRINT 20, F, YMAX, IPD(J-1)
   20 FORMAT(* FOUND PEAK, FREQUENCY = *,F8.3,* MHZ, AMPLITUDE =*,F8.3,
     1        *, INDEX = *, I5)
   25 CONTINUE
      YMIN = Y(I)
      NFLAG = 0
      YMAX = 0.0
   10 CONTINUE
      IF (NPRINT .EQ. 2) PRINT 8,I,YMIN,YMAX,Y(I),NFLAG
    8 FORMAT (* I=*,I5,*,YMIN= *,E15.5,*,YMAX= *,E15.5,*,Y=*,E15.5,
     1        *, NFLAG = *, I3)
   11 CONTINUE
      RETURN
      END
      SUBROUTINE BFIT
      COMMON/STEPIT/NV,NTRACE,CHISQ,MASK(100),
     1               X(100),DELTAX(100),DELMIN(100),NF
      COMMON /BEST/ BX(100),NFBEST,NRPBST,BCHISQ
C
C     THIS SUBROUTINE STORES THE PARAMETERS RELATED TO THE BEST FIT
C
C     BX     - PARAMETER ARRAY
C     NFBEST - # OF THE FUNCTIONAL EVALUATION
C     NRPBST - # OF DATA PEAKS REJECTED
C     BCHISQ - BEST CHI SQUARED
C
      DO 10 I = 1,NV
      BX(I) = X(I)
   10 CONTINUE
      NFBEST = NF
      BCHISQ = CHISQ
      RETURN
      END
    0.635.64327E+06        2.70                                0.3
   0.0127  1.000E05        1.07                                1.84
1011101          3.0E06       15.0E06AL/ADHESIVE/AL SANDWICH-T6R095-VARY C
```

APPENDIX C

DOPPLER STUDIES

Submitted for publication in IEEE Transactions on Sonics and Ultrasonics.

MEASUREMENT OF THE RADIAL-BOLT-HOLE CRACK SIZE USING THE DOPPLER-SHIFT TECHNIQUE

by

N. K. Batra

ABSTRACT

The Doppler effect can be used to estimate the size of radial-bolt-hole cracks in mechanically fastened aircraft structures. A sample having a radial crack is mounted on a rotating platform in a water bath and interrogated using a train of tone bursts from a stationary, focused transducer. The Doppler-shift spectrum of the backscattered ultrasonic beam from the rotating crack is recorded. The maximum Doppler shift is then related to the radial size of the crack. The merits and limitations of this technique are discussed.

MEASUREMENT OF THE RADIAL-BOLT-HOLE CRACK SIZE USING THE DOPPLER-SHIFT TECHNIQUE

by

N. K. Batra *

I. INTRODUCTION

A major problem in extending the operational life of aircraft is the detection and measurement of the size of fatigue cracks in highly stressed areas of the airframe. The cracks that present the most serious threat to flight safety are those which grow from the bolt holes in mechanically fastened structures. These flaws are among the most difficult to detect for several reasons. First, these fatigue cracks most often occur under the heads of counter-sunk bolts at the base of the bolt holes. Second, the use of new high-strength structural alloys has necessitated the detection and size measurement of very small flaws in these crack-intolerant materials. At present the inspection procedure for detecting these defects consists of removing the fastener and inserting an eddy-current probe into the hole. Since the average cost of this inspection is approximately $150.00/bolt and large cargo aircraft may contain 20,000 critical fasteners, the economic incentive to develop semi-automatic instrumentation is readily apparent.

* Systems Research Laboratories, Inc., 2800 Indian Ripple Road, Dayton, OH 45440.

This research is sponsored in part by the Air Force Materials Laboratory, AFML/LLP, Wright-Patterson Air Force Base, OH 45433, under Contract F33615-77-C-5022.

60

Although several commercial instruments have been developed to detect these flaws, they do not have the capability to measure the size of the flaw. However, crack size has been estimated using a number of ultrasonic techniques[1] involving amplitude,[2] time,[3] and acoustic-spectrum methods.[4,5] Methods of size estimation which make use of the amplitude of the reflected sound wave are inaccurate for many reasons, the principal one being the differing reflectivities of fatigue cracks. Such methods also disregard several other important factors such as crack orientation, shape, and quality of the acoustic coupling--all of which affect measurement accuracy. Timing methods[3] have been used to estimate crack dimensions from the time delay of a signal returning from a crack relative to the excitation pulse, or some known scattering point on the fastener hole. These methods are cumbersome, and the best results are obtained for very large cracks such as those found in welded steel structures.

Because of the circular symmetry of the bolt-hole, a method based upon the Doppler Effect has been developed to measure radial crack size. This method does not depend upon the amplitude or time delay of the reflected signal from the crack. The maximum dimension of the crack is proportional to the maximum Doppler shift of the backscattered signal from the crack. The method is potentially more accurate than those used previously.

II. THEORETICAL DEVELOPMENT

The classical Doppler effect refers to the change in frequency which occurs when a sound wave is backscattered (reflected) from a discontinuity moving in the medium of the incident wave. A Doppler shift of the sound wave also

occurs when the wave enters a medium which is in motion relative to its source. The magnitude of the frequency shift can be used to estimate the size of a crack or reflector in the moving medium. In this section the equation used to estimate crack size is developed.

The schematic representation of the experiment is shown in Fig. 1. An ultrasonic transducer is in a water bath along with an aluminum plate rotating with angular velocity Ω in the x_1, x_2 plane. The wave-number vector, $\vec{k}$, of the incident longitudinal wave is shown in the x_1, x_3 plane. Several points concerning this physical arrangement should be noted. First, a Doppler shift in the frequency of the incident sound wave occurs both when the wave enters and exits the sample at the water/aluminum boundary. Second, since the angle of incidence of the beam is above the first critical angle (~ 13° for a water/aluminum interface), only a vertically polarized shear wave is transmitted into the sample. Finally, the incident beam is backscattered to the transducer only when the reflector is nearly at right angles to the incident-wave vector $\vec{k}$. Therefore, the plane of polarization of the sound beam is nearly perpendicular to the centripetal-acceleration vector during the backscattering process. For this reason, it can be assumed that any Doppler shift measured as a result of backscattering is independent of this acceleration. The magnitude of the Doppler shift of a backscattered tone burst from a rotating medium can be derived by performing a simple coordinate transformation. In Fig. 1(b) the position vector $\vec{r}^*$ at time t, in the rotating coordinate frame, is represented by

$$\vec{r}^* = R \cos (\theta - \Omega t)\hat{x}_1 + R \sin (\theta - \Omega t)\hat{x}_2 \qquad (1)$$

where R is the magnitude of vector $\vec{r}^*$ and $\hat{x}_1$ and $\hat{x}_2$ are unit vecotrs along the x_1 and x_2 axis, respectively. In the rotating coordinate system, the amplitude is given by

$$A(\vec{r}^*,\omega') = A_o \exp j(\vec{k} \cdot \vec{r}^* - \omega' t) \tag{2}$$

where $j = \sqrt{-1}$ and ω' is the circular frequency of the sound wave in the rotating frame. The transformation to the laboratory coordinate frame is given by

$$\vec{r} = \vec{r}^* + \dot{\vec{r}}^* t \tag{3}$$

where the dot refers to a time derivative. To the observer in the laboratory, the wave is described by

$$A(\vec{r},\omega) = A_o \exp j[\vec{k} \cdot \vec{r} - (\vec{k} \cdot \dot{\vec{r}}^* + \omega')t] \tag{4}$$

If the frequency of the incident beam in the moving system, ω', is related to the observed frequency, ω, in the laboratory system, the following relationship is obtained:

$$\omega = \omega' + \vec{k} \cdot \dot{\vec{r}}^* \tag{5}$$

If i is the angle of incidence in the x_1, x_3 plane, the wave vector $\vec{k}$ can be written as

$$\vec{k} = \hat{x}_1 |\vec{k}| \sin i + \hat{x}_3 |\vec{k}| \cos i \tag{6}$$

Using Eqs. (1), (5), and (6), the expression for the Doppler-shifted frequency can be written as

$$\omega = \omega' - |\vec{k}| R\Omega \sin i \sin (\Theta - \Omega t) \tag{7}$$

where $|\vec{k}| = \omega/c$ and c is the sound speed in the incident medium. A Doppler shift occurs when the wave enters the rotating media and again when the wave backscattered from the crack exits the disk. The wave vectors of the incident and backscattered waves are $\vec{k}$ and $-\vec{k}$, respectively. Therefore, the Doppler-shifted angular frequency, ω'', of the backscattered wave in the laboratory reference frame is given by

$$\omega'' = \omega' + |\vec{k}| R\Omega \sin i \sin (\Theta - \Omega t) \tag{8}$$

Hence, the Doppler-shifted angular frequency in the laboratory reference frame is given by

$$\omega_D = \omega'' - \omega = 2 |\vec{k}| R \Omega \sin i \sin (\Theta - \Omega t) \tag{9}$$

The net change in frequency of an incident wave after backscattering by a point reflector at radial distance R in a rotating medium is given by

$$f_D = \frac{4\pi R}{cT} f_o \sin i \sin (\Theta - \Omega t) \tag{10}$$

where T is the period of rotation of the rotating reference frame, and is defined by $T = 2\pi/\Omega$, and f_o is the frequency of the incident sound wave. Since back-scattering occurs only in a small angular range where $\Theta - \Omega t \approx 90°$, Eq. (10) may be simplified to

$$f_D = \frac{4\pi R}{cT} f_o \sin i \qquad (11)$$

A Doppler-frequency shift f_D will occur for every point at radial distance R along a crack or defect for which acoustic energy is backscattered from the rotating coordinate system. The maximum value of this shift should, therefore, yield the maximum radial dimension of the defect, provided the beam is backscattered from the tip of the crack.

III. EXPERIMENTAL PROCEDURE

In these experiments 21 aluminum (6061-T6) disks 6.35 mm thick and 8.9 cm in diam. having 6.35-mm-diam. central holes were used. Six disks contained radial electro-discharge-machined (EDM) slots extending radially from the central hole. The slots were from 1.02 to 2.84 mm in radial length and their shape approximated a quarter circle, as shown schematically in Fig. 1. One disk contained two radial EDM slots, 180° apart. Four disks contained three square EDM slots, each of a different size and placed at different radial distances from the center of the specimen. Nine disks contained radial fatigue cracks. These cracks were obtained by placing an EDM slot in the center of each plate, cyclically loading the plate in three-point bending to grow a fatigue crack in the slot, and then drilling a hole in the plate such that the crack alone extended from the base of the hole. The fatigue cracks were all approximately quarter-circle shape. Figure 2 is a micrograph of such a crack.

To test the viability of this technique in detecting flaws in the second layer of multilayered structures, several samples were constructed which consisted of two aluminum plates bonded together with a silicon (RTV)[6] rubber that

simulated the sealant used in aircraft construction. As shown in Fig. 3, the second aluminum contained the crack or EDM slot. Care was taken during bonding of the two plates to ensure that the RTV did not enter the slot. The silicon-rubber inner layer was nominally 0.30-mm thick.

From the theoretical development it is apparent that either the transducer or the sample containing the crack may be rotated. For mechanical convenience, the experiments were conducted using a rotating sample with a stationary transducer as shown in Figs. 1 and 3.

Each sample was mounted on a platform which was rotatable at a constant angular velocity Ω. The platform was placed in a water bath which served as a couplant. A focused transducer was used to transmit a 10-MHz tone burst, typically 35 μsec in duration, at a repetition rate of 10 KHz. This ultrasonic beam was incident at an angle, i, which ranged from 14 to 28° with respect to the normal to the disk. At this angle of incidence, the longitudinal wave mode converted to a shear wave at the water/aluminum interface. The position of the transducer relative to the hole was adjusted in such a way that the refracted shear wave propagated tangentially to the circumference of the hole. Care was taken to ensure that the beam did not intersect the hole for small cracks and that it covered the tip of the crack for large cracks.

The instrumentation used in these experiments is shown schematically in Fig. 4. The received signal containing the Doppler shift was heterodyned with the transmitted signal in a double-balanced mixer. The sum-frequency band from the mixer was rejected by a low-pass filter (1-100 Hz), while the difference band

was fed into a Hewlett-Packard HP 3580A low-frequency spectrum analyzer and recorded on an X-Y plotter. A 100-sec/div. window having a 5-Hz frequency span/division at a bandwidth resolution of 1 Hz was used. This sampling rate was adequate to avoid aliasing of signals band-limited to frequencies less than 50 Hz. Data were also taken with an HP 3582A real-time dual-channel spectrum analyzer which has better bandwidth resolution. Both analyzers were used in the free-running mode with the RMS average of the spectrum taken on the HP 3582A. Since the backscattered signal from the crack is transient (occurs only once during the period of rotation of the disk), a uniform filter was used on the HP 3582A to achieve optimum results.

IV. RESULTS AND DISCUSSION

The Doppler shift in the backscattered signal from the crack is linearly dependent [Eq. (11)] upon the frequency of the incident wave, f_o, and the angular speed, Ω, of the disk. To ensure that the backscattered signal was due to the Doppler effect, the frequency shift corresponding to the maximum amplitude of the backscattered signal was measured as a function of the frequency of the incident wave and the angular speed of the disk. In both cases a linear relationship resulted, as shown in Figs. 5(a) and (b).

The scan of a disk without a notch is shown in Fig. 6. The spectrum is flat except for the slight hump around 30 Hz caused by a slight eccentricity in alignment of the transducer and the central hole of the aluminum disk which results in scattering from the hole for a small sector in the

revolution of the disk. Since this signal also has a Doppler shift, it may be interpreted as resulting from a crack, thus illustrating the need for careful alignment of the transducer, especially for small cracks.

A typical output for the Doppler experiment is shown in Fig. 7. It can be seen that the rotating crack, with its radial distribution of velocities, does indeed produce a broadened Doppler peak. The spikes in the envelop of the spectrum are due to the slow sampling rate of the HP 3580A swept analyzer. The maximum frequency of the Doppler shift (the point at which the peak enters the noise level) is 29.0 Hz. If Eq. (11) and the experimental parameters are used, this frequency corresponds to a reflector having a maximum radial dimension of 4.53 mm. With an a priori knowledge of the hole size (3.18 mm), the maximum slot dimension is calculated to be 1.35 mm. The actual size (1.52 mm) was determined by optical microscopy. Figure 8 shows the Doppler spectrum from a disk containing a 0.94-mm EDM slot taken with a HP 3582A operated in the RMS mode. The maximum Doppler-shift frequency for this spectrum occurs at 43 Hz, yielding a maximum radial dimension for the slot of 4.16 mm. A calculated radial size of 0.98 mm is in excellent agreement with the actual size of 0.94 mm.

When the Doppler-shift technique is used to determine flaw-size, it is necessary to ensure that the focal spot of the ultrasonic beam will cover the tip of the crack. To accomplish this it is necessary to scan the crack moving the focal spot radially outward (along x_2) from the point of tangency to the hole to the tip of the crack. When the maximum frequency of the spectra ceases to increase, the focal spot covers the

maximum extent of the flaw. Figure 9 shows the Doppler spectrum taken at four different locations on a disk containing a 2.84-mm EDM slot. As expected, the Doppler spectrum attained a maximum frequency of 20 Hz. The amplitude of the spectrum began to decrease after this point since less of the ultrasonic energy in the focal spot was reflected from the flaw. Consequently, it is concluded that so long as the focal spot of the beam intersects the tip of the flaw and does not intersect the hole, the beam need not be tangential to the circumference of the hole.

When a real-time analyzer was used, it was possible to detect multiple radial cracks in the time domain. However, with a swept analyzer, the size of the multiple radial slots could be detected and measured simultaneously at different angular positions because the Doppler spectra of the flaws are superimposed. From a maximum Doppler shift from each peak, the maximum radial dimension for each slot could be calculated. With a real-time spectrum analyzer, the spectrum for each flaw could be obtained by time gating.

Figure 10 shows the Doppler spectrum obtained from a sample containing a fatigue crack. The spectrum is complex since fatigue cracks are diffuse scatterers. When the procedure outlined above was used, the crack size was estimated to be 1.39 mm. Microscopic examination revealed the radial dimension to be 1.40 mm. The data collected on all disks are shown in Fig. 11. It should be noted that the data for each flaw size were taken from several disks having identical size slots or cracks, with at least three replicates of the spectra being taken on each disk. The agreement between the acoustic and optical size estimates is quite good.

Data were also taken on the three-layered samples containing radial EDM slots at the upper surface of the lower disk. One difficulty in taking data on these samples was that the frequency of the incident wave had to be such that no standing waves were generated in the RTV inner layer. Also, because of the high attenuation of the incident signal in the RTV layer, a power amplifier was inserted into the output circuit to achieve the desired signal-to-noise ratio. Figure 12 gives the experimental results from these measurements. Again the agreement between the optical and acoustic results is quite good.

Results in Figs. 11 and 12 show that it is possible to measure the radial size of cracks under the holes in single and multilayered structures. Measurement accuracy is estimated to be within 20%. It should be mentioned that the most frequent error encountered was failure to achieve the required tangency to the central hole for small flaws. In one case, the measurement error was caused by a slight error in the position of the hole--its center was not at the rotational center of the plate. Since the reflection from an eccentrically rotating hole is identical to that of a crack, it may appear that a crack is present when, in fact, it is not.

Several curved fatigue cracks were also studied. As expected for the nonradial cracks, only the maximum radial dimension of the crack could be measured.

V. CONCLUSIONS

It has been demonstrated that the radial size of cracks which extend radially from bolt holes in both single and multilayer mechanically fastened structures can be measured using the Doppler-shift technique. The technique is free from the many

70

uncertainties associated with size measurement by amplitude and timing methods. However, the method is susceptible to external vibration and also requires adjustment of the direction of the incident beam to avoid its intersecting the hole during rotation. In practice, this method could provide a reliable estimate of the maximum radial extent of cracks which eminate from bolt holes in aircraft structures.

REFERENCES

[1] P. A. Doyle and C. M. Scala, "Crack Depth Measurement of Ultrasonic A Review," Ultrasonics, vol. 16, pp. 164-170, 1978.

[2] S. Krautkramer, "Determination of the Size of Defects by the Ultrasonic Impulse Method," Brit. J. Appl. Phys., vol. 10, pp. 240-245, 1959.

[3] M. G. Silk and B. H. Lidington, "The Potential of Scattered or Diffracted Ultrasound in the Determination of Crack Depths," Non-Destructive Testing, vol. 8, pp. 146-151, 1975.

[4] L. Alder, K. V. Cook, H. L. Whaley, and R. W. McClung, "Flaw Size Measurements in a Weld Sample by Ultrasonic Frequency Analysis," Materials Evaluation, vol. 35, pp. 44-50, 1977.

[5] M. D. Fox, "Multiple Crossed-Beam Ultrasound Doppler Velocimetry," Sonics and Ultrasonics, vol. SU-25, pp. 281-286, 1978.

[6] Registered Trademark of the General Electric Co., Silicon Products Operation, Waterford, NY.

FIGURE CAPTIONS

<u>**Figure**</u>

1 (a) Schematic representation of rotating aluminum disk in water bath. $\vec{k}$ is wave vector of incident longitudinal wave.

(b) Experimental arrangement of ultrasonic beam and rotating crack. Angle of incidence, i, is chosen such that only shear wave propagates in aluminum disk.

2 Optical micrograph of a typical fatigue crack used to obtain the Doppler data. The bolt hole is in the lower left-hand corner of the micrograph.

3 Experimental arrangement for Doppler experiments on layered samples.

4 Block diagram of electronic set-up for Doppler-shift studies of radial cracks.

5 (a) Doppler-frequency shift as a function of frequency of incident beam. Note linear dependence of Doppler-shift peak upon frequency of incident beam.

(b) Doppler-shift frequency f_D vs angular speed of crack. Note linear dependence.

6 Doppler-shift spectra taken on disk containing no flaws or slot. Low-amplitude hump around 30 Hz is due to a slight eccentricity of beam with respect to the hole. f_o = 11.65 MHz, T = 4.5 sec/rev, i = 23°, r = 3.18 mm.

Figure

7 Doppler-shift spectra for radial EDM notch. Low-amplitude hump under main peak is caused by eccentricity in beam alignment. f_o = 11.65 MHz, T = 4.515 sec/rev, i = 17°, $\left(f_D\right)_{max}$ = 29 Hz, c = 1.48 × 10^5 cm/sec, r = 3.18 mm, a = 1.35 mm.

8 Doppler-shift spectra for 0.94-mm radial slot taken with real-time analyzer. f_o = 12.76 MHz, T = 3.24 sec/rev, i = 18°, $\left(f_D\right)_{max}$ = 43 Hz, r = 3.18 mm, a = 0.98 mm.

9 Doppler-shift spectra taken on disk with slot greater than ultrasound focal spot size. Note that maximum Doppler frequency (20 Hz) does not change as beam is moved across rotating slot but the amplitude of Doppler peak drops once the focal spot does not cover the slot. Spectra D is for the case where beam does not intersect slot. f_o = 12.76 MHz, T = 10.0 sec/rev, i = 18°, $\left(f_D\right)_{max}$ = 20 Hz, r = 3.18 mm, a = 2.79 mm.

10 Doppler-shift spectra for real fatigue crack. f_o = 12.76 MHz, T = 3.40 sec/rev, i = 18°, $\left(f_D\right)_{max}$ = 45 Hz, r = 3.18 mm, a = 1.39 mm.

11 Plot of crack size as measured in Doppler studies as function of actual crack size for single-layer samples. The following notation is used: o Round EDM slot

* Square EDM slot

\+ Fatigue crack

12 Plot of crack size as measured in Doppler studies as function of actual crack size for multi-layered samples.

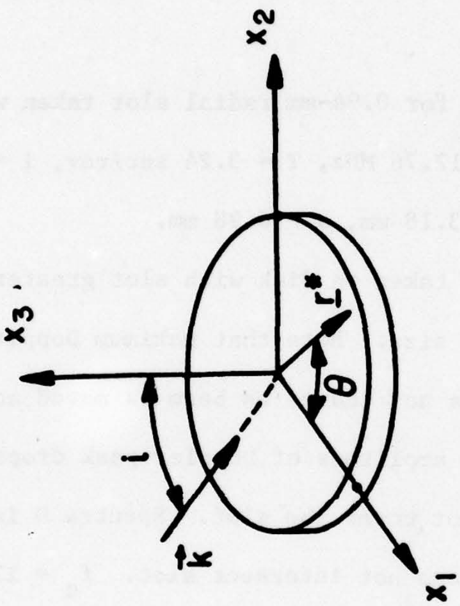

Fig. 1(a)

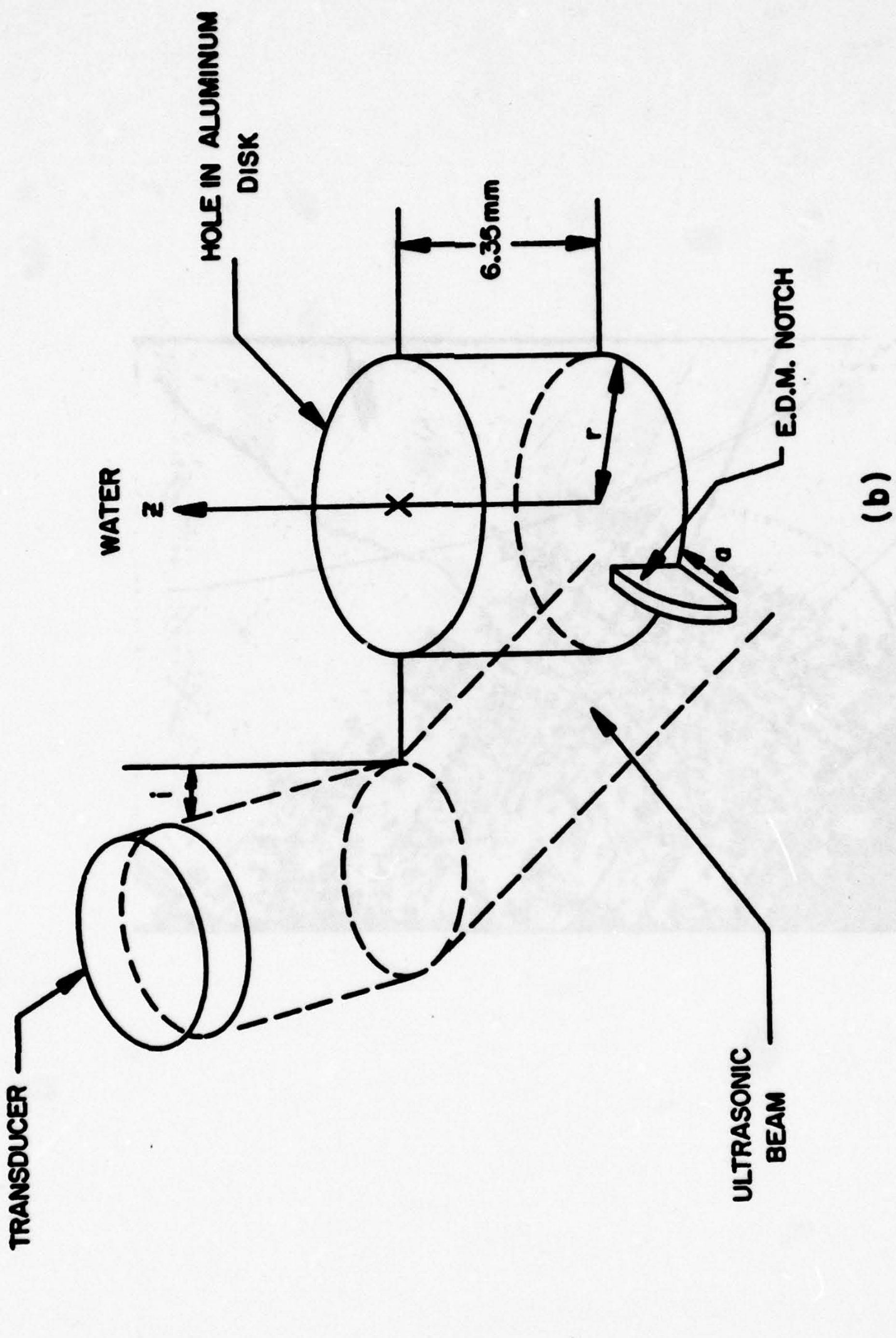

TRANSDUCER
i
WATER
z
HOLE IN ALUMINUM DISK
6.35mm
r
E.D.M. NOTCH
a
ULTRASONIC BEAM
(b)

Fig. 1(b)

Fig. 2

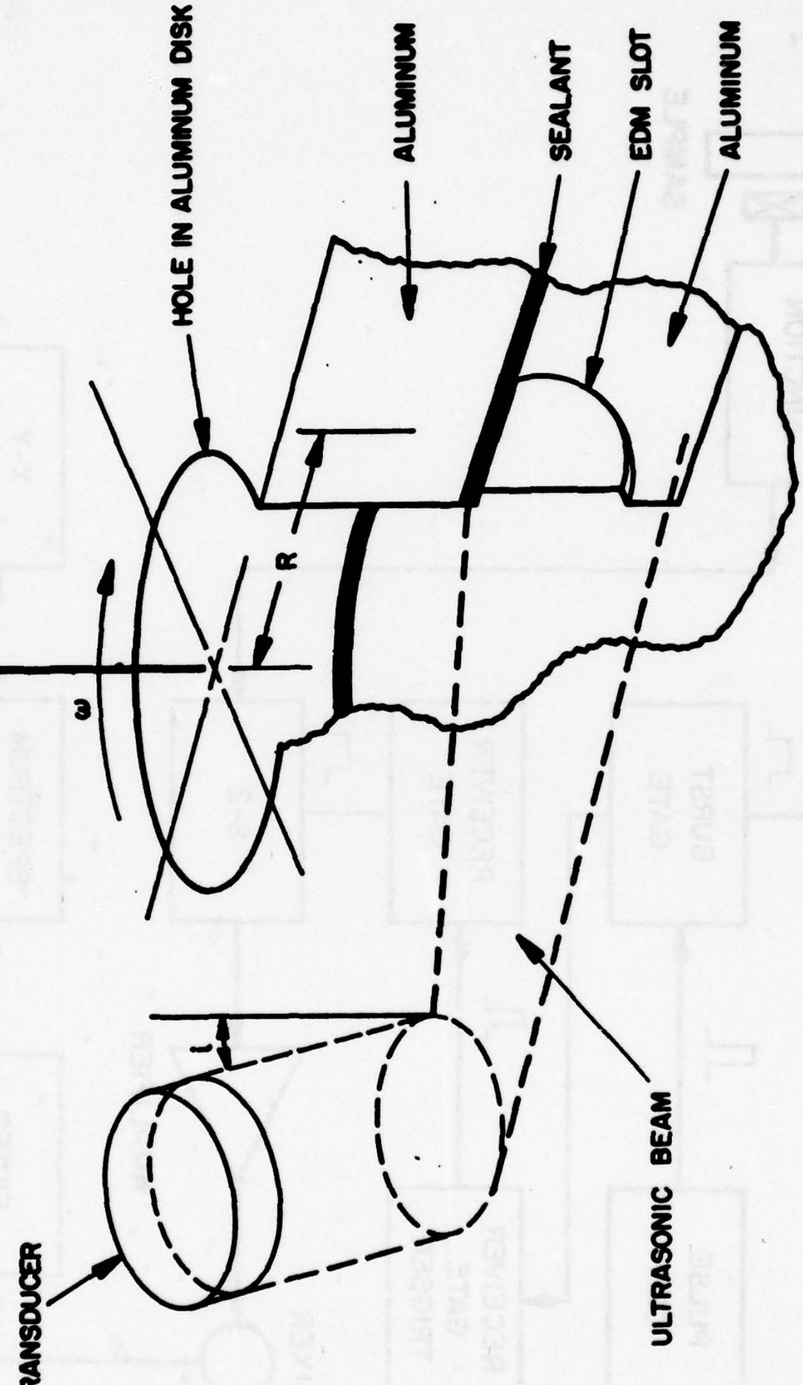
TRANSDUCER
ULTRASONIC BEAM
WATER
Z
ω
R
HOLE IN ALUMINUM DISK
ALUMINUM
SEALANT
EDM SLOT
ALUMINUM

Fig. 3

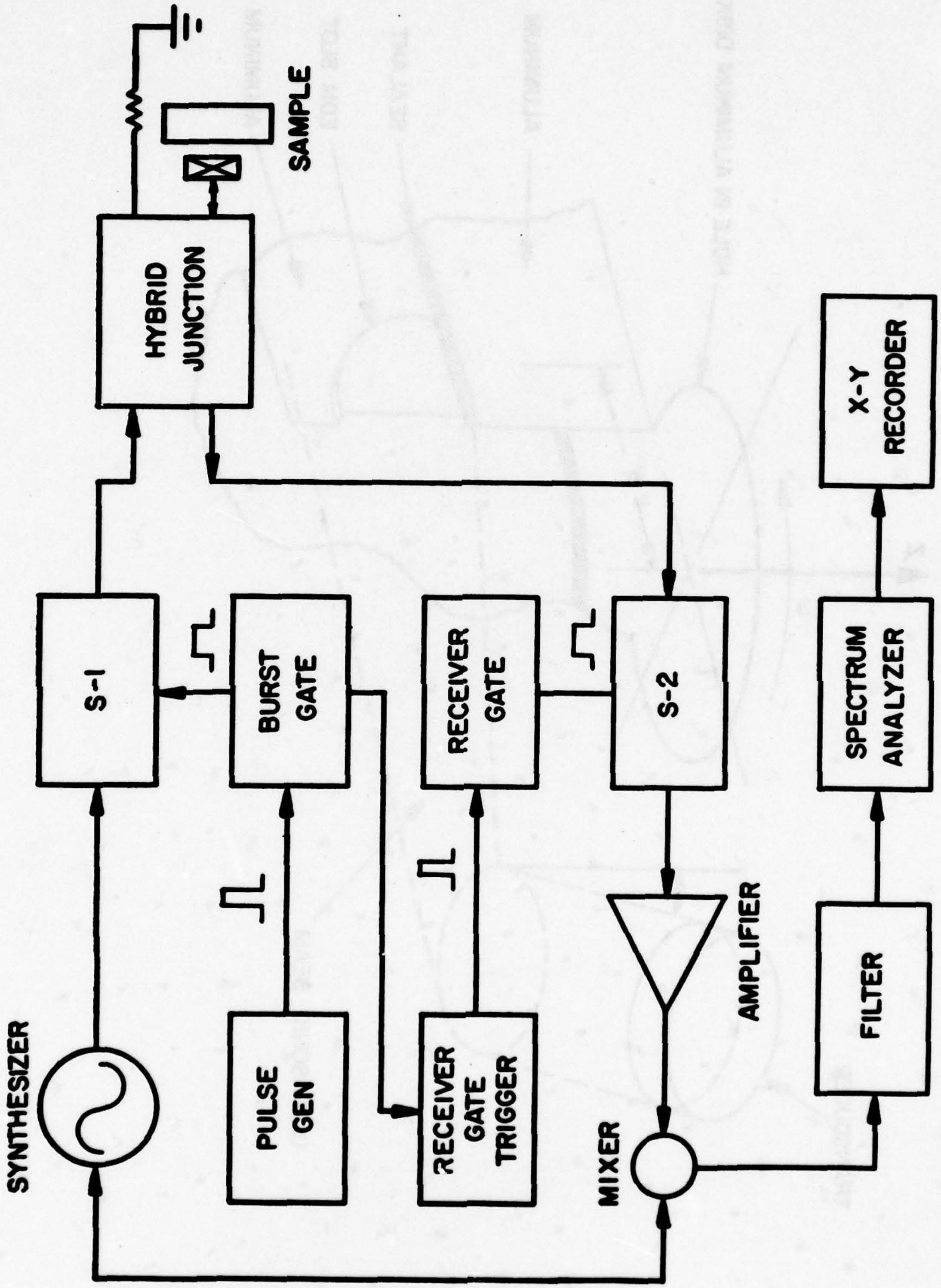
SYNTHESIZER
S-1
HYBRID JUNCTION
SAMPLE
PULSE GEN
BURST GATE
RECEIVER GATE TRIGGER
RECEIVER GATE
S-2
MIXER
AMPLIFIER
FILTER
SPECTRUM ANALYZER
X-Y RECORDER

Fig. 4

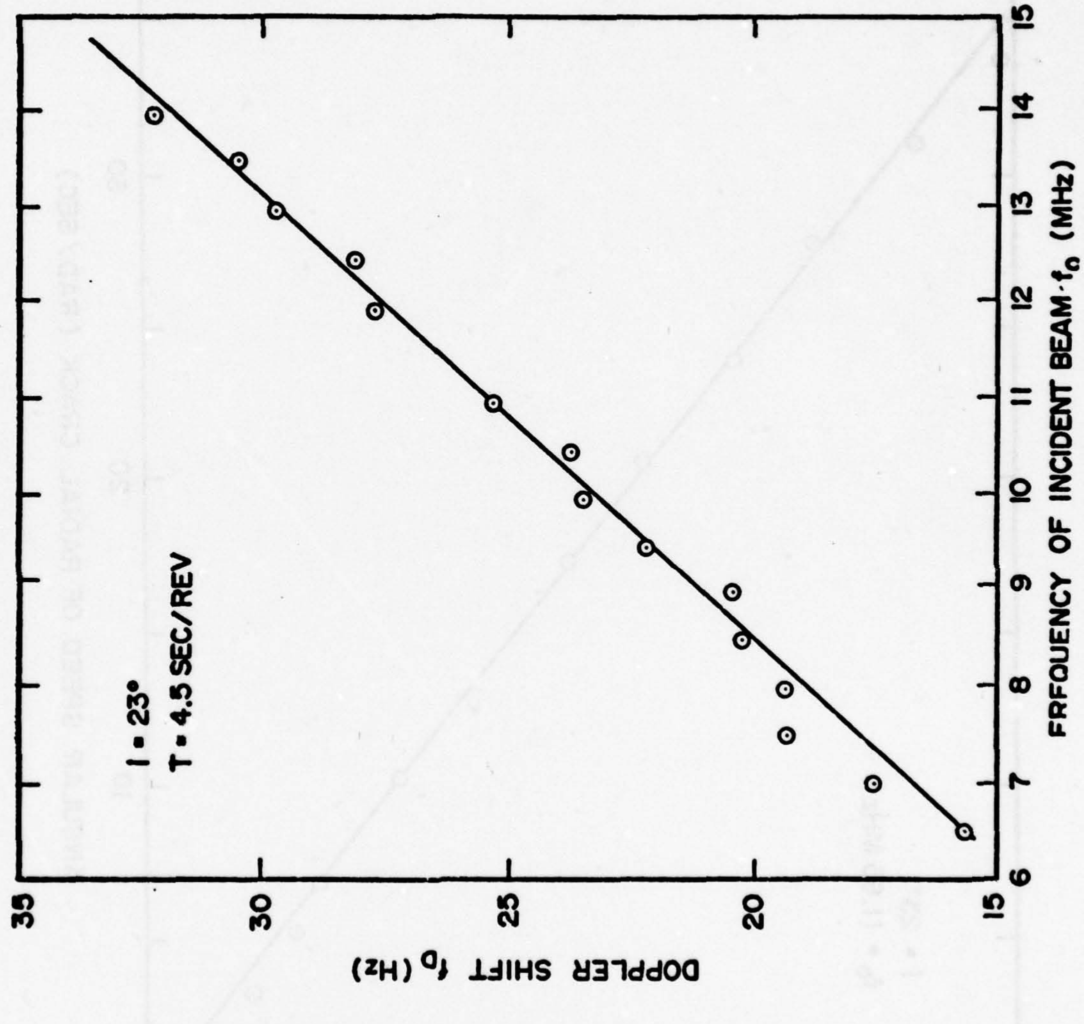
I = 23°
T = 4.5 SEC/REV
DOPPLER SHIFT f_D (Hz)
FRFQUENCY OF INCIDENT BEAM f_o (MHz)
35
30
25
20
15
6
7
8
9
10
11
12
13
14
15

Fig. 5a

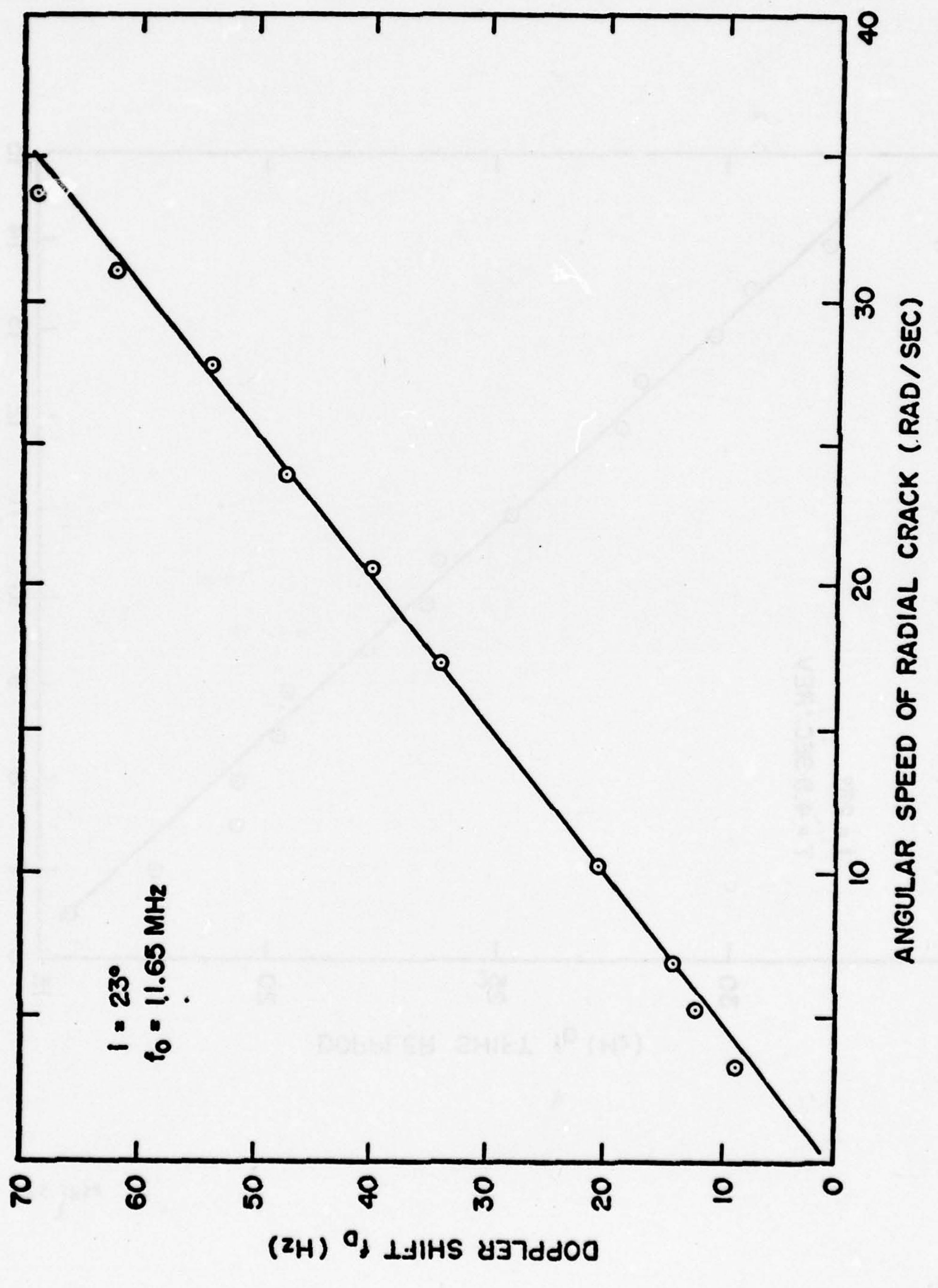
DOPPLER SHIFT f_D (Hz)
ANGULAR SPEED OF RADIAL CRACK (RAD/SEC)
θ = 23°
f_0 = 11.65 MHz
0
10
20
30
40
50
60
70
10
20
30
40

Fig. 5b

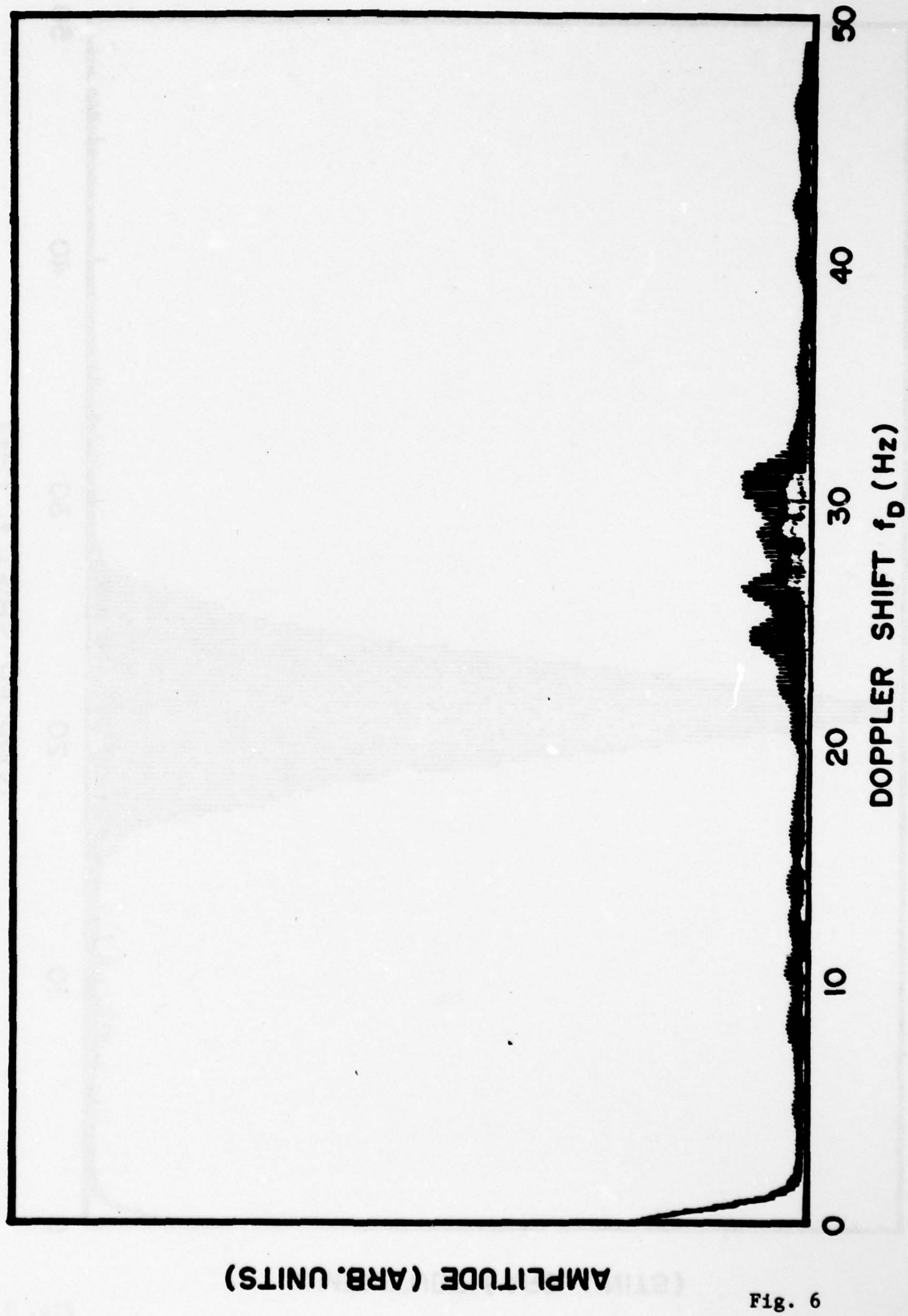

Fig. 6

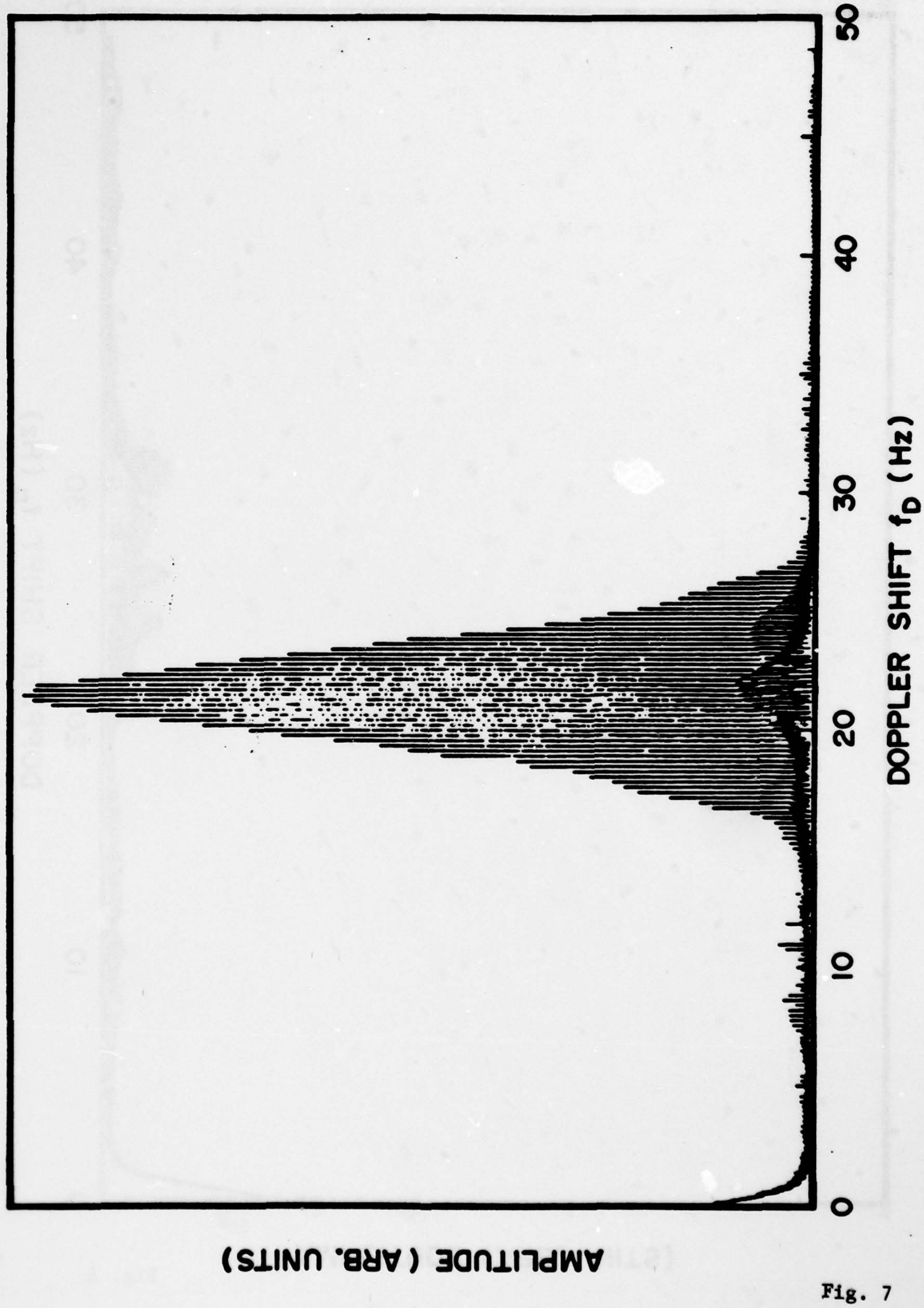

Fig. 7

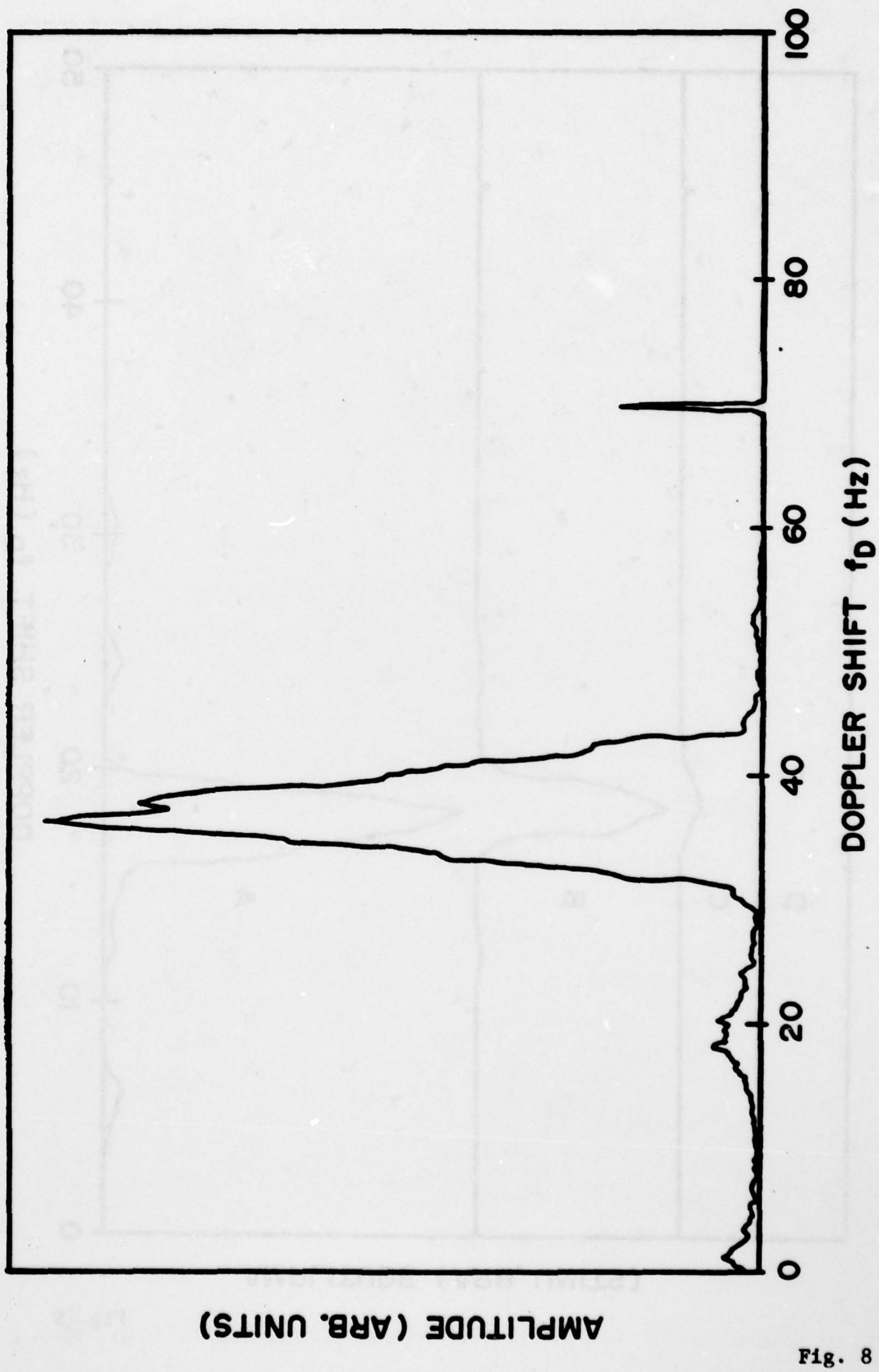

Fig. 8

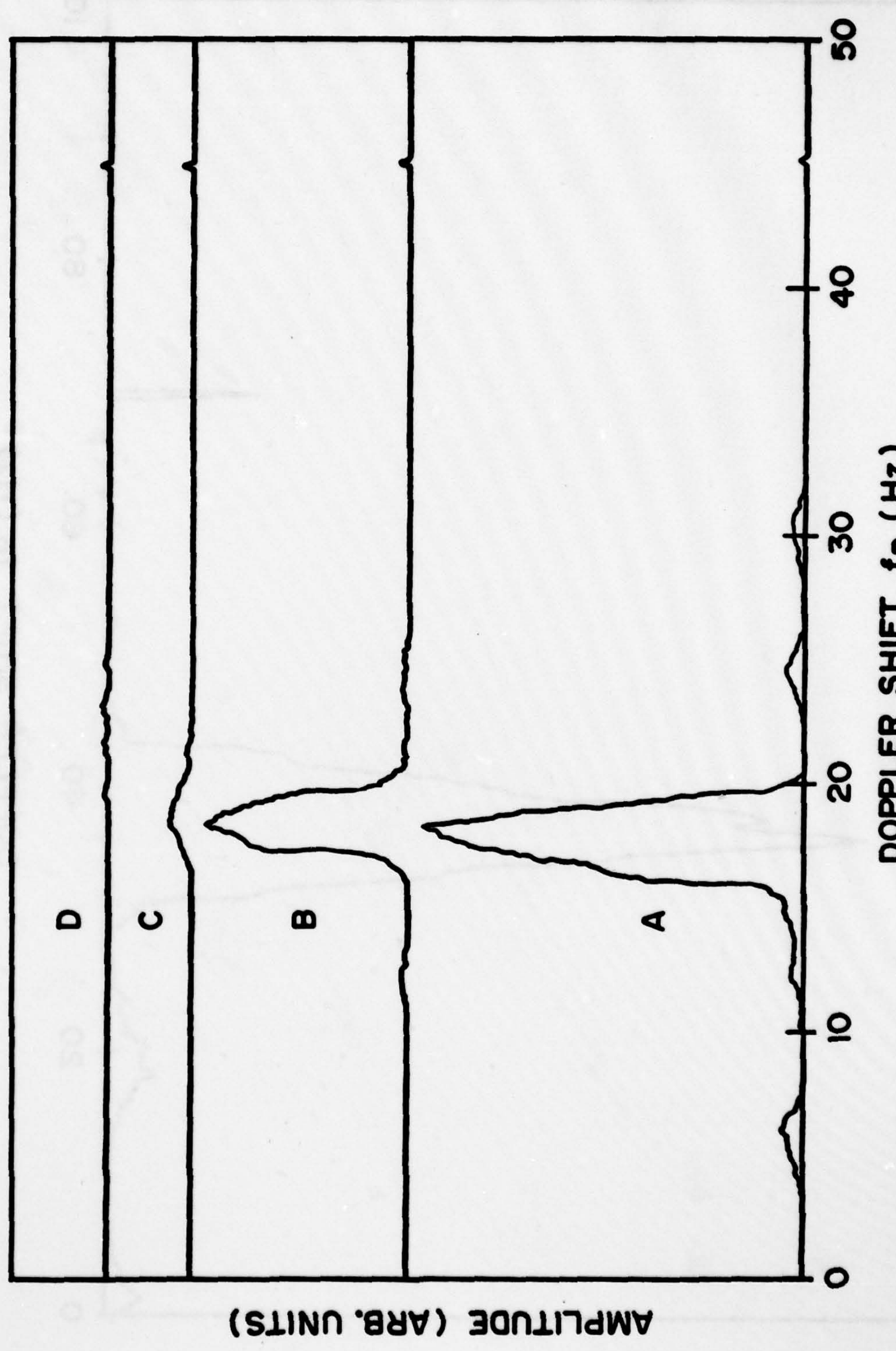

Fig. 9

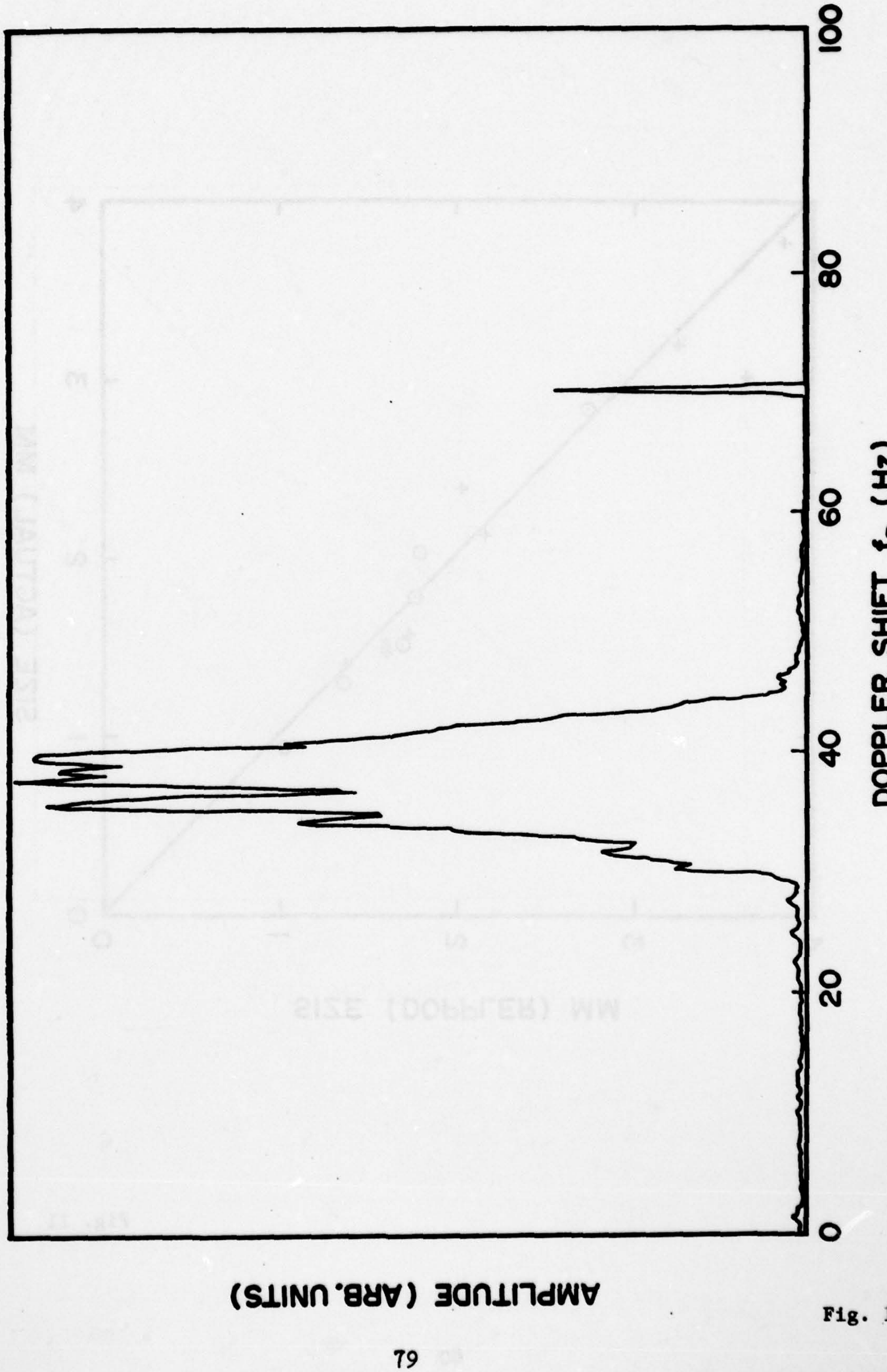

Fig. 10

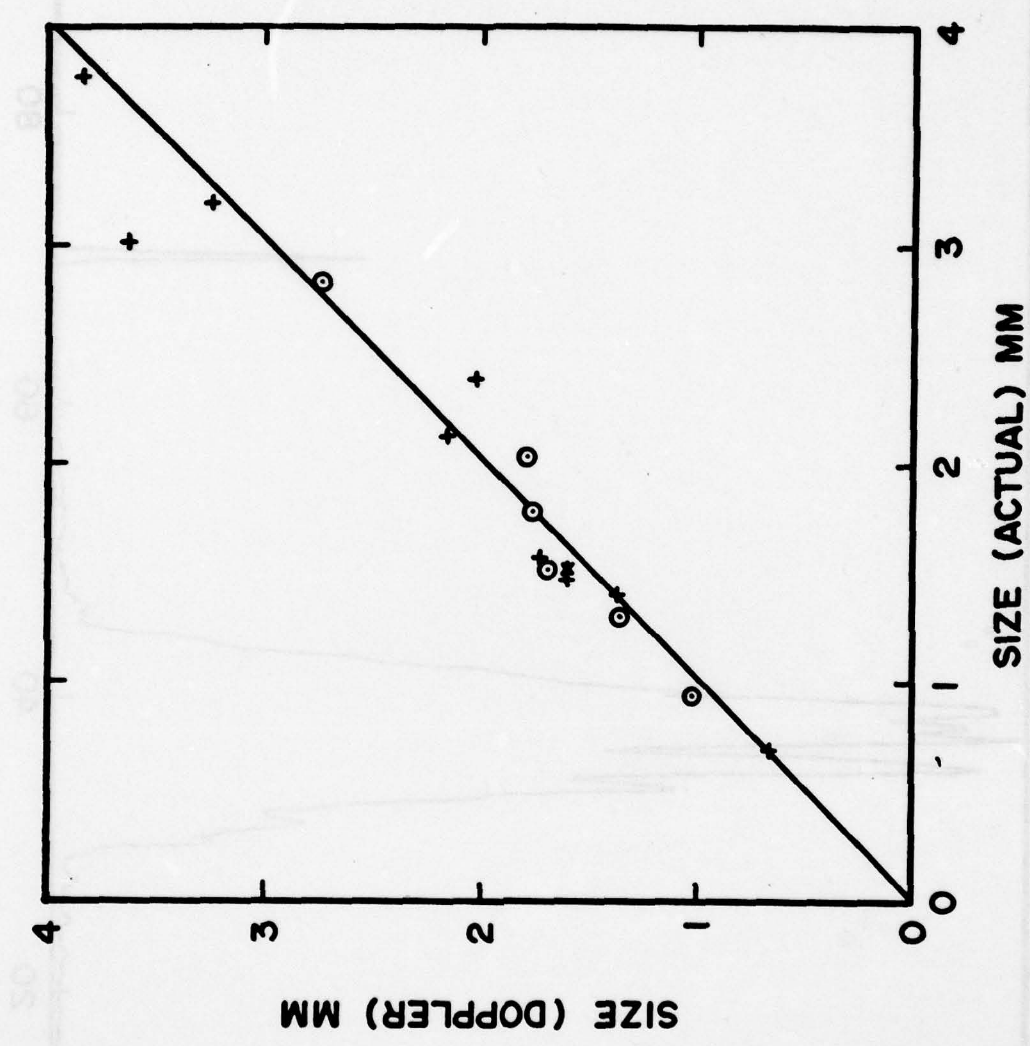

Fig. 11

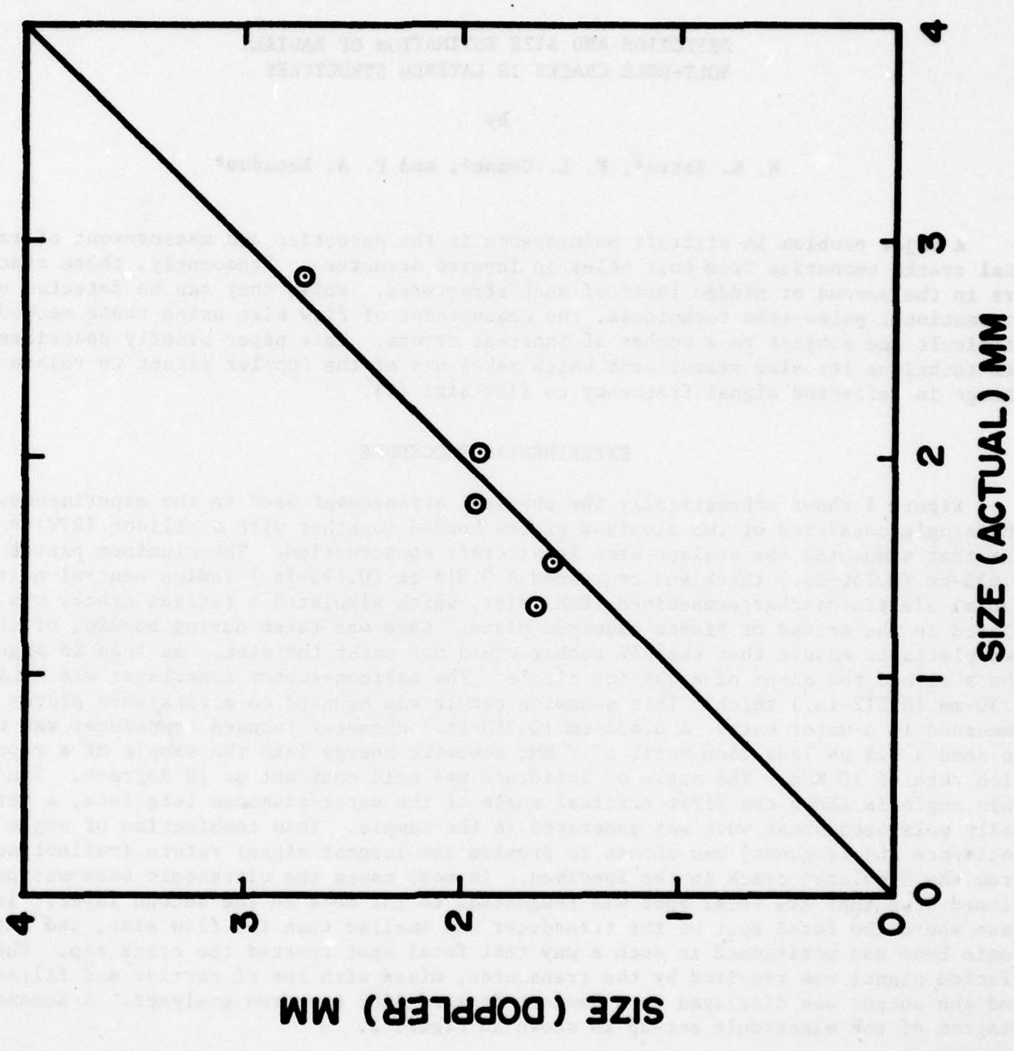

Fig. 12

Published in Paper Summaries, National Fall Conference, American Society for Nondestructive Testing, San Diego April 2-5, 1979, (American Society for Nondestructive Testing, Columbus, OH, 1979), pp 169-174.

DETECTION AND SIZE ESTIMATION OF RADIAL BOLT-HOLE CRACKS IN LAYERED STRUCTURES

by

N. K. Batra*, R. L. Crane+, and P. A. Benadum*

A major problem in aircraft maintenance is the detection and measurement of radial cracks emanating from bolt holes in layered structure. Frequently, these cracks are in the second or hidden layer of such structures. While they can be detected using conventional pulse-echo techniques, the measurement of flaw size using these methods is difficult and subject to a number of inherent errors. This paper briefly describes a new technique for size measurement which makes use of the Doppler effect to relate the change in reflected signal frequency to flaw size (1).

EXPERIMENTAL PROCEDURE

Figure 1 shows schematically the physical arrangement used in the experiments. The sample consisted of two aluminum plates bonded together with a silicon (RTV)** rubber that simulated the sealant used in aircraft construction. The aluminum plates were 0.635-cm (0.250-in.) thick and contained a 0.318-cm (0.125-in.) radius central hole. A radial electro-discharge-machined (EDM) slot, which simulated a fatigue crack, was placed in the second or hidden aluminum plate. Care was taken during bonding of the two plates to ensure that the RTV rubber would not enter the slot. As seen in Figure 1 the slot had the shape of a quarter circle. The silicon-rubber innerlayer was nominally 0.30-mm (0.012-in.) thick. This sandwich sample was mounted on a rotatable platen and immersed in a water bath. A 0.635-cm (0.250-in.) diameter focused transducer was used to send a 3.5 μs long tone burst of 7 MHz acoustic energy into the sample at a repetition rate of 10 KHz. The angle of incidence was held constant at 18 degrees. Since this angle is above the first critical angle of the water/aluminum interface, a vertically polarized shear wave was generated in the sample. This combination of angle of incidence and frequency was chosen to provide the largest signal return (reflection) from the simulated crack in the specimen. In most cases the ultrasonic beam was positioned such that its focal spot was tangential to the hole in the second layer. In the case where the focal spot of the transducer was smaller than the flaw size, the ultrasonic beam was positioned in such a way that focal spot covered the crack tip. The reflected signal was received by the transducer, mixed with the rf carrier and filtered, and the output was displayed on a Hewlett-Packard 3582 spectrum analyzer. A schematic diagram of the electronic set-up is shown in Figure 2.

---

*Systems Research Laboratories, Inc., Dayton, OH
+Air Force Materials Laboratory, Wright-Patterson AFB, OH

**Registered Trademark of the General Electric Co., Silicon Products Operation, Waterford, NY

THEORY

The Doppler effect typically refers to the change in frequency which occurs when a sound beam is reflected from a discontinuity that is moving in the medium of an incident wave. A Doppler shift can also occur when the sound wave enters a medium that is in motion relative to the emitter. This latter case is applicable to the experiment described schematically in Figure 1. Here the ultrasonic wave experiences a frequency shift at the water/aluminum interface both upon entering and exiting the sample. This Doppler shift has a range of frequencies as a result of the radial distribution of velocities across the beam spot on the upper surface of the sample. As a result, the extent of reflection of the signal by the crack determines the extent of the Doppler shift. It should be noted that the reflection of the signal occurs over a very small angular range because of the physical arrangement of the experiment and the small focal spot size of the transducer. With these considerations in mind, it is possible to derive a mathematical relationship relating the Doppler shift to the crack dimensions (1). The frequency shift of an ultrasonic wave that enters a rotating media at radial distance R and is reflected back into a non-moving media is given by,

$$f_D = \frac{4\pi f_o R}{c\tau} \sin i \qquad (1)$$

where f_D is the Doppler frequency, f_o is the incident frequency, c is the wave speed of sound in water, τ is the period of rotation of the sample, and i is the angle of incidence of the ultrasonic beam in water. This equation can easily be used to establish the maximum extent of the crack. With a priori knowledge of the hole size, the crack dimension can be determined.

RESULTS AND DISCUSSION

The data from a typical experiment is shown in Figure 3. The time record of the wave reflected from the EDM slot is shown in Fig. 3A, while the spectrum of the signal is shown in Fig. 3B. The bandwidth of the Doppler spectrum extends from approximately 16 to 35 Hz. Using Equation (1) and the data shown in Figure 3, this corresponds to radial reflector dimensions of 2.6 mm (0.1 in.) to 5.9 mm (0.23 in.). Assuming the ultrasonic focal spot completely covers the slot, then these data indicate a radial EDM slot dimension of 3.3 mm (0.13 in.). The actual dimensions of 3.175 mm(0.125 in.) for the radius of the hole and 3.0 mm (0.12 in.) for the slot correspond favorably to the predicted sizes. Note that it is the maximum frequency of the Doppler shift or the maximum radial slot dimension that is important rather than the absolute distances. For actual measurements the hole size is known a priori, eliminating the uncertainty in the measurement of one parameter. Figure 4A shows the time record of data taken on a sample containing two radial EDM slots 180^o apart, one being 1.24 mm and the other 1.32 mm. Figure 4B is an expanded region of the time record which shows that a slot is in view for only 0.185 seconds. Figure 4C shows the Doppler spectrum from one of the slots. It was possible using the HP3582 spectrum analyzer to detect multiple radial cracks using the time mode; here, however, it was not possible to estimate the size of a slot uniquely when two or more such slots were present. However, it would be possible to measure the size of one slot uniquely if the motion of the platform could be synced with the spectrum analyzer.

Table I contains a summary of the data taken thus far for sandwich samples containing both EDM slots and fatigue cracks. It is apparent that the Doppler technique is quite capable of yielding a reasonable estimate of flaw size in layered or sandwich aircraft structure. An experimental bound on the error in these measurements has been found to be about 20 percent. While it is possible to achieve much better accuracy if

40

TABLE I. Summary of Experimental Results

Sample No.	Measured Crack Size (Optical)		Estimated Crack Size (Doppler)	
	mm	in.	mm	in.
1	1.32	0.052	1.65	0.065
2	1.52	0.060	1.57	0.062
3	1.79	0.070	1.93	0.076
4	2.03	0.080	1.91	0.075
5	2.84	0.112	2.72	0.107

great care is taken, such effort does not seem to be warranted at this time. It should be mentioned that the most frequent error encountered was the failure to achieve the required beam tangency to the central hole. In one case the measurement error was caused by a slight error in the position of the hole, such that its center was not at the rotational center of the plate. Since the reflection from an eccentrically rotating hole is quite similar to that of a crack, it may appear that a crack is present when, in fact, it is not. Also, with the existing experimental set-up, alignment of the ultrasonic beam with the central hole is quite difficult. Again a reflection from the hole can mimic a crack.

Another possible difficulty--one that plagues all ultrasonic inspections of layered aircraft structure--is the total reflection of ultrasonic energy from a layer that is (n+1)/4 wavelengths thick. This problem is well known to those using wide-band ultrasonic techniques. In the Doppler experiment, the problem can become acute because of the use of a tone burst or single-frequency ultrasonic energy. When this problem was encountered in the present study, the frequency of the incident wave was changed.

CONCLUSIONS

It has been shown that the Doppler effect may be used to estimate the size of radial crack-like flaws in multilayer aircraft structures. The technique is capable of predicting crack size with an accuracy of better than 20 percent. While this technique may not be used to detect cracks emanating from bolt holes, it does represent a possible method of estimating defect size. Also it does not suffer from many of the inherent errors that limit amplitude methods for measuring crack size.

REFERENCES

1. Batra, N. K. and Crane, R. L., "Measurement of Radial Bolt Hole Crack Size Using Doppler-Shift Techniques", to be published.

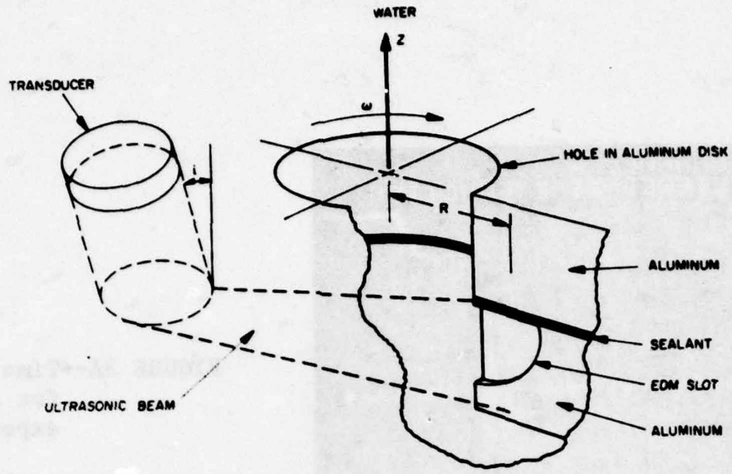

FIGURE 1--Experimental arrangement of Doppler experiments.

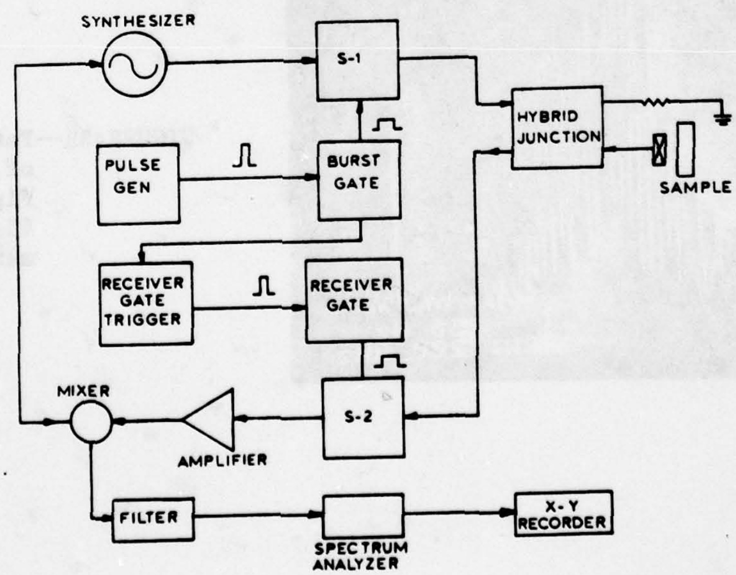

FIGURE 2--Block diagram of electronic set-up used in Doppler experiments.

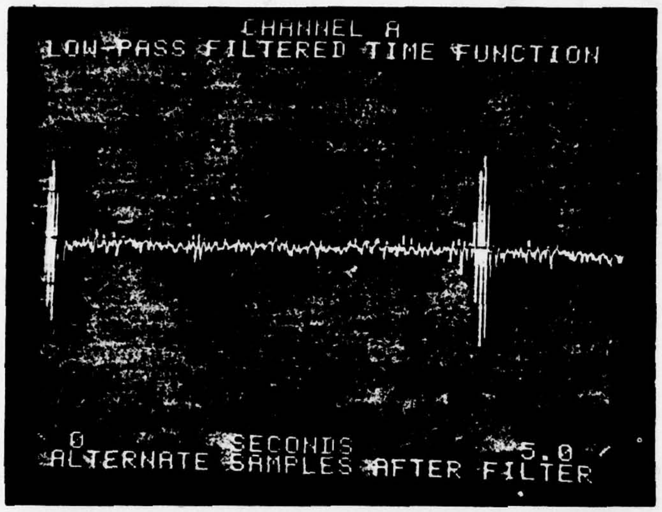

FIGURE 3A--Time record output for a typical Doppler experiment.

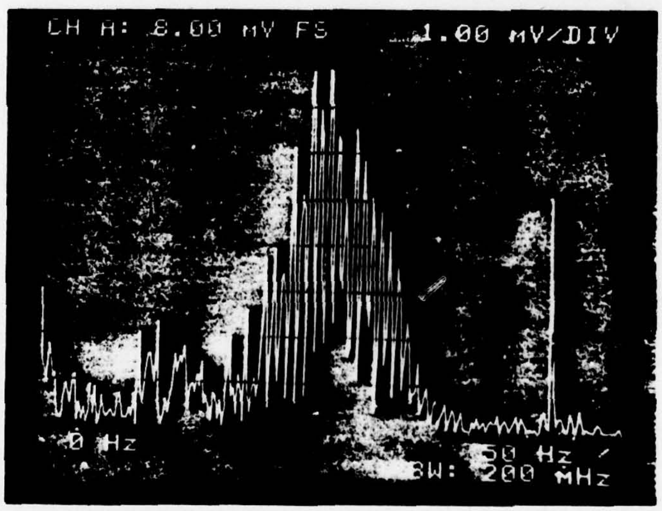

FIGURE 3B--Fast-Fourier analysis of time record of Fig. 3A. Spike at 45 Hz is reference marker.

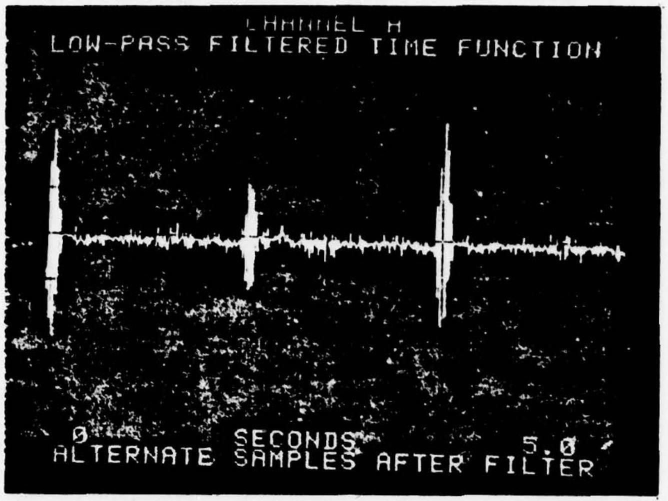

FIGURE 4A—Time record output for sandwich specimen containing two EDM slots.

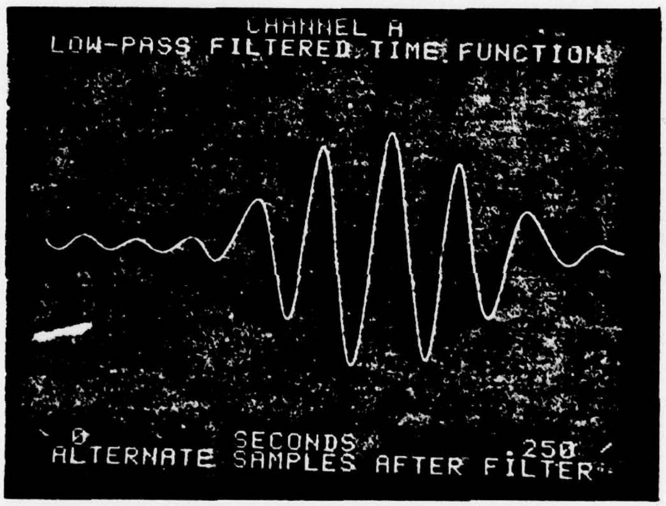

FIGURE 4B—Time expanded version of one of the echoes in Fig. 4A.

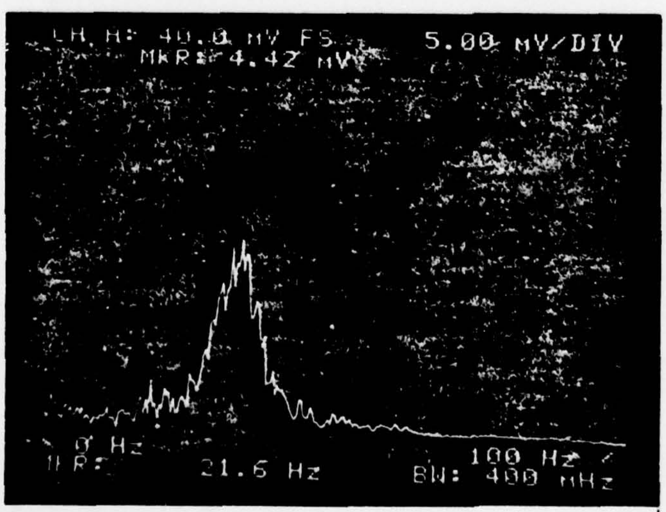

FIGURE 4C—Spectral analysis of one of the slots indicated in Fig. 4A.

APPENDIX D

ULTRASONIC PSEUDORANDOM-SIGNAL-CORRELATION SYSTEM

Submitted for publication in IEEE Transactions on Sonics and Ultrasonics.

An Ultrasonic Pseudorandom-Signal-Correlation System

CHARLES M. ELIAS, Student Member IEEE

ABSTRACT

A working ultrasonic pseudorandom signal-correlation system is described which, unlike ultrasonic random signal-correlation systems, does not require an acoustic delay line. Elimination of the delay line allows faster data acquisition and better range resolution. The system uses two identical shift-register-type generators to produce pseudo-noise bursts which are subsequences of a 65 535-bit complementary m-sequence. One generator produces the transmitted bursts while the other generates identical reference bursts which start at a variable correlation delay time after the transmitted bursts. The reference bursts are cross-correlated with the received echoes to obtain the approximate impulse response of the transducer/specimen system under test. Range sidelobes are reduced by transmitting and correlating many bursts at a given correlation delay before incrementing the delay. Signal-to-sidelobe ratios of greater than 47 dB have been obtained using this method.

Limitations of the system due to sampling constraints and the pseudo-noise power spectrum are discussed, and the system design and implementation are outlined. Results of experimental characterization of the system show that the pseudorandom signal-correlation system has approximately the same range resolution as a conventional pulse-echo system but can yield a significant increase in signal-to-noise ratio.

AD-A080 969 SYSTEMS RESEARCH LABS INC DAYTON OHIO RESEARCH APPLI--ETC F/G 14/2
STUDY OF NONDESTRUCTIVE EVALUATION METHODS FOR LAYERED STRUCTUR--ETC(U)
NOV 79 N K BATRA, C M ELIAS, J S LEFFLER F33615-77-C-5022
UNCLASSIFIED SRL-6492 AFML-TR-79-4162 NL

2 OF 2
AD-
A080969

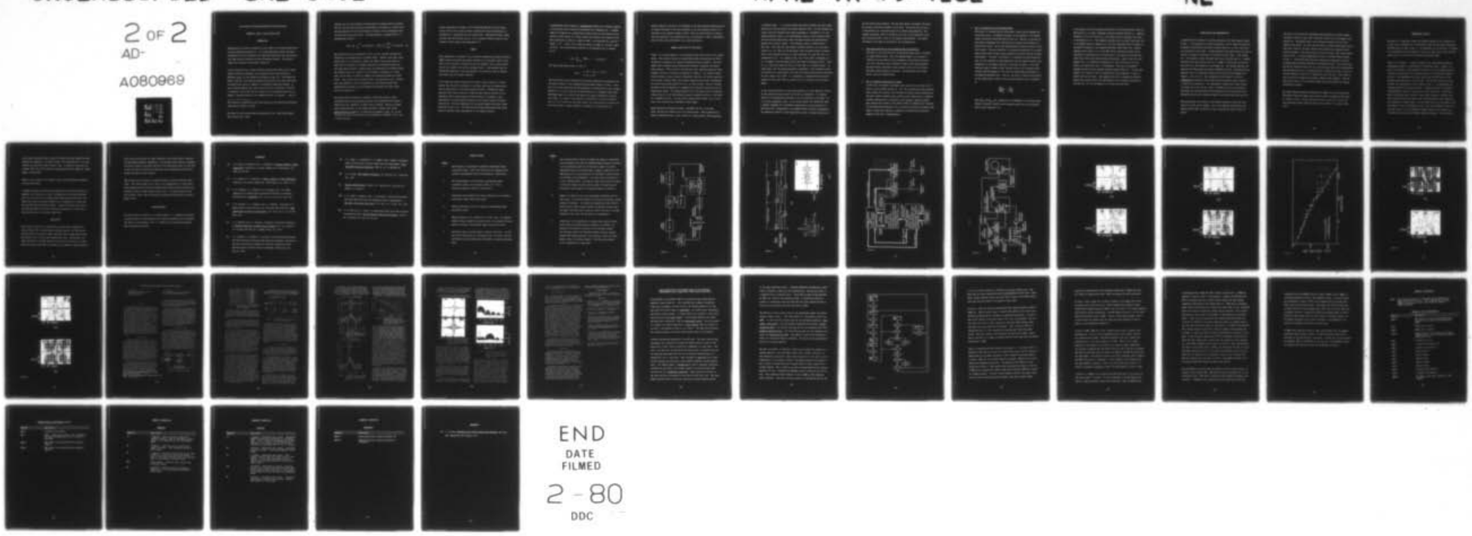

END
DATE
FILMED
2-80
DDC

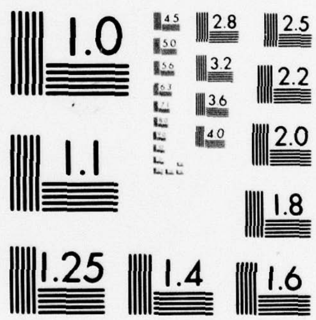

MICROCOPY RESOLUTION TEST CHART
NATIONAL BUREAU OF STANDARDS-1963-A

An Ultrasonic Pseudorandom-Signal-Correlation System

CHARLES M. ELIAS, Student Member IEEE

INTRODUCTION

Random-signal correlation techniques are well known in the radar-systems field as pulse-compression methods [1]. In a pulse-compression system, the pulse transmitted has a wide bandwidth (for high-range resolution) and long duration (for high velocity resolution and high transmitted energy). The received echoes are processed to obtain short pulses [2].

In the ultrasonics area a pulse-compression system which makes use of random signal-correlation techniques for flaw detection has been described by Furgason, et al. [3] and evaluated by Bilgutay, et al. [4]. This system was shown to provide a much improved signal-to-noise ratio and a much lower peak-to-average power ratio as compared to conventional pulse-echo methods. In the correlation method used, random noise bursts are transmitted, therefore, a "reference" noise burst that is a replica of the transmitted burst, but is delayed τ seconds relative to the transmitted burst, is required. τ must be

---

This research is sponsored by the United States Air Force Materials Laboratory under Contract F33615-77-C-5022.

The author is with Systems Research Laboratories, Inc., 2800 Indian Ripple Road, Dayton, Ohio 45440

variable over the time interval in which echoes of interest will be received. That is, the correlation process as performed by the system is a finite interval approximation of the cross-correlation function of the transmitted burst f(t) and the received burst g(t). This approximation, designated $\overline{C}(\tau)$, is mathematically given by

$$\overline{C}(\tau) = \frac{1}{T} \int_{0}^{T} f(t-\tau)g(t)dt \doteq \lim_{T \to \infty} \frac{1}{T} \int_{-T/2}^{T/2} f(t-\tau)g(t)dt \quad (1)$$

The reference bursts are analogous to $f(t-\tau)$ in (1), and the averaging and integration are simulated with a low-pass filter. However, since each transmitted burst is, by definition, unique, the signal from a noise source is split into two channels, one channel producing the transmitted bursts and the other, which contains a variable delay line, producing the reference bursts. The variable delay line consists of two ultrasonic transducers in a water bath, and the delay is varied by changing the separation between the transducers. Such a delay line is bulky and has a slow mechanical scan. Furthermore, the presence of the two transducers in the reference signal path significantly decreases the path bandwidth and degrades the range resolution of the system [5].*

The present paper describes an ultrasonic correlation system in which pseudorandom binary noise generators produce the transmitted and reference noise bursts and, therefore, no delay line is required. Results of experimental characterization of the system are given. Similar work, using phase-modulation techniques, is being done by Chapelon, et al. [6] at the

*Although not explicitly mentioned, this degradation is implicit in Eq. (34) of this reference.

Institut National de la Sante et de la Recherche Medicale in Bron, France. At the time of this writing, however, insufficient detailed information is available for a comparison with the present work. Pseudorandom binary coding has also been used by Waag, et al., in an ultrasonic Doppler system for non-invasive cardiac chamber flow measurement [7].

THEORY

Pulse compression is obtained in the ultrasonic pseudorandom signal-correlation (UPSC) system by deriving the impulse response of the "system", which is composed of the ultrasonic transducer(s) and the specimen, from a cross correlation of the received echo and the reference bursts. (This assumes that the transmitting amplifier, receiving amplifier, and correlator have no significant effect upon the impulse response.)

It is known from systems theory that if "white" noise is input to a linear system, then the cross correlation of the input noise and the system output will be proportional to the system impulse response. Although the theory specifies white noise, which has a constant power density spectrum for all frequencies and an autocorrelation function which is an impulse, a good approximation of system impulse response can be obtained using band-limited noise bursts. This was demonstrated in the random signal-correlation system mentioned earlier [3,4]. The UPSC system utilizes pseudorandom binary noise bursts to provide a good approximation to the impulse response.

A pseudorandom binary sequence or pseudo-noise sequence is a periodic sequence of bits having certain properties associated with randomness [8]. A maximal length or m-sequence is a pseudo-noise sequence which can be obtained as the serially clocked output of a binary linear shift register when specific feedback connections are made by a modulo-2 adder. An m-sequence has a period or length $p = 2^n - 1$ bits, with n being the number of stages in the shift register [8,9]. The autocorrelation function of an m-sequence $\{a_k\}$ is defined as [8],

$$C(\tau) = \sum_{k=1}^{p} a_k a_{k+\tau} \qquad \tau = 0, \pm 1, \pm 2, \ldots \tag{2}$$

For $\{a_k\}$ having binary values +1 and -1,

$$C(\tau) = \begin{cases} p & \text{if } \tau = qp,\ q = 0,1,2,\ldots \\ -1 & \text{if } \tau \neq qp \end{cases} \tag{3}$$

This relationship can be obtained from the known properties of m-sequences and the result from Ref. 8 for m-sequences having binary values of 0 and 1. From Eq. (3) it can be seen that the autocorrelation of pseudo-noise is not a single impulse at $\tau = 0$, as in the case of white noise, but a triangular pulse which has height equal to p, width at its base of two units, and period p units on the τ axis. If, however, an m-sequence is considered as a burst of length p bits or if it is broken up into short bursts, the autocorrelation function will have other peaks or "range sidelobes" in addition to the main peak [1].

100

Another important property of an m-sequence is its power spectrum which has nulls at integer multiples of the clock frequency f_c and line spacing inversely proportional to the sequence length p [8,10]. Thus, by proper choice of p and f_c, the power spectrum of the pseudo-noise can, in principle, be made to approximate that of white noise sufficiently for a given application.

GENERAL DESCRIPTION OF THE SYSTEM

Figure 1 is a block diagram of the experimental UPSC system used in this investigation. This system utilizes two pseudorandom binary noise generators--PNG #1 and PNG #2--to generate the required pseudorandom binary sequences. The PNG's employ shift registers having exclusive NOR feedback to generate the pseudo-noise sequence. PNG's #1 and #2 use identical shift registers having the same feedback circuitry to produce an m-sequence of length p. The feedback connections determine a unique, periodic m-sequence; therefore, if initial conditions are the same, identical PNG's will produce identical pseudo-noise subsequences (or noise bursts) when enabled for N ($N < p$) clock periods. This is precisely how PNG's #1 and #2 generate the transmitted and reference noise bursts in the experimental system. The timing diagram of Fig. 2(a) shows several transmitter cycles, where Q is the time between successive transmitted bursts or the period of a transmitter cycle, τ is the initial reference burst delay, and t_e is the time to the received burst (assuming a fixed target).

System operation proceeds as follows: both PNG's are set to the same state, and the burst length is set to N clock periods. PNG #1 generates the initial transmitted burst. After a delay of τ clock periods, PNG #2 generates

a reference burst. $\tau + \Delta\tau$ clock periods after PNG #1 produces the next transmitted burst, PNG #2 produces the second reference burst. As this process continues, with the reference burst delay increasing in increments of $\Delta\tau$, the analog multiplier output is the instantaneous product of the reference burst and the received signal which, after low-pass filtering and amplification, becomes the correlator output. The correlator output is illustrated in Fig. 2(b). Note that the time between successive points on the correlated output is $Q + \Delta\tau$; that is, one new point of the correlated output is generated for each transmitted burst (or, more precisely, for each time that τ is incremented by $\Delta\tau$). A $\Delta\tau$ change on Fig. 2(a) ("real time") corresponds to a $Q + \Delta\tau$ change in the correlated output time frame ("correlation time"). Since $Q >> \Delta\tau$, then $\Delta\tau/Q$ yields the ratio of "real time" to "correlator time". In other words, with the system operating as described, if the correlator output is observed on an oscilloscope, the scope time base setting would be multiplied by 1/Q to obtain "real time". Or, conversely, a response which would take t seconds in "real time" would be traced out in $Q \cdot t$ seconds at the correlator output.

In the above description of the system operation, one very important feature of this system has been omitted for the sake of simplicity. For reasons which will be subsequently explained, it is not desirable to increment τ by $\Delta\tau$ in every transmitter cycle. In the actual system, the correlation delay τ remains unchanged for I transmitter cycles prior to each increase of $\Delta\tau$. This means that I subsequences are transmitted and I reference subsequences are generated by PNG #2 at some fixed delay τ prior to being increased by $\Delta\tau$

and the process being repeated. Now the scale factor 1/Q becomes 1/QI since the previous description assumed I to be unity. The reason for the use of I "repetitions" per correlation point is to reduce range sidelobes. The "signal-to-sidelobe ratio" is defined as the ratio of the amplitude of the main correlation peak to that of the largest range sidelobe. The signal-to-sidelobe ratio might be increased in the following ways:

1. Continuous Operation of the Transmitter PNG (cw Operation)

   This mode is very attractive for certain applications since it produces no range sidelobe peaks. While the maximum range of a cw system is limited by the periodicity of the m-sequence autocorrelation function [1], this limitation can be overcome by using a very long m-sequence. The most serious limitation of the cw mode is that its use virtually precludes single-transducer operation. For this reason the cw mode was not used in the UPSC system.

2. Use of a Complete m-Sequence as a Burst

   In this case, the signal-to-sidelobe ratio should be on the order of $\sqrt{p}$ where p is the sequence period [1]. But, for a system where many different burst lengths are required, this alternative presents design complications. The shift register feedback logic would be quite complex since a different feedback configuration is required for each change in sequence length. Such complex logic would not only tend to limit the highest clock frequency of the pseudo-noise generators, but it would also nullify two primary advantages of using shift registers to generate the pseudo-noise sequences: simplicity and ease of implementation.

3. Use of I Repetitions per Correlation Point

The process of transmitting and correlating I bursts before changing the correlation delay τ is somewhat analogous to the operation of the random signal correlation system described earlier [3]. However, to the best of the author's knowledge, this technique has not been used previously in a pseudo-noise system. Use of this method greatly simplifies control of the burst length. This was considered to be especially important in an experimental system where as many system parameters as possible should be easily controllable. Of course, an increase in I increases the data-acquisition time, but the trade-off of data-acquisition time for signal-to-noise ratio enhancement is an inherent property of this type of system. Slow range scanning (large I) allows a lower low-pass filter cutoff frequency which provides improved signal-to-noise ratio and simultaneous improvement in the signal-to-sidelobe ratio. That is, the ratio of signal-to-noise power at the system output to that at the receiving amplifier can be expressed as

$$\frac{SNR_{out}}{SNR_{in}} \propto \frac{BW_{in}}{BW_{out}} \tag{4}$$

where BW_{in} and BW_{out} are, respectively, the bandwidth at the system input (usually transducer limited) and the system output (set by the low-pass-filter cutoff frequency) [3].

It is apparent from the foregoing description of the system operation that the UPSC system is, in effect, sampling an impulse response waveform at a sampling frequency of $1/\Delta\tau$ Hz (recall that a new sample datum is available each time τ is incremented by $\Delta\tau$). This sampling frequency must be greater than twice that of the highest spectral component of significant amplitude which is present in the impulse response of the transducer/specimen system under test. Another sampling effect which occurs in the UPSC system correlation process can be explained by considering the autocorrelation of two pseudo-noise bursts when these bursts have some arbitrary phase relationship. Refer to Fig. 2(a) and suppose that τ is repeatedly incremented by $\Delta\tau$ and the product of the two bursts is obtained each time τ is incremented. This can be considered a sampling process with the sampling frequency again, being $1/\Delta\tau$. In this case, however, $1/\Delta\tau$ should be twice the pseudo-noise clock frequency in order to sample twice per bit time. This sampling rate will be adequate in practice because the received bursts are band-limited by the transducer/specimen system (see Fig. 2(c) for an example of an actual received burst).

SYSTEM DESIGN AND IMPLEMENTATION

A simplified block diagram of the logic subsystem of the UPSC system is shown in Fig. 3. The subsystem is totally synchronous, and all timing functions are performed by presettable synchronous counters which are, in turn, controlled by the primary control logic. Storage registers hold numbers which are used as values for counters or directly by the primary control logic. These numbers are: burst length, initial reference burst delay (initial value of τ) maximum reference burst delay (final value of τ), number of repetitions per correlation point (I), and transmitter cycle length (Q). The storage registers are selected and loaded using front-panel thumbwheel switches. Each pseudo-noise generator uses a 16-stage shift register with exclusive NOR feedback from Stages 1, 3, 12, and 16. This configuration will produce a 65 535-bit <u>complementary</u> m-sequence (this sequence having properties nearly identical to those of an m-sequence). The complementary sequence was chosen because it permits use of the all-zero state, a forbidden state in the m-sequence. This means that initialization of the generators can be performed for most integrated-circuit shift registers simply by activating the clear input [9].

The system master clock period is the minimum increment by which any time interval or delay can be changed. Due to the sampling considerations discussed earlier, PNG's #1 and #2 are run at one-half the master clock frequency.

The logic in this system was implemented using (primarily) Schottky-clamped transistor-transistor logic (TTL) integrated circuits with wire-wrapped interconnections. The highest master clock frequency obtained with error-free operation was 25 MHz. No effort has been made to increase system speed beyond this point; however, the logic speeds in this system do not approach state-of-the-art speeds. With faster logic and careful design, a much faster system could be built. A typical experimental set-up for the UPSC system is shown in Fig. 4. A Philips PM 3265 dual-trace multiplier oscilloscope is used as a variable-gain broad-band amplifier and analog multiplier. The received signal and the reference bursts are fed to the vertical inputs of the oscilloscope. The oscilloscope is set in the multiply mode to permit the product of the two vertical amplifier outputs to be available at the Y OUT jack. This output is fed to an active low-pass filter having variable cutoff frequency. The low-pass-filter output is the correlated signal and can be observed on a second oscilloscope as shown.

The logic subsystem supplies synchronization signals for both oscilloscopes. The bipolar converters employ burst and gate inputs to change the TTL bursts to "bipolar" bursts. Bipolar pseudo-noise burst trains were used because they experience miniman transient effects when applied to ac coupled amplifiers.

EXPERIMENTAL RESULTS

The result of a comparison between the impulse response of two transducers in a water bath as measured with a conventional pulse-echo ultrasonic system and the UPSC system is shown in Fig. 5. The similarity of the responses is striking. It is noteworthy that the Panametrics unit used a 390-V pulse, while the UPSC system used a 2-V p-p burst in obtaining the response shown.

Figure 6 is an example of signal-to-sidelobe ratio improvement obtained by increasing the number of repetitions per correlation point. Figure 7 is a plot of the maximum sidelobe magnitude (relative to the correlation peak) as a function of repetitions per correlation point for a fixed burst length of 375 bits. The experimental data were taken using the UPSC system in the through transmission mode in a water bath. Two raw data sources were used to obtain the experimental results plotted in Fig. 7: an oscilloscope and a Northern Model NS-575 signal averager. Agreement between the calculated and experimental results is excellent up to 100 repetitions. Beyond this point, the computer model predicts a more rapid decrease in sidelobe level with increasing repetition number, while the experimental values appear to be following the original slope. At the present time it is not known if this discrepancy is due to experimental errors, since the sidelobes are near system noise levels, or to an inadequate computer model of the system (e.g., the model does not take into account transducer effects). For the 375-bit

burst length, sidelobe levels at least 47 dB below the peak height have been obtained experimentally. As stated in Ref. [11], obtaining the -47 dB ratio required an acquisition time of almost 2 min. It should be noted that the sidelobe level can also be reduced by increasing the burst length for a given number of repetitions.

Figure 8 is an example of the signal-to-noise ratio improvement obtainable with the UPSC system.

A simple experiment was performed to demonstrate that system resolution is degraded by the presence of a pair of transducers in the reference-signal path, as is the case for the random signal correlation system of Ref. [3]. Figure 9(a) shows the impulse response of two transducers in a water bath with the UPSC system operating normally. Figure 9(b) shows the result of the same experiment but with two additional transducers in a water bath being inserted into the reference signal path.

CONCLUSIONS

This study has shown that a UPSC system can yield results comparable to those obtained with a random signal correlation system. The UPSC system has been shown to have better range resolution than a random signal system which makes use of a narrow band variable delay line. Nevertheless, the range resolution of the UPSC system can be no better than that of an ideal pulse-echo system since both are limited by the transducer impulse response.

Like a pulse-echo system, the range resolution of the UPSC system is improved by using higher-frequency transducers. For the UPSC system, however, consideration must be given to the power spectrum of the pseudo-noise which is 3-db down at about one-half the pseudo-noise-generator clock frequency and has nulls at integer multiples of that frequency.

UPSC systems could be applied to signal detection in highly attenuative materials. Such systems might also be used in the implementation of those quantitative nondestructive evaluation techniques which employ spectral analysis and, therefore, require a large signal-to-noise ratio. If long acquisition times are a problem, faster logic and parallel processing using multiple correlators might be used.

ACKNOWLEDGEMENTS

The author wishes to thank Dr. J. A. Moyzis and Mr. K. D. Shimmin for devising a computer model of autocorrelation as it would be performed by the instrument. The author is also grateful to Dr. T. J. Moran for his advice and encouragement throughout this project.

110

REFERENCES

[1] C. E. Cook, M. Bernfeld, and C. A. Palmieri, in Radars, Volume 3 - Pulse Compression, edited by D. K. Barton, Dedham, MA: Artech House, Inc., 1975, pp. 127-129.

[2] H. O. Ramp and E. R. Wingrove, in Radars, Volume 3 - Pulse Compression, edited by D. K. Barton, Dedham, MA: Artech House, Inc., 1975, p. 75.

[3] E. S. Furgason, V. L. Newhouse, N. M. Bilgutay, and G. R. Cooper, "Application of Random Signal Correlation Techniques to Ultrasonic Flaw Detection," Ultrasonics, Vol. 13, No. 1, pp. 11-17, Jan. 1975.

[4] N. M. Bilgutay, E. S. Furgason, and V. L. Newhouse, "Evaluation of a Random Signal Correlation System for Ultrasonic Flaw Detection," IEEE Transactions on Sonics and Ultrasonics, Vol. SU-23, No. 5, pp. 329-333, Sept. 1976.

[5] V. L. Newhouse and E. S. Furgason, "Ultrasonic Correlation Techniques," in Research Techniques in Nondestructive Testing, Vol. III, edited by R. S. Sharpe, New York, NY: Academic Press, Inc., 1977.

[6] J. Y. Chapelon, D. Cathignol, C. Fourcade, "A New Pseudo-Random Binary-Code Phase Modulated Ultrasonic High Resolution Echograph," presented at the Third International Symposium on Ultrasonic Imaging and Tissue Characterization, National Bureau of Standards, Gaithersburg, MD., June 5-7, 1978.

[7] R. C. Waag, J. B. Myklebust, W. L. Rhoads, and R. Gramiak, "Instrumentation for Noninvasive Cardiac Chamber Flow Rate Measurement," Proc. 1972 IEEE Ultrasonics Symposium, IEEE Cat. No. 72 CHO708-8 SU.

[8] S. W. Golomb, Shift Register Sequences, San Francisco, CA: Holden-Day Inc., 1967.

[9] Motorola McMOS Handbook, Phoenix, AZ: Motorola Inc., New York, NY: Chapter 11, Section D.

[10] S. E. Craig, W. Fishbein, and O. E. Rittenbach, "Continuous Wave Radar with High Range Resolution and Unambigous Velocity Determination," IRE Trans. on Military Electronics, Vol. MIL-6, pp. 153-161, Apr. 1962.

[11] C. M. Elias and T. J. Moran, "A Pseudorandom Binary Noise NDE Ultrasonic Correlation System," 1978 Ultrasonics Symposium Proceedings, IEEE Cat. No. 78 CH1344-1 SU, 1978, pp. 311-315.

FIGURE CAPTIONS

Figure

1	Block diagram of experimental ultrasonic pseudorandom signal correlation system. PNG #1 and PNG #2 are the transmitter and reference pseudorandom binary noise generators, respectively.
2	(a) Timing diagram of the ultrasonic pseudorandom signal correlation system, (b) Correlator output, (c) Actual receiving transducer signal for 30-bit burst.
3	Simplified block diagram of the logic subsystem of the ultrasonic pseudorandom signal correlation system.
4	Typical experimental setup for ultrasonic pseudorandom signal correlation system.
5	Impulse response of two transducers in a water bath. (a) Response obtained using a Panametrics pulser/receiver, (b) Response obtained using the ultrasonic pseudorandom signal correlation system.
6	Correlator output for burst length of 100-bits (20 μsec). (a) Output with 10 repetitions per correlation point, (b) Output with 100 repetitions per point showing the improvement in signal-to-sidelobe ratio.

Figure

7 Plot illustrating the effect of varying the number of repetitions per correlation point upon the maximum sidelobe magnitude (relative to the correlation peak) for a fixed burst length of 375-bits. Calculated points were obtained from a computer simulation of the UPSC system for an autocorrelation (no transducer or water effects are included in the simulation). The solid line is a linear fit to the calculated data. The break in slope occurs when the product of the burst length (in bits) and the number of repetitions per correlation point exceeds the m-sequence length (65 535-bits).

8 Example of signal-to-noise ratio improvement obtainable with the UPSC system. The received signal is the first echo through a highly attenuative specimen. (a) Signal from Panametrics Model 5052 PR pulser/receiver using maximum "energy" and maximum receiver gain, (b) Signal from UPSC system using the receiver section of the same Pauametrics unit (with the same gain) as a preamplifier.

9 Illustration of the degradation in system range resolution which occurs when the reference-channel bandwidth is reduced by the addition of an acoustic delay path in the reference channel. (a) Correlator output with digitally delayed reference channel (normal UPSC system operation), (b) Correlator output with fixed acoustic delay in reference channel. This delay was produced by two transducers in a water bath.

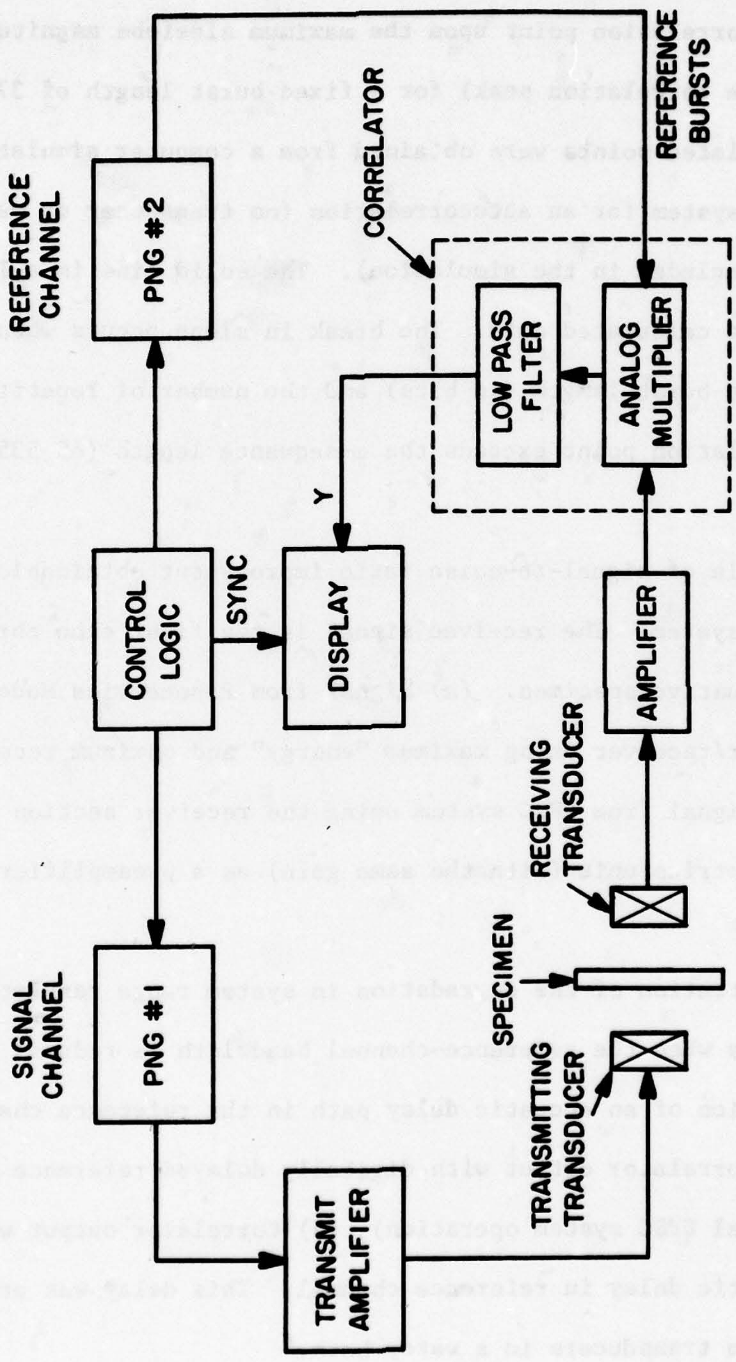
SIGNAL CHANNEL
PNG #1
TRANSMIT AMPLIFIER
CONTROL LOGIC
SYNC
DISPLAY
Y
REFERENCE CHANNEL
PNG #2
CORRELATOR
LOW PASS FILTER
ANALOG MULTIPLIER
REFERENCE BURSTS
AMPLIFIER
RECEIVING TRANSDUCER
SPECIMEN
TRANSMITTING TRANSDUCER

Figure 1.

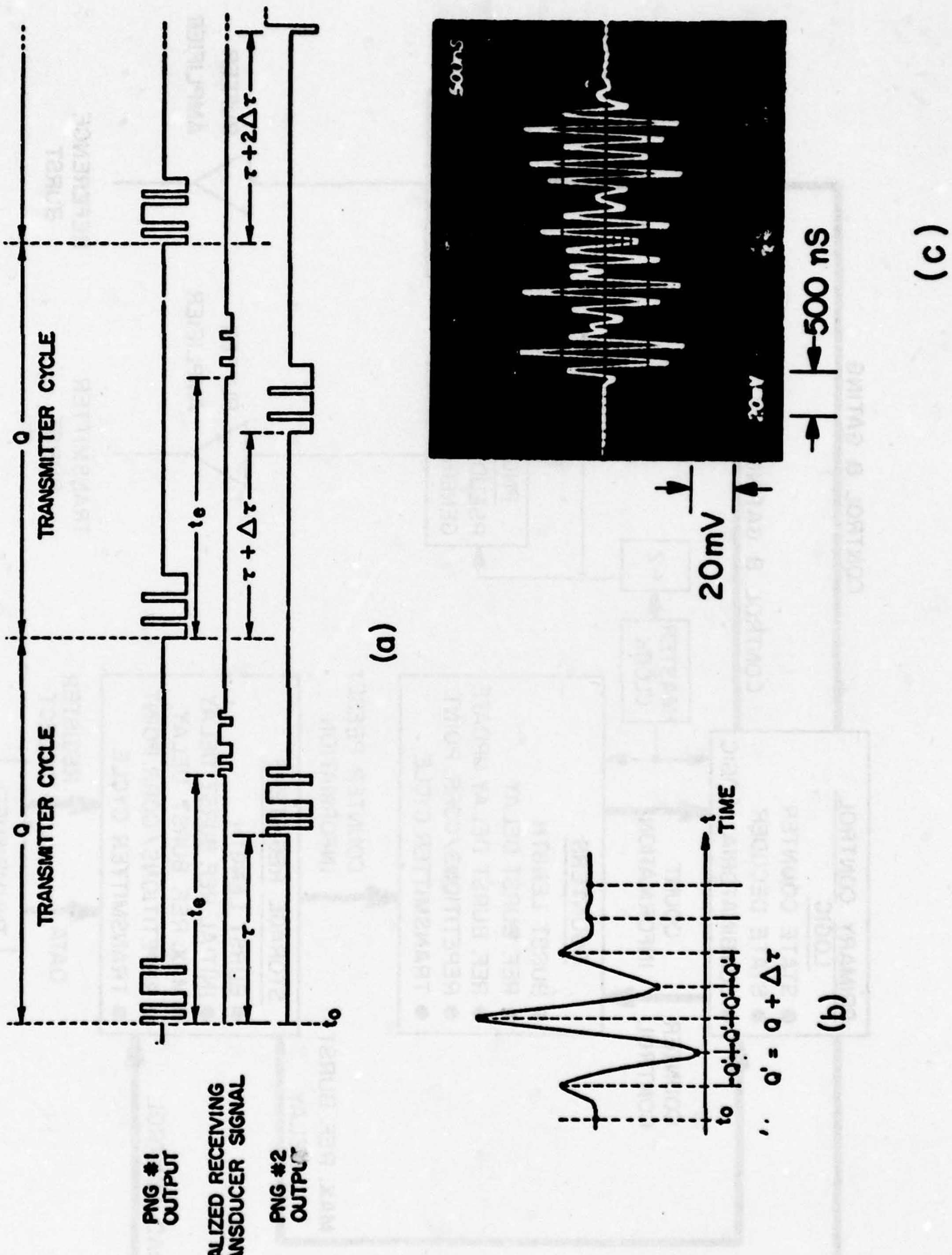
PNG #1 OUTPUT
IDEALIZED RECEIVING TRANSDUCER SIGNAL
PNG #2 OUTPUT
TRANSMITTER CYCLE
TRANSMITTER CYCLE
(a)
TIME
(b)
20mV
500 nS
(c)

Figure 2.

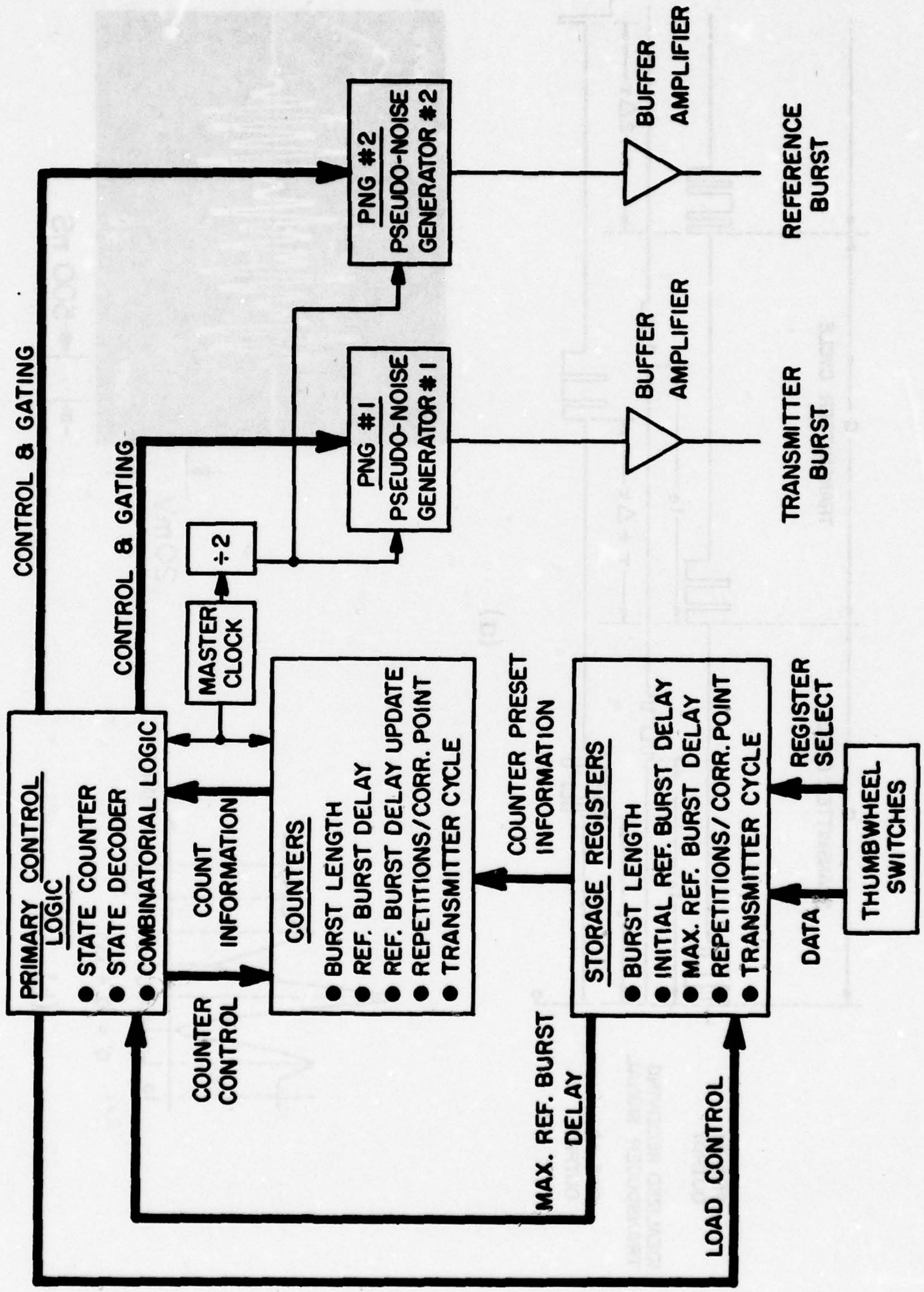
PRIMARY CONTROL LOGIC
● STATE COUNTER
● STATE DECODER
● COMBINATORIAL LOGIC
CONTROL & GATING
CONTROL & GATING
MASTER CLOCK
÷2
PNG #1
PSEUDO-NOISE GENERATOR #1
PNG #2
PSEUDO-NOISE GENERATOR #2
BUFFER AMPLIFIER
BUFFER AMPLIFIER
TRANSMITTER BURST
REFERENCE BURST
COUNT INFORMATION
COUNTER CONTROL
COUNTERS
● BURST LENGTH
● REF. BURST DELAY
● REF. BURST DELAY UPDATE
● REPETITIONS/CORR. POINT
● TRANSMITTER CYCLE
COUNTER PRESET INFORMATION
STORAGE REGISTERS
● BURST LENGTH
● INITIAL REF. BURST DELAY
● MAX. REF. BURST DELAY
● REPETITIONS/CORR. POINT
● TRANSMITTER CYCLE
REGISTER SELECT
DATA
THUMBWHEEL SWITCHES
MAX. REF. BURST DELAY
LOAD CONTROL

Figure 3.

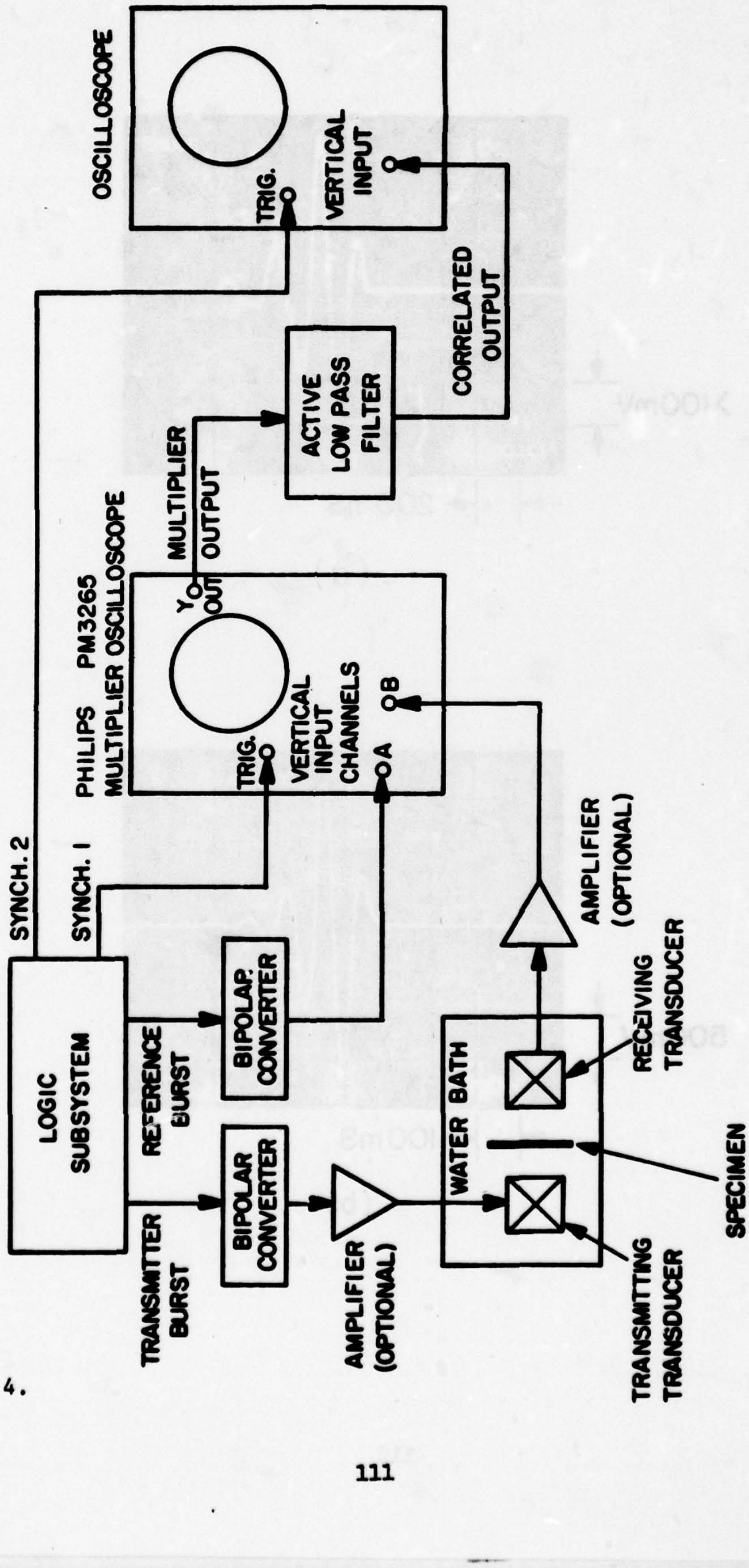
OSCILLOSCOPE
TRIG.
VERTICAL INPUT
CORRELATED OUTPUT
ACTIVE LOW PASS FILTER
MULTIPLIER OUTPUT
PHILIPS PM3265 MULTIPLIER OSCILLOSCOPE
Y OUT
TRIG.
VERTICAL INPUT CHANNELS
A
B
SYNCH. 2
SYNCH. 1
LOGIC SUBSYSTEM
REFERENCE BURST
BIPOLAR CONVERTER
TRANSMITTER BURST
BIPOLAR CONVERTER
AMPLIFIER (OPTIONAL)
AMPLIFIER (OPTIONAL)
WATER BATH
RECEIVING TRANSDUCER
SPECIMEN
TRANSMITTING TRANSDUCER

Figure 4.

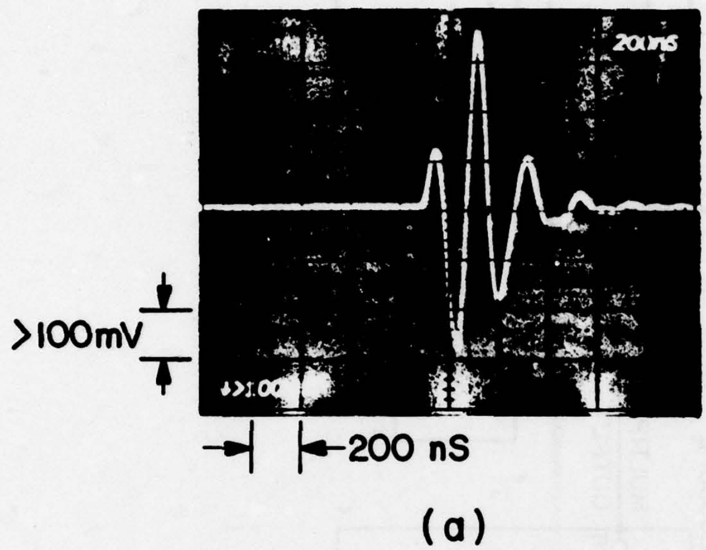

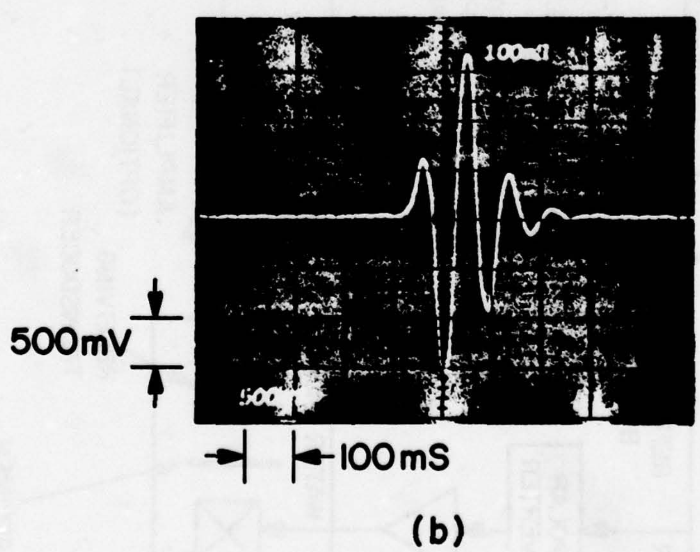

Figure 5.

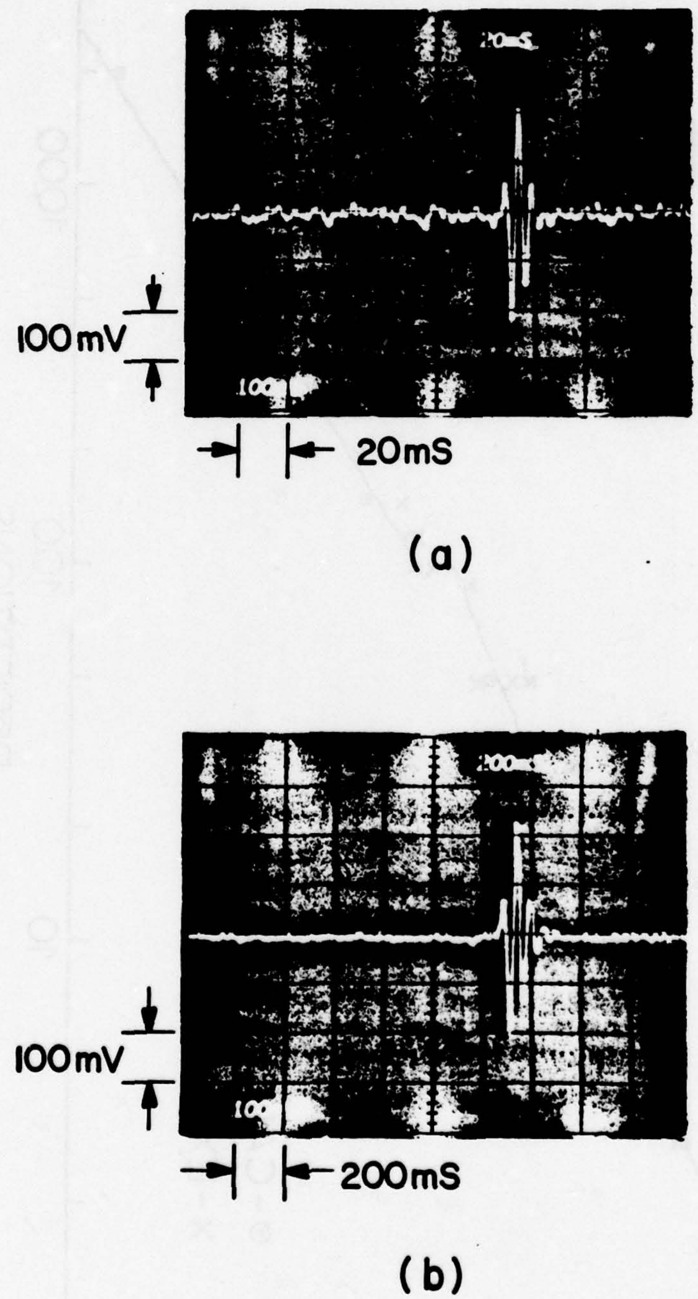

Figure 6.

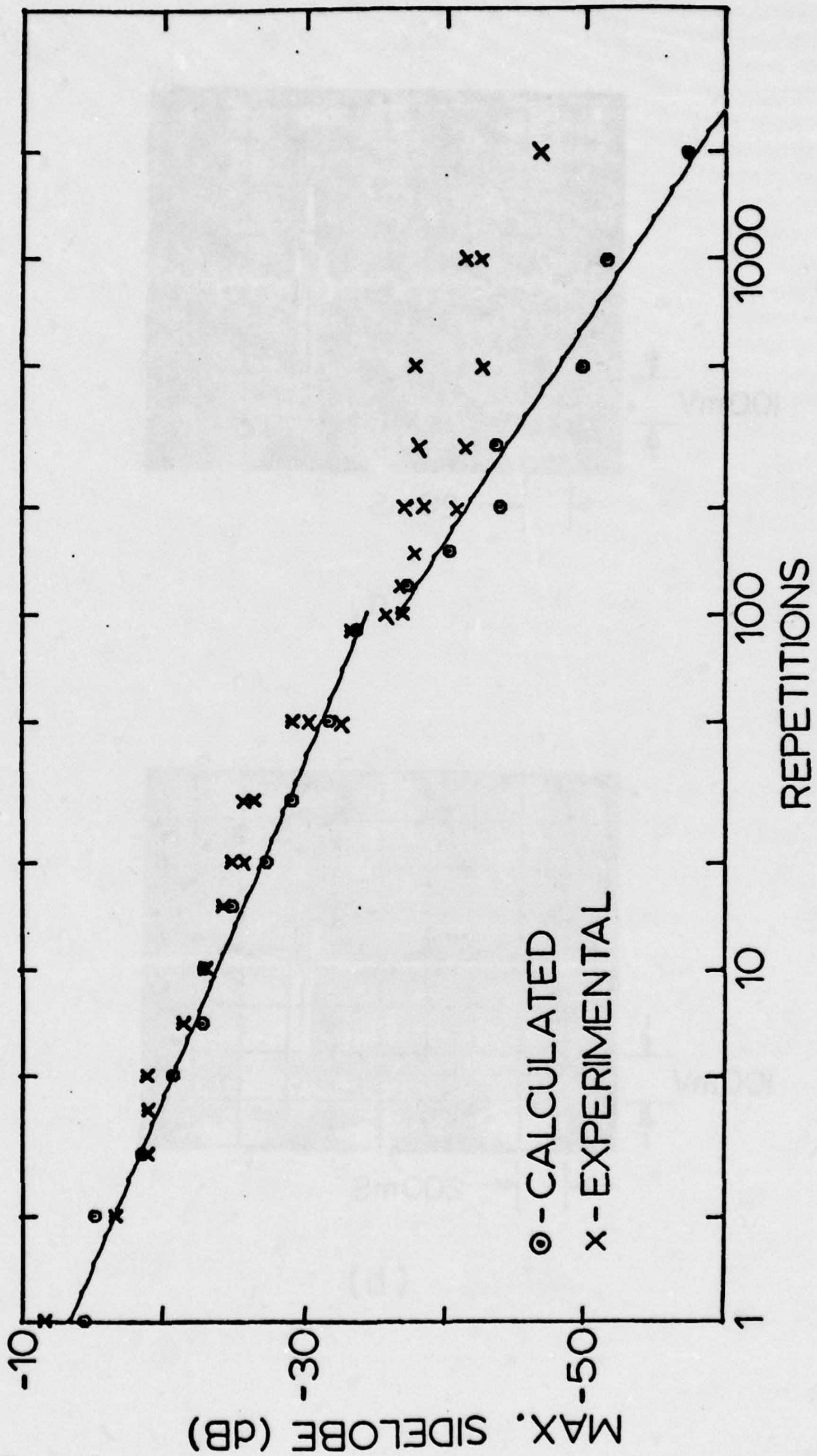

-10
-30
-50
MAX. SIDELOBE (dB)
1
10
100
1000
REPETITIONS
⊙ - CALCULATED
x - EXPERIMENTAL

Figure 7.

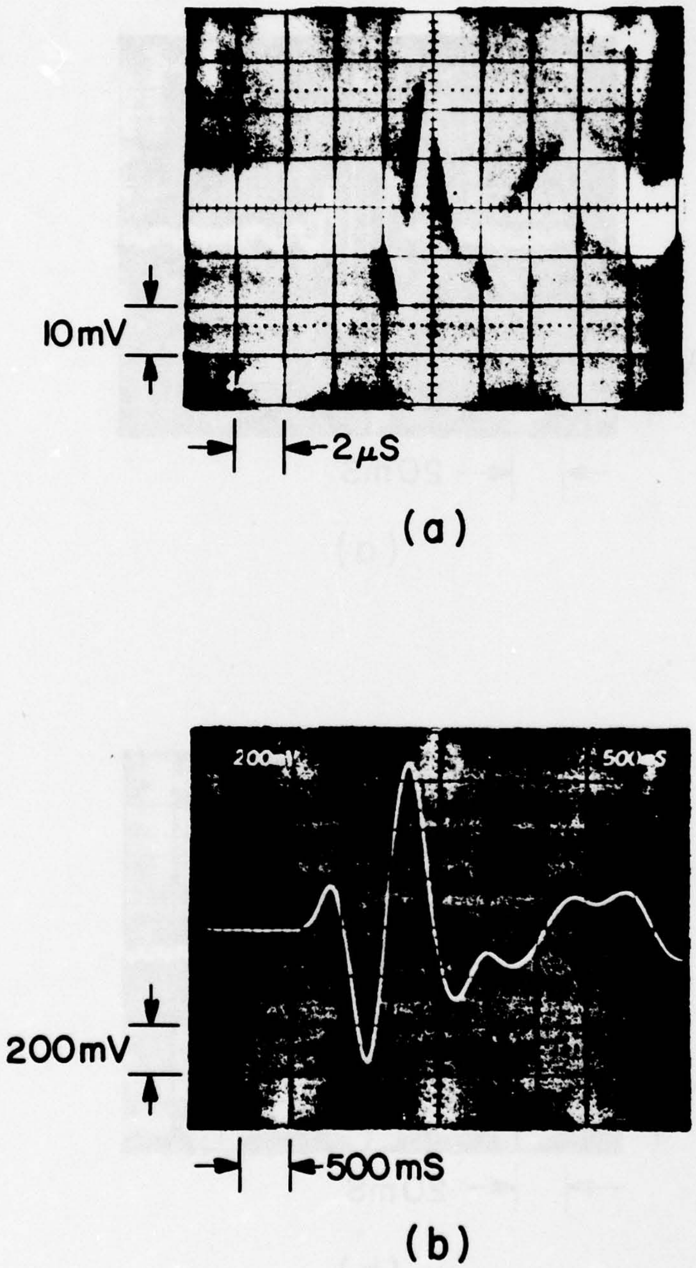

Figure 8.

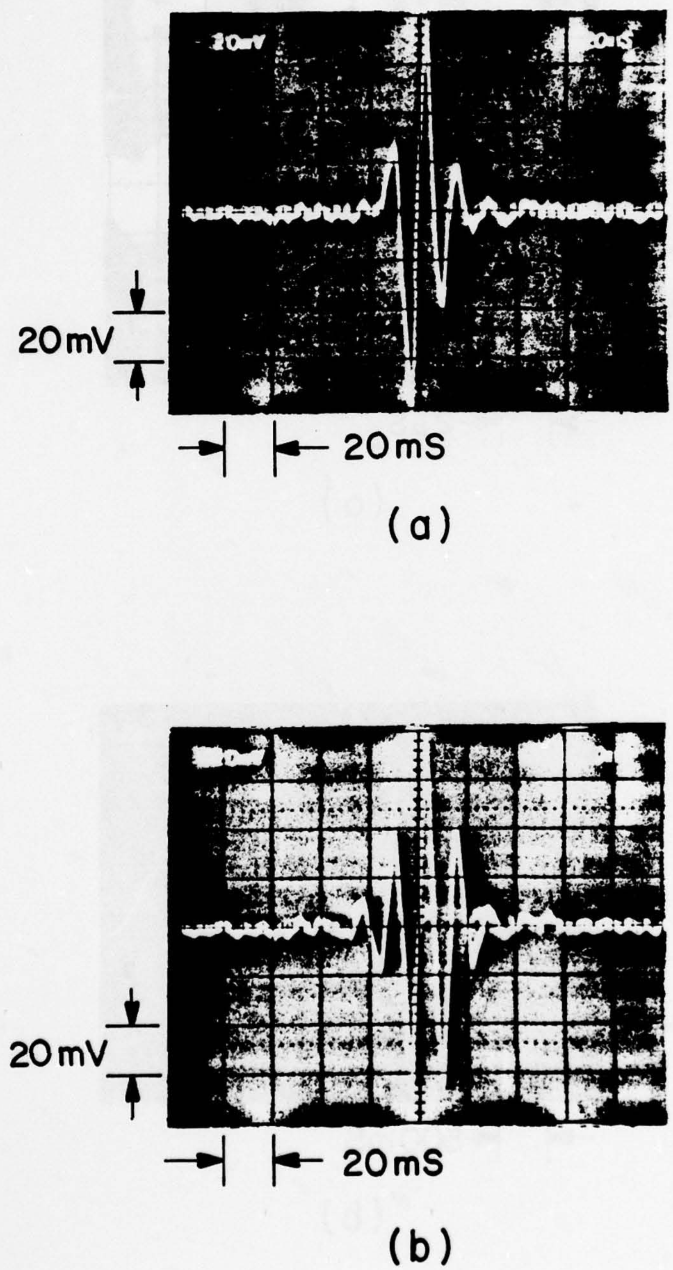

Figure 9.

A PSEUDORANDOM BINARY NOISE NDE ULTRASONIC CORRELATION SYSTEM

C. M. Elias
Systems Research Laboratories, Inc.
2800 Indian Ripple Road
Dayton, Ohio 45440

T. J. Moran
Air Force Materials Laboratory (AFML/LLP)
Wright-Patterson AFB, Ohio 45433

Abstract

A pseudorandom binary noise NDE ultrasonic correlation system has been designed which retains the signal to noise improvement capabilities of the random signal correlation system while improving data acquisition speed to near real time. A prototype instrument has been constructed using a 65K bit maximal sequence pseudorandom noise generator and its performance has been evaluated. One important consideration for the application of this technique is the presence of time sidelobes. To date, using 5 MHz immersion NDE transducers, the prototype system has shown that a correlation peak to sidelobe ratio of > 47 dB can be achieved. It has also been shown that phase modulating a cw rf carrier with the binary code allows the system to be used to measure acoustic transit time changes with ppm accuracy or to drive transducers at frequencies above the 10 MHz limit of the instrument without the modulation. Additional details of system performance and possible applications are discussed.

1. Introduction

Large improvements in the signal to noise ratio of ultrasonic signals from targets typically encountered in Nondestructive Evaluation (NDE) have been achieved in the laboratory using a random signal correlation system[1]. The random signal system achieves this improvement by driving the transducer with a long burst of white noise and correlating received signals with a replica of the drive burst. The average transmitted energy can be made much greater with the random signal system than with short pulse excited conventional systems where electrical breakdown in the transducer limits the transmitted energy. The bandwidth limiting which occurs in the correlation receiver also contributes significantly to the enhanced sensitivity.

With this system, the only way a replica of the transmitted signal can be derived is by splitting the signal from the noise source. This reference is then delayed with an ultrasonic delay line. The delay line consists of a pair of ultrasonic transducers in a water bath whose separation is mechanically varied. A sample in the signal channel is scanned by varying the reference delay over the range in which delayed signals from targets in the sample are expected to occur. Present signal acquisition times are greater than can be tolerated for field NDE use, due to a large degree to the slowness of the mechanical scan.

This paper will describe a system whereby the requirement for a mechanically scanned delay line can be eliminated and the scanning can be accomplished in near real time[2]. The new system substitutes a pair of pseudorandom binary noise (PBN) sources which produce identical output sequences for the white noise source used in the random signal system. Many of the features of the random signal system have been retained and the range resolution of the new system has been found to be superior to that of a random signal system. A prototype instrument has been constructed and its capabilities will be described.

2. System Description

A block diagram of the system is shown in Figure 1. The primary difference from the random signal system is the pair of PBN generators. Each generator consists of a sixteen stage shift register with exclusive NOR feedback chosen to produce a 65,535 bit maximal length binary sequence[3]. Figure 2 shows the first 100 bits of the sequence produced by the generators. The control logic determines the length of the noise burst, the relative time delay between the reference burst and the signal channel burst and the rate at which this delay is varied for scanning of the sample. The reference delay is stepped in increments equal to single periods of the master oscillator, resulting

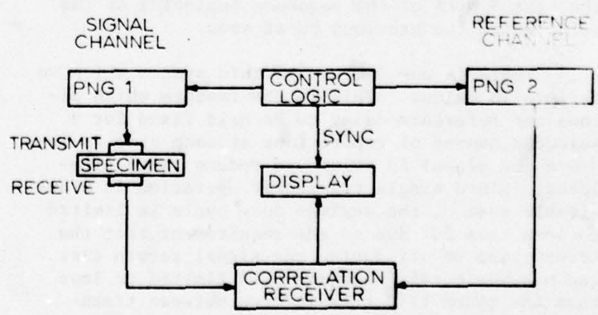

Figure 1. System block diagram

1978 Ultrasonics Symposium Proceedings
IEEE Cat. #78CH 1344-1SU
(IEEE Ultrasonics Symposium, Cherry Hill, NJ, Sept. 25-27, 1978).

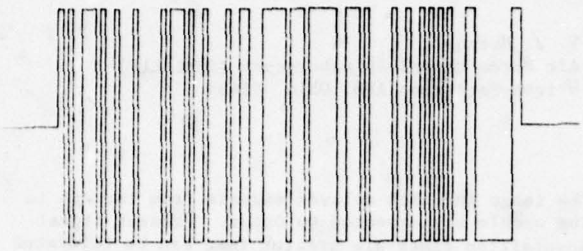

Figure 2. First 100 bits of the pseudorandom binary m-sequence used with the present instrument.

in a sampled system. To insure that the Nyquist criterion for adequate sampling is fulfilled, the master oscillator frequency is divided by two for the timing of the PBN generators, making a single bit time of the sequence twice the reference delay step.

The correlation receiver uses the multiplier function of a Phillips Model 3265 oscilloscope to multiply the signal and reference channels and a low pass filter on the scope output to perform the simulated integration. The output is displayed on a storage oscilloscope.

Figure 3 illustrates the operation of the system. In the signal channel, the burst length and cycle period are chosen to allow returning target signals of interest to be fully separated from the transmitted signals. The reference burst, which is identical to the signal burst, is initially delayed slightly less than the first return signal. The delay is then incremented in steps to a point past the delay time of any signal of interest in the signal channel. Each time the reference delay equals a signal delay, maximum correlation occurs. It may be noted from the figure that each transmitted burst differs from the previous one. In fact, if the first burst represents N bits of the overall sequence, each succeeding burst consists of the next N bits of the sequence beginning at the point where the previous burst ends.

There is one feature of this system which we believe is unique. This is the feature which allows the reference delay to be held fixed for a selected number of repetitions at each step to improve the signal to noise and reduce range sidelobes. Since single transducer operation is a desirable option, the maximum duty cycle is limited to less than 50% due to the requirement that the transmitted be off during the signal return time. The maximum burst length is also limited to less than the round trip transit time between transducer and target. For reasonable path lengths, this restricts the burst length to a maximum on the order of 25-50 μsec. These constraints led to the design decision to approximate a long sequence which has good correlation properties with a series of short bursts, each of which is a different segment of the overall sequence. This fixing of the reference delay for many repetitions tends to average out sidelobes since each burst produces a different sidelobe pattern.

The logic speed in the present prototype instrument limits the clock rate of the pseudonoise generators to approximately 13 MHz. The PBN spec-

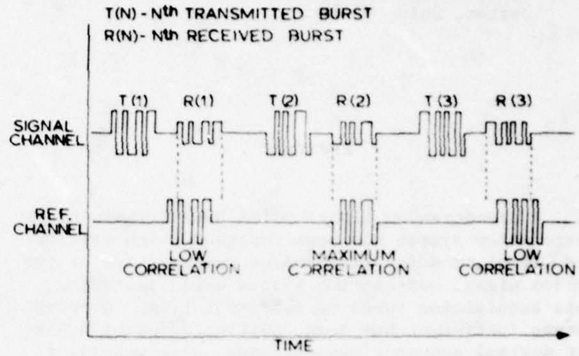

Figure 3. Simplified system timing diagram to illustrate operation.

trum exhibits nulls at integer multiples of the clock frequency[4]. This allows use of transducers with center frequencies up to ~10 MHz. Using state of the art components, it should be possible to run the logic fast enough to drive transducers with center frequencies up to 50 MHz directly. However, there is a well-known radar technique known as phase shift keying which would allow higher frequency transducers to be driven even with our present slow speed prototype instrument. The technique consists of using the PBN sequence to phase modulate a CW carrier, allowing the matching of the spectrum center frequency to the frequency of the transducer.

3. System Operation

The system was initially tested using a pair of 5 MHz transducers separated by approximately 10 cm. in a water tank to generate and receive the acoustic signals. The purpose of these tests was to determine the level of the range sidelobes and the resolution potential of the system.

The range sidelobes arise from the fact that the system operates with a burst mode. It is known that a complete maximal length sequence transmitted as a burst exhibits range sidelobes which have a maximum amplitude on the order of $1/\sqrt{N}$ times the correlation peak amplitude where N is the number of bits in the sequence[5]. Since our system uses segments of a complete sequence, we have examined the sidelobe levels experimentally and with a computer model to determine the effect of the number of repetitions per reference delay point on the sidelobe levels.

Figures 4 and 5 show examples of the data which must be analyzed to evaluate system performance. Figure 4 shows the correlation peak and the close-in sidelobes on a linear and log plot for a short burst (12.5 μsec) and a small number (10) of repetitions. The peak sidelobe levels for this case are on the order of 20 dB below the correla-

tion peak height. When the burst length is increased to 50 μsec and the number of repetitions to 99, the sidelobe levels are reduced to approximately 36 dB below the peak as is shown in Figure 5. To determine in a systematic way the effect of varying the repetition number, a computer model

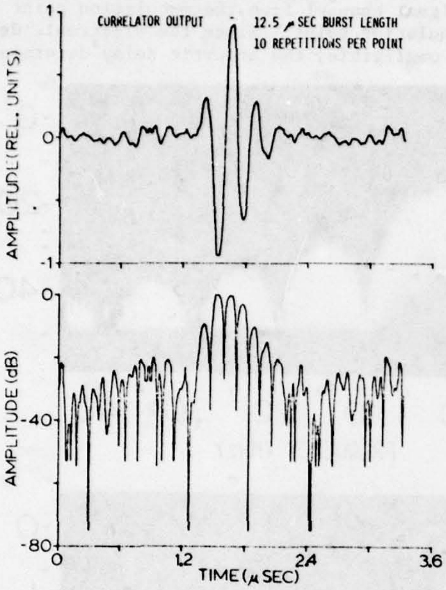

Figure 4. Correlation peak for short burst length and small number of repetitions per reference delay.

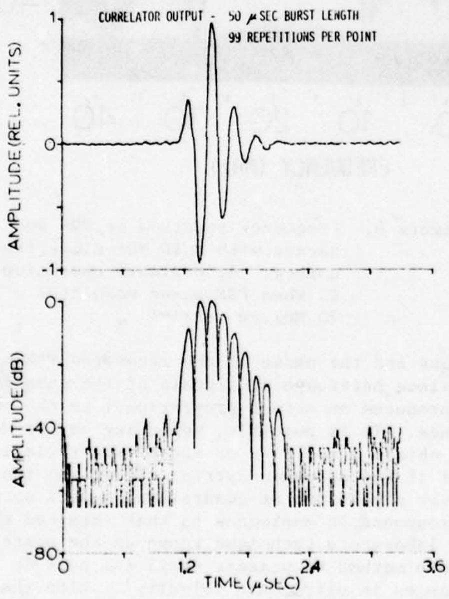

Figure 5. Correlation peak for a longer burst and a typical number of repetitions per reference delay.

of the system was devised and the autocorrelation function of the signal and reference bursts was calculated. Figure 6 shows the results of the calculation for a burst length of 375 bits with repetitions between 1 and 2000 per delay point. The amplitude of the maximum sidelobe is plotted vs repetitions. In addition, experimental results

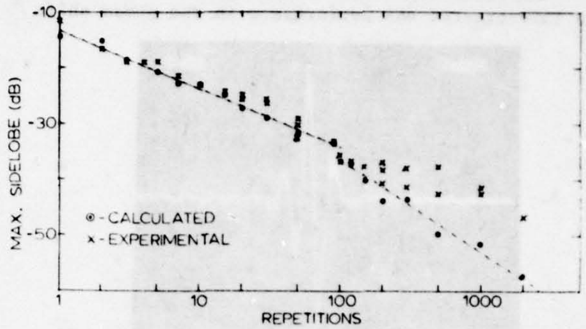

Figure 6. Experimental and calculated maximum sidelobe level for a 375 bit burst length as a function of the number of repetitions at each reference delay.

obtained both visually from the oscililoscope and with a Northern Model NS-575 signal averager are shown in the same figure. Agreement between the calculated and experimental results is excellent up to 100 repetitions. Above this point, where the entire PBN sequence length is exceeded at each correlation point, the computer model predicts a more rapid decrease in sidelobe level with increasing repetition number, while the experimental values appear to be following the original slope. At the present time it is not certain if this discrepancy is due to experimental errors, since the sidelobes are near the system noise levels, or to an inadequate computer model of the system. The present model does not take into account the effect of the transducer on the signal channel burst. It should be noted that we have been able to achieve sidelobe levels at least 47 dB below the peak height. The price one has to pay for such sidelobe levels is long signal acquisition times, almost 2 minutes in the case of 2000 repetitions, making it rather impractical to use such large numbers of repetitions with the present system. One possible method of improving signal acquisition time would be to use more than one reference PBN generator and parallel process the outputs. It should also be noted that an increase in pulse width with the repetition number held fixed will also reduce the sidelobe level.

The width of the correlation peak was also investigated. It was determined that this width was limited only by the transducer response. In terms of ability to resolve target signals in time, there is virtually no difference between this system and a conventional pulse NDE system. A comparison was also made between this system and the random signal system. An ultrasonic delay produced by a second pair of transducers matched to the first pair was added to the reference channel to approximate

the random signal system. Figure 7 illustrates the broadening of the correlation peak which occurs when the reference channel is also bandwidth limited as is the case with the random system.

The final aspect of system operation which was investigated was performance in the phase shift

A.

B.

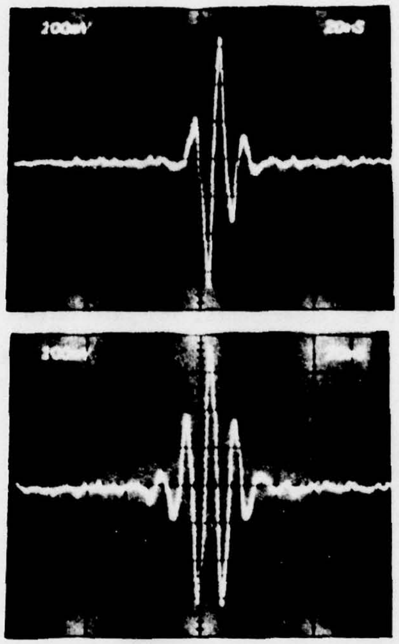

Figure 7. A. Normal PBN system correlation peak. B. Broadened peak when reference channel is bandwidth limited to simulate the random signal system.

keyed mode of operation. There are two possible ways to implement such a system. In the first, which was chosen, a cw carrier is phase modulated by the PBN sequence using a double balanced mixer and the resulting signal drives the transmitting transducer. The carrier is then removed from the receiving transducer output by heterodyning with a signal split off from the cw carrier signal generator. The second way is to produce phase modulated signals in both signal and reference channels[6]. Such a set-up would require a very broad bandwidth correlation receiver if it were desired to operate at frequencies above 20 MHz.

Figure 8A shows the spectrum of an ordinary PBN sequence operated at a 10 MHz clock frequency and illustrates the nulls at multiples of the clock frequency. Figure 8B illustrates the manner in which phase shift keying centers the spectrum at the carrier frequency, allowing high frequency transducers to be driven by a low frequency PBN sequence.

There are several points to be noted with regard to operation of the system in the phase shift keyed mode. When the modulation is confined solely to the signal channel, the phase of the PBN sequence after carrier removal on the receiver side is sensitive to the phase of the carrier. With no reflections, the phase of the carrier in the received signal is determined by the total delay time in the signal channel from the modulation point to the demodulation point. Since the electronic delays are negligible, the acoustic delay determines

A.

B.

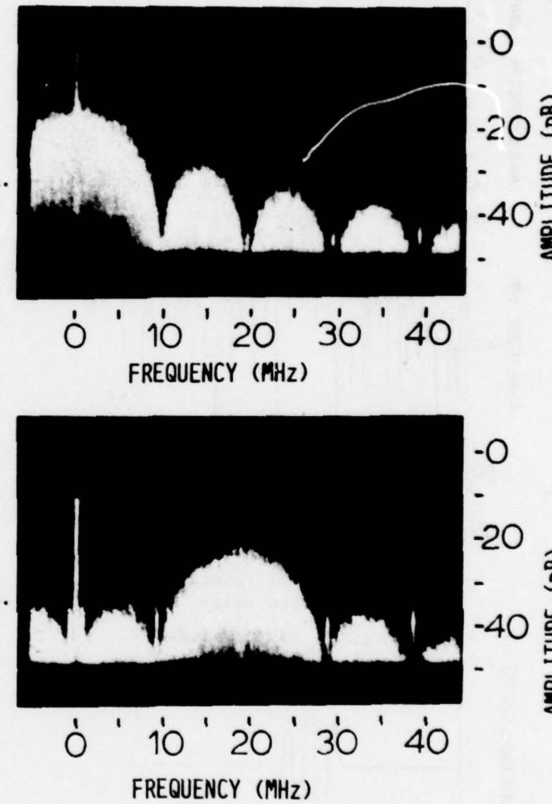

Figure 8. Frequency spectrum of PBN sequence with a 10 MHz clock frequency. A. Ordinary operation., B. When PBN phase modulates a 20 MHz cw carrier.

this phase and the phase of the recovered PBN sequence since heterodyning signals of the same frequency produces an output proportional to the phase difference. It is possible, depending on the delay, to obtain a positive or negative correlation peak, or if the acoustic carrier signal and the oscillator signal are at quadrature, a null output. Such a response is analogous to that obtained when using a laboratory technique known as the phase comparison method to measure small ($\sim$1 part in 10^7) changes in ultrasonic velocity[7]. With the phase comparison method, the transmitting transducer is excited with a tone burst and the phase of the received echoes is compared to that of a coherent cw reference. In the laboratory, temperature or some other variable is changed to produce acoustic transit time changes (caused by sound ve-

locity or path length changes). The frequency of the carrier is then varied to hold the output phase at null. In this case

$$\frac{\Delta f}{f} = -\frac{\Delta T}{T} = \frac{\Delta v}{v} - \frac{\Delta \ell}{\ell}$$

where f is carrier frequency, T is total acoustic delay time, v is sound velocity, ℓ is the acoustic path length and Δf is the frequency change needed to maintain the null condition. Electrical delays are assumed neglible as are phase variations produced by the transducer as a function of frequency.

The analogy between the outputs of the phase shift keyed PBN system and the phase comparison ultrasonic velocity measuring method indicates that it should be possible to measure small changes in velocity or thickness by recording the change in carrier frequency necessary to maintain the null during a scan of a part. This was tested experimentally by placing a pair of 9 MHz transducers 10 cm. apart in a water tank. The output was initially set to null and the spacing was then changed in 0.025 mm steps with the carrier frequency varied to return the output to null at each step. After 50 steps it was found that the maximum error in the measured Δf for a single step was 21%, with the average value for all points being within 3.5% of the expected value. The largest source of error was vibration in the water tank which produced position changes. The error in the average was probably due to error in the mechanical step distance and slight frequency variation of the transducer response. The experiment itself was not set up in an optimal fashion, but it indicated that it would not be unreasonable to expect resolution of 10 ppm changes in velocity or dimension with this system.

It should also be noted that the other way to implement the phase shift keyed system which is described in Ref. 6 would show the same phase sensitivity unless the carrier and both signal and reference PBN sequences are phase locked to ensure that the bursts are exact replicas of one another.

4. Conclusion

The primary advantage of the PBN system over conventional NDE ultrasonic systems is the increased sensitivity of the system. If the sample environment is sufficiently clean, i.e. there are no large scatterers, it is relatively easy to obtain signal noise improvements of 20 to 40 dB compared to the conventional systems. The presence of spurious scatterers such as grain boundaries, etc. would obviously produce interfering signals which would reduce or eliminate the improvement.

NDE application areas would principally be those inspections where the attenuation is large and/or deep penetration is required. Additional applications would be to improve the signal to noise ratio for spectral analysis of the signal and in imaging systems where the digital nature of the system should provide great flexibility. The phase shift keyed mode of operation provides an additional sensitivity to small dimensional and velocity variations as well as permitting the extension of flaw detection and acoustic attenuation measurements to higher frequencies using the same basic instrument.

Acknowledgements

The authors wish to thank J. A. Moyzis and K. D. Shimmin for devising the computer program used to model the instrument.

References

1. Ferguson, E. S., V. L. Newhouse, N. M. Bilgutay, and G. R. Cooper, "Application of Random Signal Correlation Techniques to Ultrasonic Flaw Detection", Ultrasonics, Vol. 13, 1975, pp. 11-17.
2. Elias, C. M., "An Ultrasonic Pseudorandom Signal Correlation System", to be published.
3. Golomb, S. W., Shift Register Sequences, (Holden-Day Inc., 1967).
4. Craig, S. E., W. Fishbein, and O. E. Rittenbach, "Continuous-Wave Radar with High Range Resolution and Unambiguous Velocity Determination", IRE Trans. on Military Electronics, Vol. MIL-6, 1962, pp. 153-161.
5. Cook, C. E., M. Bernfeld, and C. A. Pamieri, in Radars, Volume 3: Pulse Compression, edited by D. K. Barton (Artech House, Inc., 1975) pp. 127-129.
6. Chapelon, J. Y., D. Cathignol, and C. Fourcade, "A New Pseudo-Random Binary Code Phase Modulated Ultrasonic High Resolution Echograph", presented at the Third International Symposium on Ultrasonic Imaging and Tissue Characterization, National Bureau of Standards, Gaithersburg, MD, June 5-7, 1978.
7. Moran, T. J. and B. Luthi, "Elastic and Magnetoelastic Effects in Magnetite", Phys. Rev., 187, 1969, pp. 710-714.

LOGIC DESCRIPTION OF THE CONTROL LOGIC OF THE ULTRASONIC PSEUDORANDOM-SIGNAL-CORRELATION SYSTEM USING AN ASM CHART

An algorithmic state machine (ASM) is a concise and very useful means of modeling a logic system [1]. Such a machine has a number of predefined states and, in general, the next state of the machine depends on its present state and certain inputs or qualifiers. In a given state, the machine may produce certain outputs. If these outputs are a function of that state alone they are called state outputs. If the outputs depend on the state and some other condition(s), they are conditional outputs. Often the states of a machine are defined logically by a state counter; when the counter is at count S, the machine is said to be in state S. The logic which controls the counting sequence is thus the state control logic for the machine.

An ASM is represented graphically by an ASM chart. The chart uses the same rectangular box, diamond and "rounded box" symbols which are used in flow charts and, in fact, bears a superficial resemblance to a flow chart. However, in an ASM chart the operations described within a rectangular box and all branching associated with that box are executed simultaneously, not sequentially as in a flow chart. Each rectangle or state box and its associated branching and conditional output symbols represent a single machine state. The diamond symbol or decision box is used to represent conditional branching and the symbol with straight parallel top and bottom and semicircular ends is a conditional output box. State outputs are written in the state box which corresponds to the state in which they occur. The state number associated with a particular state box is written outside the box

at the upper right hand corner. A Boolean expression representing a condition or qualifier is written in the condition box. The two exit paths of a condition box are labeled H and L. The H path is taken if the qualifier is HIGH, the L path if the qualifier is LOW. A conditional output box placed in a conditional exit path indicates that those outputs written in the box will be asserted only when that path is taken.

The ASM chart for the control logic of the pseudorandom signal correlation system in shown in Fig. 1 . The "rest state" for the machine is state zero (ØØØ). In this state the operator may set the following parameters: burst length, cycle period - the time between transmitted noise bursts, initial correlation delay - the initial starting time for the reference noise burst, maximum correlation delay - the final starting time for the reference noise burst, and repetitions per point - the number of noise bursts transmitted before the correlation delay is increased. The values for these parameters are held in storage registers.

The logic term (ER-L) is asserted in state zero to enable the loading of the storage registers. The terms LNC-L, LQC-L, LPC-L, LP*C-L, and LIC-L are also asserted in state zero. These terms cause the N, Q, P*, and I counters, respectively, to be loaded or preset to the number stored in the registers. The P counter is loaded from the P* counter which is itself loaded from a storage register. ØA-L is used to set the two pseudorandom binary sequence generators to zero. Switching the RUN/HALT switch to RUN sets the GO flip-flop. GO-H causes the ASM to advance to state 1 (ØØ1) on the following clock transition. Note that the state counter for this ASM (as well as the

130

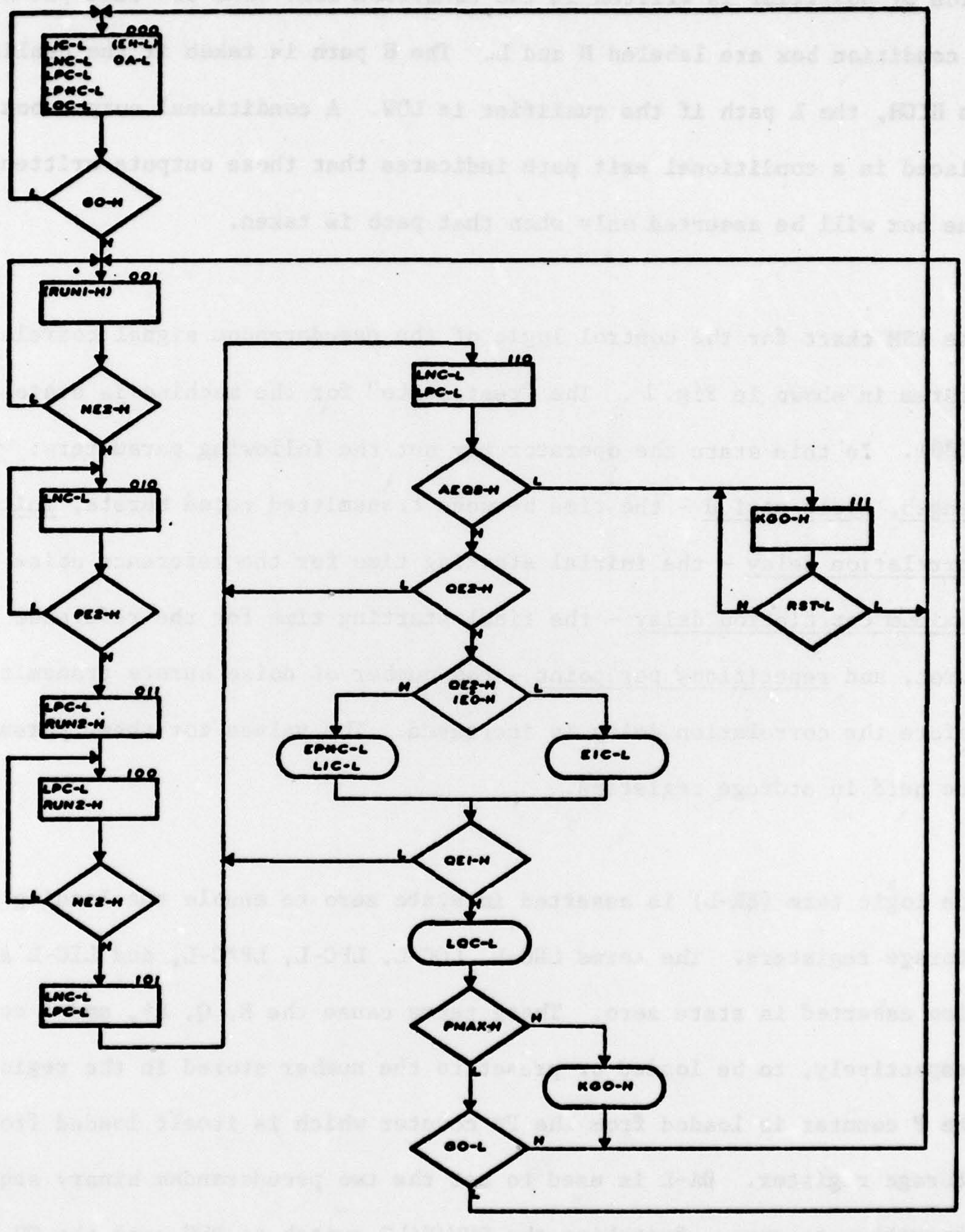
000
LIC-L
LNC-L
LPC-L
LPHC-L
QC-L
(EN-L)
OA-L
GO-H
001
(RUN1-H)
NE2-H
010
LNC-L
PE2-H
011
LPC-L
RUN2-H
100
LPC-L
RUN2-H
NE2-H
101
LNC-L
LPC-L
110
LNC-L
LPC-L
AEQB-H
111
KGO-H
RST-L
QE2-H
QE2-H
IEO-H
EPHC-L
LIC-L
EIC-L
QE1-H
LQC-L
PMAX-H
KGO-H
GO-L
H
L

Figure 1.

I, N, P, P*, and Q counters) is clocked by the system 20 MHz clock. This means that all state transitions will be synchronized with this clock. Hereafter, unless otherwise stated, the term "clock" refers to the 20 MHz system clock and "one clock time" is one period of this clock.

In state 1, (RUN 1-H) enables pseudorandom binary sequence generator number 1 (PRBS #1). PRBS #1 serial output is "anded" with (RUN 1-H) and, after level shifting and amplification, becomes the transmitted noise burst. In state 1, none of the counter "load terms" (LNC-L, LQ-L, etc.) are asserted. The control logic for the N, P, and Q counters is such that these counters count down when their load terms are not asserted. Thus, in state 1 PRBS #1 is running and the N, P, and Q counters are counting down from their preset counts. When the N counter, which controls the noise burst length, counts down to the count of 2, NE2-H is asserted and one clock time later the machine enters state 2 (Ø1Ø).

State 2 is entered with the N-counter count equal to 1. In state 2 LNC-L is asserted so that the zero count of N counter never occurs, but the counter is again preset to the number contained in the "N register" NR (burst length). In state 2 (RUN 1-H) is no longer asserted, therefore, PRBS #1 stops running, ending the transmitted noise burst. The gating term for PRBS #1 is also forced LOW in state 2. This ensures that the gated noise output is LOW even if PRBS #1 was stopped with a ONE or HIGH output condition (PRBS #2 is gated in a similar manner). In state 2 the N counter is held at its preset value, but the P and Q counters are still counting. When the P counter, which

controls the starting time of the reference noise burst, reaches the count of 2, PE2-H is asserted and state 3 (Ø11) is entered one clock time later.

In state 3, LPC-L causes the P counter to preset to the number held in the P* counter and to hold this count. RUN 2-H enables the reference pseudo-random binary sequence generator PRBS #2 and, since LNC-L is no longer asserted, the N-counter starts counting down. The ASM remains in state 3 for one clock time and then enters state 4 (1ØØ). (Due to a logic design change, state 3 is now actually not needed since the logic which was previously unique to state 3 is now implemented elsewhere.)

In state 4 (1ØØ), PRBS #1 is still running and the N and Q counters still counting down. Just as for the transmitted burst, the N counter controls the reference burst length. When NE2-H signifies that the N counter has counted down to 2, the state changes to 5 (1Ø1). RUN 2-H is no longer asserted so the reference burst ends, the N counter is again loaded with the contents of register NR, and neither the N nor the P counter is counting. Now that the reference burst has ended, both PRBS #1 and PRBS #2 should hold the same number. The parallel outputs of the shift registers used in PRBS #1 and PRBS #2 are fed to a comparator. If the contents of the registers are the same, AEQB-H is asserted. After a one clock time stay in state 5 to allow for comparator propagation delays, the ASM advances to state 6 (11Ø).

In state 6, if AEQB-H is not asserted the ASM enters state 7 (111) which is the "error state". In state 7, an error indicator on the instrument front panel is lighted and KGO-H resets the GO flip-flop. When the RESET button

is depressed, RST-L causes the ASM to return to state zero. If AEQB is asserted in state 6, state 7 is not entered. Instead, the ASM waits for QE2-H to indicate that the Q counter, which controls the time between transmitted noise bursts, has counted down to 2. When QE2-H is asserted, IEØ-H, which is HIGH when the I counter has counted down to zero, determines which of two sets of conditional outputs will be asserted. The I counter was preset (in state zero) to the number of "repetitions per correlation point". (Note that one "repetition" has already taken place before the I-counter is checked so the counter should be preset to a number which is one less than the desired number of repetitions.) If IEØ-H is not asserted, the I-counter does not contain zero and the L branch of the decision box is taken. In this case, EIC-L is asserted enabling the I-counter to count down. If the I-counter contains zero, IEO-H is asserted, the H branch is taken and LIC-L reloads the I counter with the contents of the I register IR. Also, EP*C-L enables the P* counter to count up. Since QE2-H is HIGH for only one clock time, EIC-L or EP*C-L can be asserted for only one clock time which assures that the I or P* counter will change by only one count. Since LPC-L is asserted for the duration of state 6, the P counter will have its required one clock time to preset to the updated contents of the P* counter before QE1-H causes the ASM to exit state 6.

The term PMAX-H is asserted when the contents of the P* counter equals the contents of the register PMR. PMR Holds the final or maximum value of the correlation delay. When QE1-H is asserted, LQC-L enables reloading of the Q counter. If PMAX-H is not asserted and the GO flip-flop is still set

(indicating that the RUN/HALT switch is still in RUN), state 1 (ØØ1) is re-entered and RUN 1-H starts a new transmitted burst. If the P* counter was incremented in state 6, PE2-H will be asserted one clock time later than it was for the previous state. This means that the exit from state 2, hence the start of the reference burst, will occur one clock time later. In summary, when the I counter has counted the required number of repetitions for a given preset value of the P counter (correlation delay), the P* counter--from which the P counter is loaded-- is incremented by one count thus increasing the delay by one clock time.

If PMAX-H were asserted in state 6, this would indicate that the maximum correlation delay had been reached. In this case, KGO-H resets the GO flip-flop and the ASM returns to state zero. In state zero all the counters are reloaded, PRBS #1 and PRBS #2 set to zero and, if the RUN/HALT switch is in RUN, the GO flip-flop is set and the ASM goes to state 1.

MNEMONICS INFORMATION

NOTE: **Each mnemonic consists of a character string followed by a hyphen and then an H or an L. The H implies that the logic signal is asserted when HIGH: the L means the signal is asserted when LOW.**

Mnemonics Used on ASM Diagram

Mnemonic	Description
AEQB-H	The contents of the two pseudorandom-noise-generator shift registers are numerically equal.
EIC-L	Enable the I counter.
EP*C-L	Enable the P* counter.
(ER-L)	Enable loading of data registers (actually implemented as a buffered [inverted] decoded state-count zero).
GO-H	GO flip-flop is set.
IEØ-H	I counter count equals zero.
KGO-H	K input to GO flip-flop.
LIC-L	Load I counter.
LNC-L	Load N counter.
LPC-L	Load P counter.
LP*C-L	Load P* counter.
LQC-L	Load Q counter.
NE2-H	N counter count equals 2.
PE2-H	P counter count equals 2.
PMAX-H	P* counter count equals contents of "PM" register.

Mnemonics Used on ASM Diagram (Cont'd)

Mnemonic	Description
QE1-H	Q counter count equals 1.
RST-L	Reset. Clears GO flip-flop. Also a qualifier for exit from ERROR state (111) to return to state ØØØ.
RUN1-H	RUN command for pseudorandom-noise generator number 1.
RUN2-H	RUN command for pseudorandom-noise generator number 2.

MNEMONICS INFORMATION

Registers

Mnemonics	Description
IR	I register. Holds the count to which the I counter is preset. This is the number of noise bursts to be transmitted for each correlation point.
NR	N register. Holds the count to which the N counter is preset. This represents the noise burst length.
PR	P register. Holds the initial value of the count to which the counters PC and P*C are preset. This is the initial starting time of the reference burst or the initial correlation delay.
PMR	P-Max register. Holds the final value of the correlation delay.
QR	Q register. Holds the count to which QC is preset which is the time between transmitted noise bursts.

MNEMONICS INFORMATION

Counters

Mnemonics	Description
IC	I counter. Presettable down counter. Determines number of noise bursts generated per correlation point. "P*C" counter is incremented by one count each time I has reached zero and the P*C count determines the starting value for the "P" counter.
NC	N counter. Presettable down counter. Determines noise burst length. Counts upon negation of load signal.
PC	P counter. Presettable down counter. This counter is preset with the current value of "P*" counter. The P counter determines the start time of the reference noise burst or the "correlation delay".
P*C	P* counter. Presettable up counter. Holds the current value of the correlation delay (the start time of the reference noise burst). This counter is incremented by one to increase the correlation delay.
QC	Q counter. Presettable down counter. Determines time between transmitted noise bursts. Counts upon negation of load signal.

MNEMONICS INFORMATION

Generators

Mnemonics	Description
PRBS #1	Pseudorandom binary sequence generator #1.
PRBS #2	Pseudornadom binary sequence generator #2 (reference).

REFERENCES

[1] C. R. Clare, Designing Logic Systems Using State Machines, New York, NY: McGraw-Hill Book Company, 1973.